SPSE

# Photographic
## SCIENCE AND ENGINEERING

Direct-Reading Zero-to-Six Range Densitometer Incorporating Digital Output • *Monroe H. Sweet* 97

Automatic Recording and Analyzing Densitometer for Reflection and Transmission Densities • *Monroe H. Sweet and Benjamin R. Harriman* 101

A New Method for Evaluating Sensitometric D-Log E Curves *W. H. Carnahan* 110

Some Observations on the Reproduction of Flesh Colors • *C. J. Bartleson* 114

Image Illuminance Levels in Night Photography • *William G. Cibula* 118

Hypersensitization of X-Ray Films • *Yoshitada Tomoda* 122

Effect of Derivatives of Thiourea and Related Compounds on Zeta-Potential of Silver Bromide • *Shin Suzuki and Tooru Kataoka* 127

Fungicidal Rinses for Processed Color Films • *E. S. Mackey and C. E. Johnson* 132

Photographic Developing Agents: I. Pyrimidines *R. W. Henn and Sue V. Carpenter* 135

The Calcium-Sequestering Properties of Organic Compounds in Photographic Developers • *R. W. Henn* 140

Notes from the Editor 144

Book and Journal Reviews 145

Technicalia Photographica • *Frank Smith* 152

1959 Annual Conference Notice 160

*Volume 3 · Number 3*

**MAY-JUNE · 1959**

# Editorial Policy

*Photographic Science and Engineering* is dedicated to the advancement of the knowledge and application of photography and other directly related sciences. Its pages are open to all who wish to report on new studies dealing with the theory of photosensitive systems, the design of photographic instruments and apparatus useful in the treatment of photographic materials, photographic optics and illuminants, the use of photography for scientific or engineering measurement or recording, and photographic instrumentation and data recording. Only original papers should be submitted except on special invitation.

Manuscripts should be typed double-spaced on white bond paper with $1^1/_4$-inch margins all around. Literature references should be exact, and should include titles of journals, names of authors, numbers of volumes and pages, and year of publication. Book references should include title of volume, names of authors, publisher, number of edition, year of publication, and chapter and pages cited.

Graphs, charts, and other line illustrations should conform to good usage such as given in the American Standards Association Document Y-15, "A Guide for Preparing Technical Illustrations for Publication and Projection." Continuous-tone photographs should be made on 8- by 10-inch glossy paper and should show pertinent image detail sufficiently clearly to permit reduction to fit a 3-inch column in this journal. All illustrations should be numbered in soft blue pencil on the back to correspond with captions typed on a separate page. Tables should also be submitted on separate pages appropriately identified. An abstract should accompany each manuscript.

Papers intended for publication should be submitted in duplicate to the editor, T. H. James, Research Laboratories, Eastman Kodak Co., Rochester 4, N.Y. All papers will be reviewed by members of the Editorial Review Board and if not accepted will be returned to the author. Published papers become the property of the Society and are protected by appropriate copyrights. Authors receive five copies of issues in which their contributions appear. Authors may order reprints of their papers at the time they return the galley proofs. The Society does not assume responsibility for material in transit, nor guarantee publication of unsolicited material.


# Photographic
## SCIENCE AND ENGINEERING

*official publication of the*
Society of Photographic Scientists and Engineers

**May-June 1959**

Volume 3, Number 3



**EDITORIAL STAFF**

**T. H. James,** *Editor*

**Jennie H. Allen,** *Managing Editor*

**S. C. Goddard,** *Feature Editor*

**Frank Smith,** *Feature Editor*

**Robert H. Zappert,** *Feature Editor*

**Norman A. Exley,** *Assistant Editor*

**EDITORIAL REVIEW BOARD**

**R. S. Barrows**

**R. Clark Jones**

**K. G. Leistner**

**J. A. Maurer**

**F. W. H. Mueller**

**H. F. Nitka**

**Thomas D. Smith**

**William West**



*Photographic Science and Engineering* is published six times a year by the Society of Photographic Scientists and Engineers. The publication office is at 20th and Northampton Streets, Easton, Pa. Address correspondence to the Society at Box 1609, Main Post Office, Washington, D.C. Subscription to non-members of the Society, $8.00 per year, members $4.00; single copies, $2.00 each. The Society is not responsible for the accuracy of statements made by authors and does not necessarily subscribe to their views. Second-class mail privileges authorized at Easton, Pa. This publication is authorized to be mailed at the special rates of postage prescribed by Section 132.122.


© Copyright 1959 by the Society of Photographic Scientists and Engineers, Inc. Permission to reprint any part of the contents, except in reviews and abstracts, must be obtained in writing from the Editorial Vice President.

PHOTOGRAPHIC SCIENCE AND ENGINEERING
Volume 3, Number 3, May-June 1959

# Direct-Reading Zero-to-Six Range Densitometer Incorporating Digital Output

MONROE H. SWEET, *Quantametric Devices, Inc., Binghamton, N.Y.*

**To measure the high densities encountered in graphic arts and x-ray film products, the amplifier circuit of a commercially available direct-reading photomultiplier type of densitometer of range 3 was redesigned to provide a range of 6, preserving its original accuracy, electrically uniform output, high speed of response and other desirable functional features. Whereas the original densitometer utilizes constant anode current, in the present modification the anode current is deliberately varied by means of a controlled bias voltage and a nonlinear anode load resistance. A digital reader was developed to provide an accurate and easy to use output indicator for the densitometer. The reader is a high-speed electromechanical device capable of changing from 0 to full scale (6.0 density) in less than $2\frac{3}{4}$ sec. It is nonoscillating and the circuit is entirely transistorized. With a different type of photomultiplier tube and certain additional circuit modifications the range can be increased to at least 9 or 10 density units.**

Until the early 1940's, it was uncommon to discuss photographic densities above 3.0. Probably 3.0 became the upper limit of ordinary measurements due to difficulties in the design and use of practical visual densitometers capable of reading higher densities with satisfactory accuracy.

With the development of modern photosensitive receivers and associated circuitry, the capability of measuring higher densities, and also of increasing the spectral purity of measurements in the case of color densities, promoted a trend to higher limits, and today a range of 4.0 has become relatively common. In the evaluation of transparency materials used in graphic arts work, density measurements as high as 6.0 are photographically significant. The extended range is also useful in the evaluation of x-ray film products.

## Circuit Changes to Provide Range of 0–6

### *General*

The circuit for the original instrument used has been described in several different articles.[1,2,3] In this circuit, the sensitivity of the photomultiplier tube is continuously and automatically adjusted so as to keep the output (anode) current essentially constant.

Referring to Fig. 1, assume the circuit to be in equilibrium at a particular incident light level and dynode voltage. If the incident light level is increased, the anode current will momentarily increase. This results in an increased voltage drop across resistance, R, driving the grid of the control tube more negative and reducing the dynode voltage. However, reduction of dynode voltage is accompanied by reduced photomultiplier tube sensitivity and reduced output current. If the gain of the control tube is so high that it can be treated as infinite, then the anode current will be constant at all light levels (assuming zero grid current), and the equilibrium dynode voltage can be used as a measure of the incident flux level.

Fortunately for use in densitometry, it is characteristic of multiplier tubes that the relation between dynode voltage and sensitivity is approximately logarithmic, and therefore equal changes in dynode voltage correspond to nearly equal changes in density over a wide range of dynode voltage values.

For the type of tube used in the unmodified densitometer, the relation between optical density (or − log (incident flux)) and dynode voltage is shown in Fig. 2. Although the relation between dynode voltage and density (log (sensitivity)) is quasi-linear, Fig.

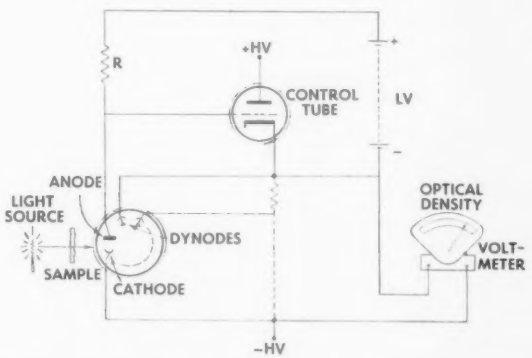


Fig. 1 Schematic diagram of ordinary dynode voltage feedback circuit (simplified).

Presented at the Annual Conference, Rochester, N.Y., 8 October 1958. Received 3 November 1958.

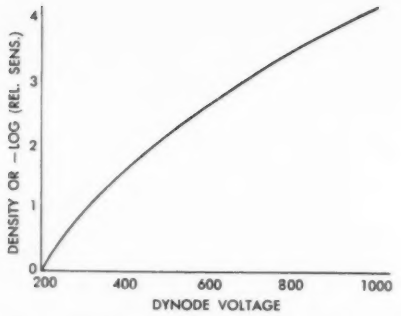


Fig. 2. Density vs. dynode voltage for simple circuit of Fig. 1.

2 shows that the slope of the curve becomes relatively shallow at maximum dynode voltage (1,000 v) and increasingly steep at the lowest voltages. The slope is only $\frac{1}{5}$ to $\frac{1}{10}$ as great at 1,000 dynode-v as at 200 v but for a limited density range it is nearly constant.

In order to confine the dynode voltage swing to reasonable values for the full range of 6 and to obtain other advantages, a method has been developed for deliberately varying the anode current with dynode voltage rather than attempting to hold the anode current constant. Among the advantages of this technique is that the approach to a strictly linear relation between density and dynode voltage can readily be improved over that obtainable with the basic circuit.

### *Analysis*

In Fig. 3, line A represents the (idealized) results obtained with the simple circuit in Fig. 1, wherein the photomultiplier anode current is held constant. In order to obtain the relationship represented by line B, the anode current must be decreased continuously as the density rises to give greater and greater net sensitivity than that obtained by simple feedback. In fact, at density 6, and 850 dynode-v, the net sensitivity must be 1000 times greater than for the simple circuit.

A feedback amplifier controlled by the dynode voltage applies a bias potential to a nonlinear anode load resistance. The "sense" or "phase" of the bias voltage must be opposite to that of the dynode voltage, so that when the incident light level increases and the dynode voltage is reduced the bias voltage increases, thereby increasing the equilibrium anode current and preventing as great a reduction in dynode voltage as would occur at constant anode current.

The relationship between dynode voltage and anode current necessary to obtain the "B" function of Fig. 3 is not obvious. In the simple circuit having constant anode current, $i$,

$\log (\text{Sens}_{d\text{-}v}) = \text{D}$, where $\text{Sens}_{d\text{-}v}$ is the photomultiplier tube sensitivity at dynode voltage, $d$-$v$, and D is density (1)*

and in order to achieve the desired results using controlled anode current and dynode voltage, it is necessary that

$$\log (\text{Sens}_{\text{net}}) = 2\text{D} \qquad (2)$$

or

$\log (\text{Sens}_{d\text{-}v} \times \text{Sens}_i) = 2\text{D}$, where $\text{Sens}_i$ is the sensitivity at anode current, $i$.

This leads to the expression

$i = 10^{\text{D}}$, which describes the relation between density and anode current to yield function "B." (3)

### *Practical 0–6 Circuit*

Silicon carbide resistance elements are available whose characteristics can be used to satisfy the requirements of Eq. (3). Figure 4 indicates how this is accomplished. The bias potential for the SiC resistor is provided by a dynode voltage feedback amplifier whose gain and phase are such as to satisfy the requirements stated above.

* Log sensitivity is *numerically* equal to density when the units of sensitivity are suitably chosen.

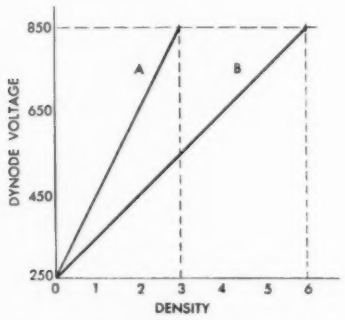


Fig. 3. Density vs. dynode voltage relationship for the circuit of Fig. 1.

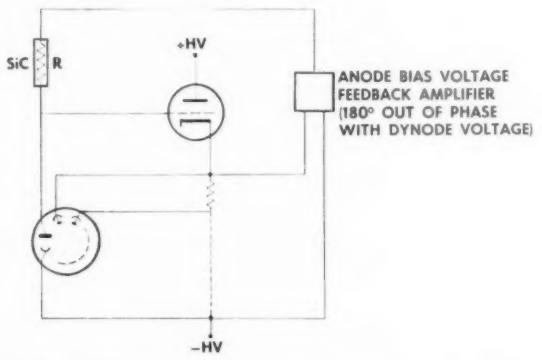


Fig. 4. Schematic diagram indicating method used for obtaining anode current control.

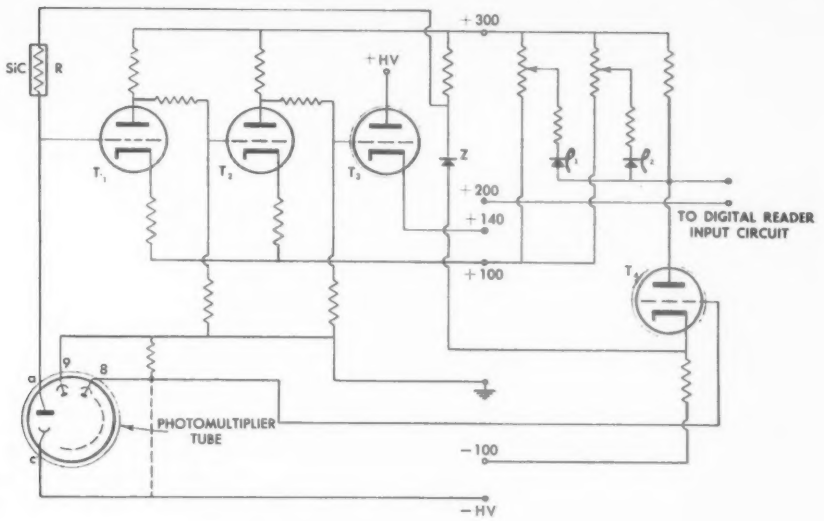


Fig. 5. Schematic diagram of simplified 0–6 density-range photomultiplier amplifier circuit.

Figure 5 is a simplified schematic diagram of the actual circuit. By using a two-stage amplifier ahead of the dynode voltage control tube, $T_3$, the potential of the photomultiplier anode is held very nearly constant under all operating conditions, and grid current in the input tube can easily be kept essentially zero.

$T_4$ serves as a cathode follower and voltage amplifier. Its input is obtained from dynode No. 8. The cathode of $T_4$ operates in a low impedance circuit and is of proper phase to provide the desired bias conditions for the SiC element, *R*. In order to obtain the proper level of operating voltage, a zener diode is used to elevate the cathode voltage as shown.

The plate swing of $T_4$ serves as the input for the digital reader.

Adjustments, not shown, permit the bias potential on the SiC resistor to be changed, as well as the rate of change of bias with changes in dynode voltage. When in proper adjustment, agreement of density readings within ±0.02 of reference standards for nearly the entire range of 6 is obtainable with little difficulty.

### *Digital Reader*

As stated earlier, in order to read a range of 6.0 density to 0.01 on even a large single-scale moving-

Fig. 6. Model 61 Digiscan Reader. Shown in use with Model 12A Densitometer.

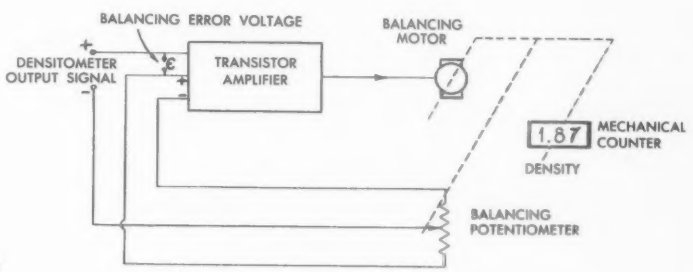


Fig. 7. Schematic diagram of digital reader.

**Fig. 8.** *Top:* **Ordinary moving-pointer densitometer scale.** *Bottom:* **Digiscan Reader. The two photographs are reproduced with the same reduction and both devices indicate 1.87 density.**

pointer meter involves prohibitive eyestrain. Since no commercially available high-speed digital readout device of suitably low cost was available, a satisfactory reader was developed and this device can be attached to any similar densitometer. It is called the Model 61 Digiscan Reader and is shown in Fig. 6.

The principles of operation of the reader are illustrated in Fig. 7. The output of the densitometer is connected to a transistor amplifier through a potentiometer having a constant applied potential. If the signal voltage and the potentiometer voltage are not equal and opposite, the result is an error voltage which excites the balancing motor.

The balancing motor drives the potentiometer in such a direction as to reduce the error voltage. This action is continuous. A large mechanical counter, especially designed for high-speed operation, is connected to the motor-potentiometer drive shafts and the whole device is calibrated directly in terms of density. The device reads well over 200 digits/sec and rebalancing time is less than $\frac{1}{3}$ sec for all ordinary readings. It is dynamically stable and the amplifier and potentiometer can be replaced without influencing the accuracy of the readings. A variation in line voltage from 50 to 140 v has no effect on the accuracy of the readings. The repeatability or precision is better than 0.002 density.

The reader can be attached to any linear signal densitometer by connecting three leads to tube pins in the densitometer amplifier. Although developed especially for this extended range densitometer it is directly applicable to ordinary 3- and 4-range direct-reading instruments.

A relay, operated by a microswitch tripped by the measuring arm, disables the reader circuit whenever the measuring arm is raised. If the microswitch is properly adjusted, the reading obtained with the measuring arm pressed against the sample is preserved when the arm is raised.

The relative ease of reading the digital reader in comparison with that of the Model 12A Moving-Pointer Meter can be judged from Fig. 8. The two photographs are of identical magnification and each reading device indicates 1.87 density.

The "sensitivity" or "span" adjustment is incorporated in the reader although the zero adjustment for the unmodified densitometer is retained.

## Equipment Performance

Practical field tests of both the expanded range circuit and the reader have been conducted for nearly two and a half years and these indicate a long service life. The calibration has remained stable and only minor mechanical servicing of one of the several readers was necessary. No servicing of any of the transistor amplifiers has been required.

As might be expected, operators report almost complete elimination of eyestrain through the use of the digital readers, greater operating speed, and a reduction in reading errors.

## Additional Remarks

The support of Haloid Xerox in this project is gratefully acknowledged. Patent protection on the novel features of the circuits and other features of the digital reader is being sought.

## References

1. Sweet, M. H., *Electronics*, *19:* No. 11, p. 105 (1946).
2. ———, *J. Soc. Mot. Pic. TV Engrs.*, *54:*35 (1950).
3. ———, *J. Opt. Soc. Am.*, *37:*432 (1947).

PHOTOGRAPHIC SCIENCE AND ENGINEERING
Volume 3, Number 3, May-June 1959

# Automatic Recording and Analyzing Densitometer for Reflection and Transmission Densities

MONROE H. SWEET, *Quantametric Devices, Inc., Binghamton, N.Y.*, AND BENJAMIN R. HARRIMAN, *Photo Products Research Department, Haloid Xerox Inc., Rochester, N.Y.*

**An instrument is described that simultaneously records the densities and computes the desired sensitometric characteristic values of test strips accurately and reliably. The new instrument accommodates both reflection and transmission strips on a 3 or 6 density range and does not require calibration or zero re-adjustment when changing ranges. Routine operation consists of feeding unmounted test strips into a slot in the measuring head. This new high-speed densitometer has adequate precision and accuracy in terms of American Standard Transmission and Reflection Density for all ordinary sensitometric work.**

One of the principal problems in photographic sensitometry is the accurate and efficient evaluation and interpretation of the densities of test strips.

After reviewing the theoretical and practical requirements for an automatic densitometer to serve the needs of a typical photographic research and development laboratory, it was recognized that none of the older instruments would be completely satisfactory. An instrument was needed that would be sufficiently versatile to evaluate transmission and reflection test strips at medium and high densities, rapidly and conveniently with sustained accuracy, and yet would be simple, compact and uncluttered.

The present instrument incorporates a number of new features as well as several improvements on old techniques combined in such a way as to satisfy these requirements. As a result, it is well suited not only for research purposes but also for high volume output of routine quality control work.

Presented at the Annual Conference, Rochester, N.Y., 8 October 1958. Received 3 November 1958.

**Fig. 1. Quantascan Model 101 Automatic Densitometer, exclusive of computer display.**

## General Description

In Fig. 1, a picture of the basic instrument, exclusive of the computer display, it may be seen that only the recorder scale and the necessary portion of the reflection head extends above the desk top. The lamp voltage stabilizer and junction box can be seen at the back of the knee-well. The photomultiplier amplifier and recorder amplifier are concealed in the desk drawer compartments.

Figure 2 shows the basic instrument in routine use. Once the instrument is in temperature equilibrium (only 1 or 2 min) normal operation consists in feeding the test strips into the strip-slot. D vs. Log E curves are delivered on chart paper to the operator on a flat plate. Generally, charts are kept in roll form, each

**Fig. 2. Basic densitometer in routine use.**

roll representing a number of charts that form a natural grouping. An automatic zero drift compensating circuit preserves the zero reading in spite of short or long term changes in photomultiplier tube or amplifier gain. Actually, it is only required that zero stability be preserved during the 5-sec reading portion of the operating cycle, but the stability is several decades better than this.

## Routine Use of the Basic Instrument

All the controls for routine operation are located on the measuring head panel shown in Fig. 3. The daily calibration check, using the glass filters for reference,

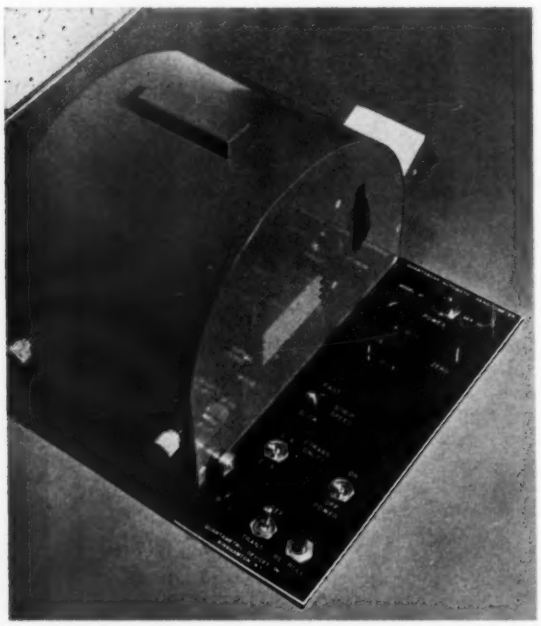

Fig. 3. Measuring head, showing arrangement of controls.

requires only a few seconds, and switching from transmission to reflection density modes is accomplished by operation of a single control switch. In the transmission position, either the 3 or the 6 density range may be used. In order that unit slope of the D vs. log E be graphically represented as a 45° line when the density range is increased from 3 to 6, the test strip drive speed is doubled. However, it is generally preferred to expand the log E scale of the recording in the 6 density range because materials having densities up to 5 or 6 usually are of such high contrast that their traces cannot be easily separated when plotted on 1:1 scale basis.

Either of two test strip channels can be evaluated by positioning the strip guide carriage, and by means of a push-button switch the chart paper can be rerolled to record additional strips on the same graph.

Once oriented for routine use, the operator simply inserts the strips into the guide slot and records the traces on the chart paper.

## System Design

One of the basic design problems was to make the choice between step-wedge and smooth-wedge exposed test strips. Step-wedge exposed strips have the advantage of permitting a relatively large sample area to be scanned, thereby minimizing the effects of unavoidable irregularities in the density of the sample. Step-wedge exposed strips are well suited for use with punched card or other digital mode recorders but are not well suited for graphical recording because the operator must (manually) draw a curve through the (automatically) plotted points after the recording is complete.

In those installations where versatile digital computers are already in company use, the punched card recording techniques may be attractive, since they permit permanent step-by-step recording of the sensitometric strip data in convenient form; these data may be used immediately as well as at any later time for evaluation of the test strips with respect to new criteria for speed, gradation, exposure scale, etc.

The adoption of continuously exposed test strips permits the ink recording of the complete D vs. log E curve and the use of analog computers in such a way that the sensitometric characteristic values can be computed during the recording cycle. There are obvious advantages to the availability of a graphical display of the D vs. log E function, but if a series of tests is conducted for which graphs are not needed, the computer section of the equipment can be used alone. For these reasons, the continuous type of test strip was selected for the present system design.

Figure 4 illustrates a series of ten repeat recordings of a typical test strip on the same section of chart paper.

Another design problem was that of choosing between an optical null (double beam) system and a variable intensity (single beam) system. The optical null method is theoretically capable of superior performance because, if it is well designed, short term drift problems are absent and long term drift is minimized. However, the single beam system is simpler and if a detector-amplifier can be constructed which maintains precision commensurate with the accuracy required in the practical sensitometric process, it is the more attractive choice. Most null instruments require the use of calibrated strips as practical reference standards so the requirement to use these in calibrating the single beam instrument is not a disadvantage, comparatively speaking. Recent improvements in a photomultiplier tube amplifier circuit assured the instrument designers that a satisfactory level of precision could be maintained, in routine daily use, with the single beam technique. Therefore the latter mode was adopted, and has proven itself through actual performance over a period of a year and a half.

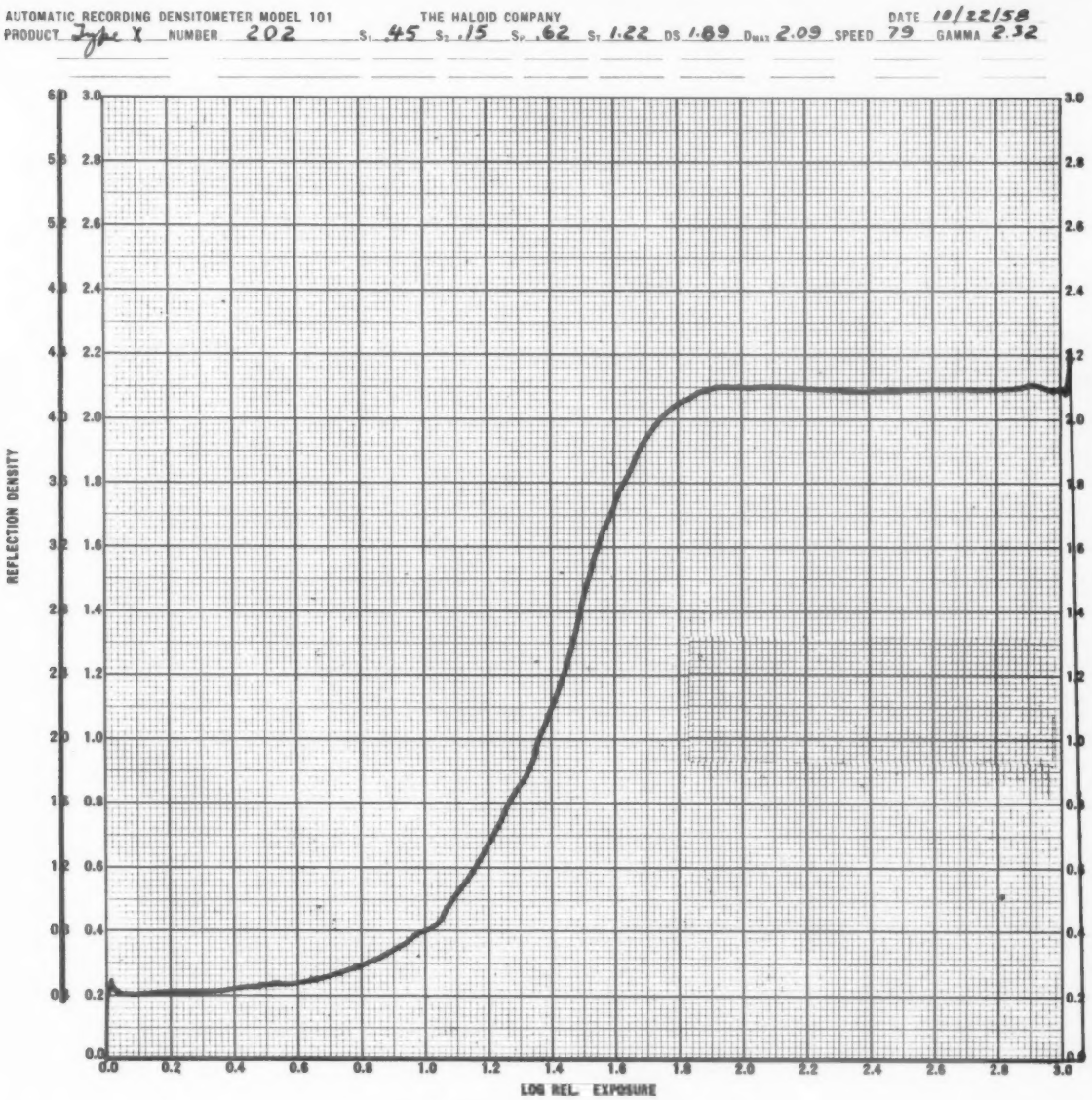


Fig. 4. Trace of ten repeat recordings of a typical test strip.

## Description of Components

### *Measuring Head*

Figure 5 is a schematic diagram of the optical system. For transmission measurements, lamp $L_T$ is energized and its flux is collected and focussed on an opal glass plate at "$D_1$" by lenses $1_1$ and $1_2$. Plane mirror $M_1$ permits use of a "folded" system and provides a more compact arrangement than is otherwise possible. The opal glass, $D_1$, is a nearly perfect diffuser and the transmitted flux irradiates the test sample at all angles of incidence.

The specularly transmitted component of the flux is collected by lens $1_3$ and after reflection by a second plane mirror $M_2$, the image of the specimen is focused in the plane of the exit aperture A. A diffusing screen $D_2$ helps distribute the flux over the photo surface of the photomultiplier tube P.

The geometry of this system obviously conforms closely with the basic requirements for American Standard Diffuse Transmission Density. The minor errors that occur at minimum densities, due to interreflections between the opal glass and the specimen, can usually be ignored in practice, although they can

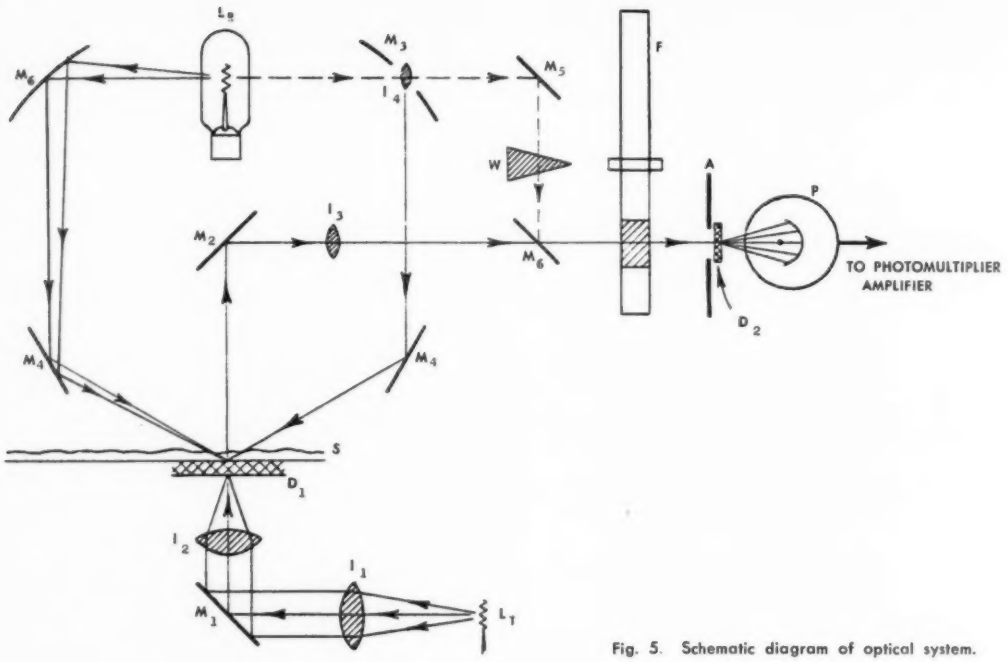


Fig. 5. Schematic diagram of optical system.

be compensated electrically in the output circuit if desired.

In the reflection system, flux from lamp $L_R$ is collected by the concave annular mirror, $M_2$, and focused on the specimen after reflection by the simple annular mirror $M_4$. Light reflected by the sample is collected by the same optical system as that for transmission. The mode of this arrangement corresponds in every respect to the requirements for the proposed American Standard Photographic Reflection Density.

In the case of transmission measurements, the optical flux reference for zero density is of course that received by the phototube when the sample is absent.

In the reflection density mode, the zero reference is that of a perfectly diffuse reflector of substantially 100% reflectance.* Since there is no practical physical sample to represent this ideal, a small fraction of flux from $L_R$ is collected by lens $L_4$ and directed on the photomultiplier tube after reflection by plane mirrors $M_5$ and $M_6$ and partial absorption by wedge W. Once wedge W is adjusted so that the flux received by the phototube is of the same magnitude as that which would be received from an ideal zero density specimen, this beam can be used thereafter to obtain the zero reference density signal. Mirror $M_6$ is carried on a lever arm, solenoid operated. It is located in the position shown, when the instrument is in the "STANDBY" condition and between the reading of individual strips. Wedge W is positioned by a simple transport mechanism operated by a control knob located at the left side of the measuring head housing.

* A specially prepared magnesium oxide surface is specified in the proposed standard.

Mirror $M_6$, which also serves as a shutter to obstruct light reflected from the specimen S, is locked out of position during transmission readings.

The reflection system is obviously very efficient and dense color filters can be used without restricting the density range beyond the limits of practical interest.

A filter wheel, F, contains a series of filters used primarily for calibration checks. Since both the transmission and the reflection systems conform with the desired standards, a density reading of 1 should correspond to an attenuation of 90% in the zero density beam. Therefore, when the response of the recorder is adjusted to agree with the known values of the whole series of neutral density filters in the filter wheel, the operator is assured that the calibration of the instrument is correct.

Figure 6 shows the measuring head removed from the desk. A multiple conductor plug connects the unit to the junction box. The photomultiplier tube leads are led directly to the amplifier chassis. The filter wheel can be seen protruding from the side of the housing.

### *Mechanical Arrangement*

The mechanical arrangement, shown in Fig. 6, consists of a strip drive mechanism having two drive rollers, one on each side of the measuring aperture. When the strip is inserted in the slot, it trips the first of two microswitches. This closes the strip drive motor circuit and the first roller firmly engages the strip and pushes it against a second microswitch. The second switch starts the chart drive motor and the strip enters the measuring aperture. As the operation proceeds, the strip is gripped by the second

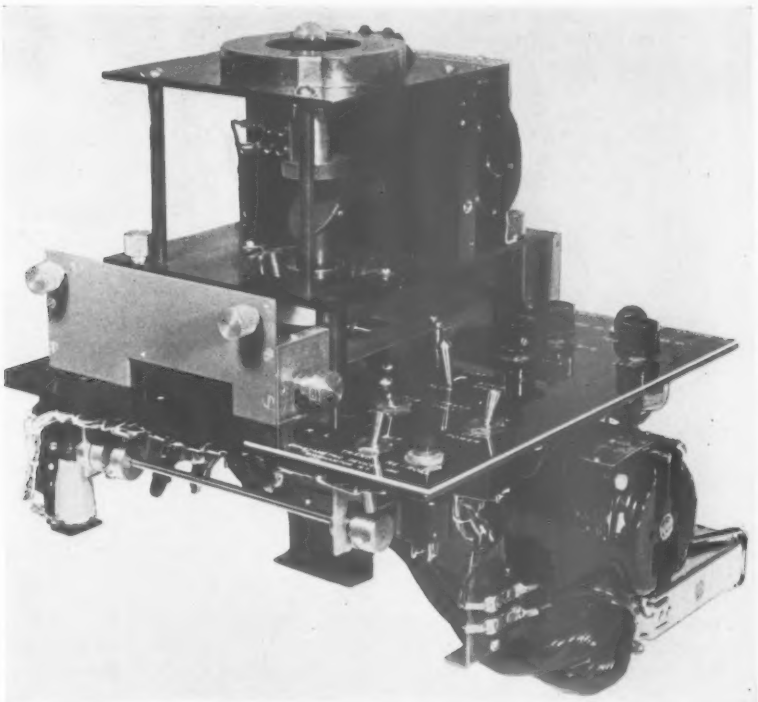

Fig. 6. Measuring head with cover removed.

roller. Circuits in the recorder keep the strip drive motor running until after the strip leaves the second roller.

The mechanical drive system is designed so that nothing touches the strips along the channels measured.

In Fig. 5, showing the optical system, it is indicated that the backing for the reflection and transmission strips is opal glass. Actually, this is not the case. Several operations are performed when the function switch is moved from the "TRANSMISSION" to the "REFLECTION" position, and among them is the replacement of the opal glass with a white painted metal tab. This provides a backing surface of characteristics required by the proposed Reflection Density Standard. The opal glass used for transmission measurements has a suprisingly high reflection density (0.85) and when used as a backing material for thin base test strips it leads to density readings that are several hundredths too high. The paint used for the backing tab has a reflectance of well over the 85% minimum specified in the standard.

Another mechanical function performed by the REFLECTION – TRANSMISSION switch is the control of the solenoid-operated reference mirror, $M_6$. When the switch is placed in the "TRANSMISSION" position, the mirror is moved out of the optical path and locked. In the "REFLECTION" position, it is released so that the solenoid can push it into position when its coil is energized between strip measurements.

Interlock switches prevent the strip drive motor from operating when other switches are not in their proper positions.

### *Densitometer Amplifier*

The densitometer amplifier circuit is similar to one developed by one of the present authors several years ago.[1,2] The basis for this circuit is that the dynode voltage for the photomultiplier tube is continuously and automatically adjusted, in the presence of changes in incident light, so that the anode output current is held constant. When the photomultiplier serves as a receiver in a densitometer, the dynode voltage is used as a measure of the density of the sample. This circuit has many unique advantages and has become widely used in photometric equipment since its original publication.

Several substantial improvements are incorporated in the present amplifier, and patent protection on these as well as on the novel features of the instrument is being sought.

An entirely new anode circuit is used for the 6 density range. The anode current is deliberately varied, in a nonlinear way, with dynode voltage. This permits operation of the photomultiplier tube at higher sensitivity and over a much wider range of flux levels than with the original circuit.

The anode circuit for the 3 density range provides more nearly constant anode voltage operation at a lower input grid current level than originally. This provides improved stability.

Automatic zero drift compensation is provided by

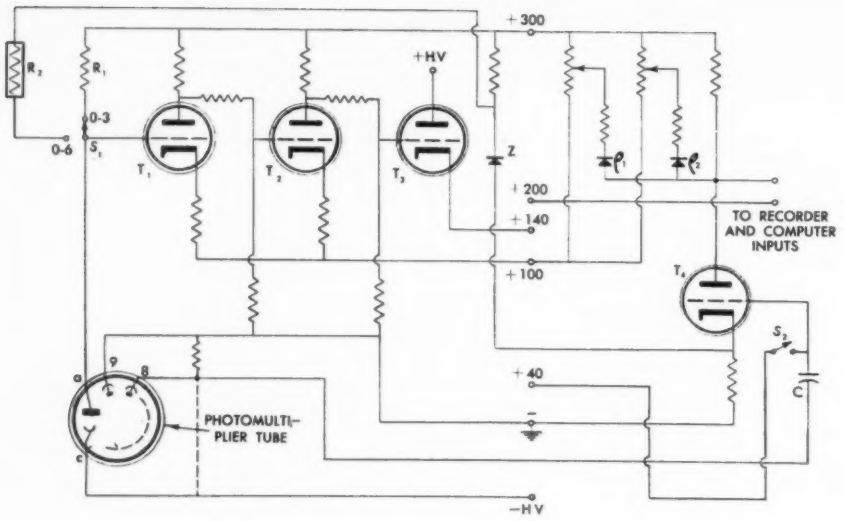


Fig. 7. Simplified schematic diagram of photomultiplier amplifier circuit.

means of a "holding" condenser located between the dynode bleeder and the output cathode follower control grid.

The output circuit does not add to the high voltage supply current drain. It derives its signal directly from the dynode bleeder network and operates the control grid of a cathode follower and voltage amplifier. The use of silicon rectifiers in the reverse direction as zener diodes, as well as in the forward direction to replace hard tubes and gaseous tubes, helps reduce the total power consumption of the amplifier to only a few watts.

Figure 7 is a simplified schematic diagram illustrating these features. Whether in the 3 or 6 density range position, the potential of the grid of input tube $T_1$ depends on the anode current of the photomultiplier tube. When the light received by the photomultiplier tube is increased, the grid of $T_1$ is driven more negatively, momentarily. However, this causes its plate potential to become more positive and with it the grid of tube $T_2$. Therefore the plate of $T_2$ is driven in a negative directon, carrying with it the grid of the high voltage control tube $T_3$. The dynode voltage controlled by $T_3$ is reduced. This action reduces the sensitivity of the photomultiplier tube and restricts the anode current. An equilibrium anode current is reached almost instantaneously. The voltage gain of the two-stage "buffer amplifier" for $T_3$ is relatively high and yet the use of the two cathode load resistors provides sufficient degeneration to give excellent stability. The net result is that over the whole operating range of the circuit, the potential of the grid of tube $T_1$ is very nearly constant. Furthermore, since the operating conditions for $T_1$ are such that the grid current is negligible ($10^{-10}$ amps), the photomultiplier anode current is maintained very nearly constant.

The output signal is derived from the cathode follower tube $T_4$. $T_4$ is driven through the coupling condenser C by the voltage developed between dynodes 8 and 9. Therefore, to a close approximation, the plate-cathode current of $T_4$ varies linearly with dynode voltage. In the standby condition, switch $S_2$ is closed. This holds the grid of $T_4$ at a constant value such as to give a plate load drop of 100 v as drawn and produce zero recorder signal. The effects of drift of photomultiplier-tube sensitivity and lamp output, as well as minor changes in efficiency of the optical system are therefore eliminated during each standby switching cycle.

A calibration compensating circuit similar to one used in the original circuit is incorporated in the plate circuit of $T_4$.

The theory and practice of the 6 density range circuit is discussed in some detail in the preceding paper (see page 97, this issue of *PS&E*).

### Recorder Modifications

For recording, a Minneapolis-Honeywell $\frac{1}{4}$-sec full-scale ink recorder was selected, although punched cards, electric typewriter or magnetic tape systems with suitable encoders could of course be substituted. With respect to the photomultiplier-amplifier and recorder, a chart drive speed corresponding to a 1-, $1\frac{1}{2}$-, or 2-sec cycle would be practical, but, as originally designed, simultaneous computer* considerations made it desirable to reduce this speed somewhat. A recent computer design improvement has removed this speed restriction entirely.

It is unfortunate that this type of recorder is intrinsically so sensitive because the photomultiplier amplifier itself provides a large power signal and the need to discard most of the available signal energy and then rebuild it to the point where it controls the

* By "simultaneous computer" we mean a computer which determines the test strip characteristics at the same time the curve is being plotted.

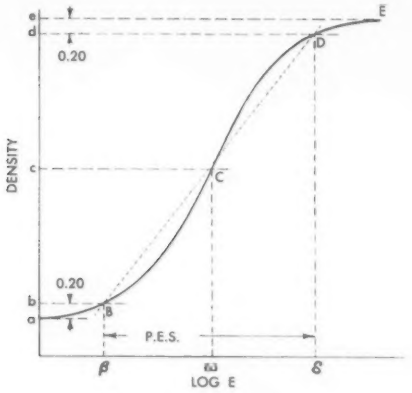


Fig. 8. D vs. log E curve.

relatively powerful balancing motor is a poor system feature. The recorder input is sensitive to stray signal and noise pickup. Careful shielding, grounding, and routing of the input cables are required. This requirement has been considerably minimized by simplifying and otherwise completely revising the slidewire potentiometer circuit of the recorder, reducing its sensitivity somewhat. These changes permitted the elimination of unnecessary thermal-compensating and span-compensating circuits.

The chart drive mechanism on the recorder was completely redesigned in order to provide a positive cycling operation through a Geneva movement and to provide a cam on one of the drive shafts to operate a microswitch which keeps the strip drive motor operating until the test strip has passed completely through the measuring head. Another cam-operated microswitch operates the automatic zero relay, opening the switch circuit during the recording phase of the operating cycle.

### Computer*

The present instrument was designed as a system, incorporating an analog computer in order to virtually eliminate subjective errors in test strip evaluation and to accelerate the evaluation process. A number of relatively sophisticated approaches were considered, but the advantages of simplicity, reliability, and versatility favored the present analog approach. Haloid Xerox is particularly interested in the parameters of photographic papers determined according to U.S. Air Force Specifications P 4672-A.

Figure 8 shows some of the cardinal points on the D vs. log E curve from which important sensitometric characteristic values are computed according to these Air Force specifications. Other characteristic values could, of course, be computed if desired. In the Air Force method, speed is measured in terms of the log E value, $\omega$, corresponding to point C, where C is the point on the curve whose density, $D_c$ is $\frac{1}{2}$ (D-min + D-max). The partial exposure scale is defined as log $E_\delta$ − log $E_\beta$ where $\beta$ corresponds to D-min + 0.2, and $\delta$ corresponds to D-max − 0.2.

To determine these values during the recording operation an arrangement is used whose principles are indicated in Fig. 9.

As the test strip progresses through the measuring head, potentiometers $P_1$ and $P_2$ are balanced so as to provide a voltage equal to the densitometer output signal voltage. Immediately after the strip enters the measuring beam, potentiometer $P_1$ is balanced, then its balancing motor is interrupted. The potentiometer output setting is therefore a measure of the minimum strip density (D-min). Potentiometer $P_2$ is connected in the circuit until just before the strip leaves the measuring aperture. At this instant, its balancing motor circuit is interrupted and its pick-off voltage is a measure of the maximum strip density (D-max).

Resistors $R_1$ and $R_2$ are of equal value and as drawn, voltage AC is a measure of $D_c$. The strip is now reinserted in the measuring head in the reverse direction but in this case the timer motor $M_3$ drives potentiometers $P_3$ and $P_4$, through clutches $K_1$, $K_2$ and the settings of $P_1$ and $P_2$ remain fixed. The clutch $K_1$ for $P_3$ engages immediately upon insertion of the strip and

* A number of additional refinements in the design and operation of the computer were in progress during the preparation of this paper. Therefore only the principles are described here, based on actual operation of the computer in its earlier form. Another paper describing the final design of the computer is planned for early publication.

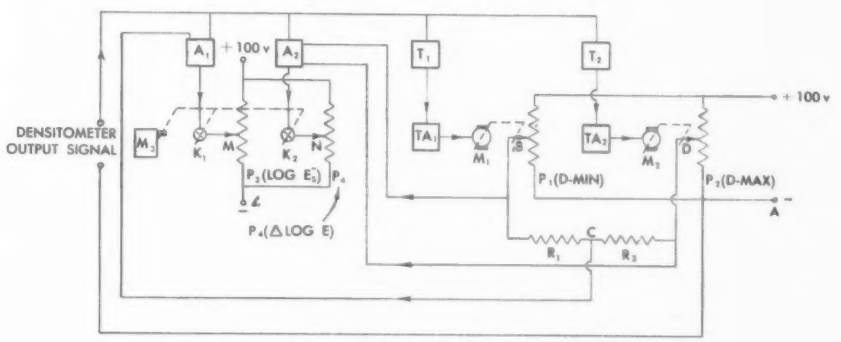


Fig. 9. Simplified schematic diagram of computer data recorder.

releases when the densitometer signal reaches a value equal to $\overline{AC}$, due to operation of trigger amplifier $A_1$. Therefore the setting of $P_3$ is a negative measure of speed in terms of log $E\omega$.

Clutch $K_2$ engages only after the densitometer output drops to a value equal to D-max − 0.2; i.e., when the signal voltage drops to $\overline{AD} - m$, where $m$ is a fixed voltage corresponding to 0.2 density; it releases when the signal drops to $\overline{AB} + m$, corresponding to D-min + 0.2. Therefore the setting of potentiometer $P_4$ is a measure of the partial exposure scale (P.E.S.).

From the data recorded on potentiometers $P_{1-4}$ the following sensitometric characteristics can be read directly or determined by further computation.

1. D-min
2. D-max
3. Density range
4. Speed
5. Partial exposure scale
6. Gradation

From the outset, it was planned to display the four most important sensitometric characteristics in digital form immediately above the recorder shown in Fig. 2, or, if desired, to print the values on tape or card printers.

In the interim device, a single digital reader of the type discussed in the earlier paper has been used to display the computed data. A multitap switch serves to select the values desired and these are noted in turn.

As mentioned earlier, the original computer concept involved the use of stepper relays and the recorder speed was restricted to accommodate the relays. In the present design there is no such restriction and the speed could be increased to a ½-sec cycle or faster if the obvious mechanical modifications were made and if the chart recorder performance were ignored.

Furthermore, the need for two strip runs, as described above, is circumvented by exposing a D-max section of the test strip along the leading edge and rearranging the circuits accordingly.

## Calibration

Both the transmission and the reflection systems conform with American Standard requirements. However, the response of the photomultiplier tube to incident flux is nonlinear and must be calibrated by suitable techniques.

It is the authors' view that the calibration of any densitometer can be guaranteed only by obtaining agreement with specimens whose density values are accurately known from fundamental measurements, i.e., through the use of inverse square-law techniques or other techniques of equal rigor. Therefore, the calibration of the instrument is obtained by bringing the recorder readings into agreement with fundamentally derived values of step-wedges. At the same time, the response of the recorder to neutral densities located in the filter wheel are noted. Thereafter, for the purposes of routine calibration, it is only necessary to check the response of the recorder to the neutral densities of the filter wheel.

## Performance

The instrument has been in virtually continuous operation for one and a half years and the improved features have proven their merits. In addition to ease and speed of operation, high accuracy was of course sought. The stability of the instrument is demonstrated by the following experiment. After the instrument was turned off for 15 hours, a series of recordings were made at geometrically progressive time intervals. The experimental test sample was a dual density level reflection strip. At each time interval, two recordings were made from the test strip. After 45 sec, the zero and sensitivity adjustments were made. After 1 min, the strip having a density of about 1.40 was run through twice. After 2 min, this procedure was repeated. After 4 min, it was repeated again. After 7½ min, the zero and the sensitivity adjustments were rechecked, but the only change necessary was to reduce the sensitivity by 0.01 density when reading the 1.0 density reference filter. No further adjustments were made during the test. The density characteristics of the strip were recorded again at 8, 16, 32, 64, 128, and 256 min. After the 64-min recording and between each two of the subsequent cycles, a number of normal daily samples were recorded.

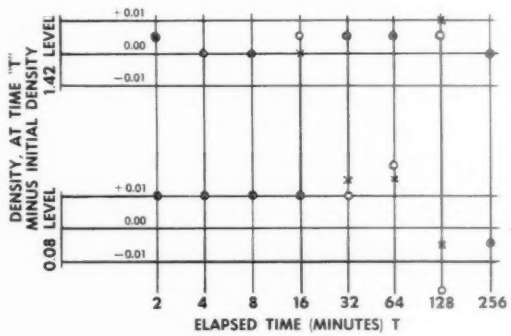


Fig. 10. Density difference vs. operating time.

The data are plotted in Fig. 10. Note that the average deviation from the initial recordings at the 1.4 density level is considerably less than 0.005 density. We attribute the fact that the lower density sample showed much larger deviations after the second 64-min recording to the accumulation of sample defects during the test.* Even so, for the eleven pre-

* Since, in the vicinity of 0.00 density, the instrument operates as an optical null device and variations in amplifier and recorder gain have negligible effect on the results. Furthermore, any shifts in the zero reference beam would have upset the 1.4 density readings equally.

ceding readings, the average deviation was essentially zero.

## Summary

The Quantascan Automatic Recording and Analyzing Densitometer plots the reflection or transmission densities of unmounted sensitometric strips rapidly and automatically on a linear 3 or 6 density scale. The instrument is more stable than ordinary photomultiplier instruments, and the geometry of both the transmission and the reflection optical systems conform closely with American Standard requirements. Computers attached to the basic instrument enable selected sensitometric characteristic values to be read immediately upon completion of the scanning cycle. Because of its intrinsically high sensitivity and stability, the densitometer is also suited for color densitometry and small aperture densitometry.

## Acknowledgments

The development work on this equipment was performed by Quantametric Devices, Inc., with the technical and financial assistance of Haloid Xerox. Special acknowledgment is due James H. Casterlin of Quantametric Devices, Inc., for the many ingenious mechanical features incorporated in this instrument.

## References

1. Sweet, Monroe H., *Electronics, 19:* No. 11, p. 105 (1946).
2. ———, *J. Soc. Mot. Pic. TV Engrs., 54:* 35 (1950).

PHOTOGRAPHIC SCIENCE AND ENGINEERING
Volume 3, Number 3, May-June 1959

# A New Method for Evaluating Sensitometric D-Log E Curves

W. H. CARNAHAN, *Paper Service Division, Eastman Kodak Company, Rochester, N.Y.*

**The calculation of meaningful parameters from sensitometric curves has been one of the main problems in sensitometry. A method is presented whereby a given sensitometric curve is described as a modification of a universal standard curve. The method has been applied primarily to papers. In general, three quantities are expressed: speed, grade number, and maximum density, each of which is based on the characteristics of the whole curve. The standard curve on glass is placed in a parallel beam of light. The curve is rotatable about the ordinate through the midpoint. The image is projected onto the curve to be evaluated. The latter is rotatable about an axis passing through the zero density abscissa. Rotation of the standard compresses or expands the projected log exposure scale. Rotation of the curve to be evaluated changes the apparent slope of the projected curve by altering all densities proportionally. With these two movements it is possible to match the curve shape of the standard to the curve to be evaluated. Lateral movement of the curve measures speed. Graphical methods instead of optical projection are also possible. Examples are given of the range of curve shapes which can be evaluated.**

The large number of requirements for photographic products today has resulted in the manufacture of a correspondingly wide number of photographic products. One of the standard methods of expressing the characteristics of papers and films is in terms of the characteristic curve. Such a curve tells the quality control man the amount of density which is produced by any and all degrees of exposure. Elaborate precautions are taken to standardize the conditions of exposing and processing and the densitometry of the test samples, because all these variables are known to influence the characteristics. The characteristic curve contains practically all the necessary information concerning factors which influence photographic quality, but not in a form convenient to use for control purposes. For control, one needs numbers which can be tabulated, averaged, plotted, etc. Thus the problem becomes one of evaluating the characteristic curve to determine speed, contrast, etc., quantitatively. Many methods have been suggested for doing this. All have merit, but the chief difficulty of most previous methods is that they emphasize only a portion of the curve. There is a need for a system of evaluation that will be responsive to as much of the curve as possible. One solution that appears in the literature is that of Morrison, who describes a method of simulating the D-log E curve shape by a metal strip bent according to stated parameters.[1]

The problem is complicated by the large number of different kinds of curves to be evaluated. Some typical characteristic curves of photographic papers are shown in Fig. 1. Obviously they differ in several ways from each other — some are higher, some lower, some flat, some steep, and a few (the reversal papers) are backwards from the rest.

One of the requirements of a system for evaluating curves for test purposes is that it be simple to apply in a production test situation and meaningful to those responsible for quality control.

Recently an optical projection method has been developed to aid in the evaluation of characteristic curves and to furnish the type of information which can be derived mathematically by the use of vector parameters.[2] The principle of operation of this de-

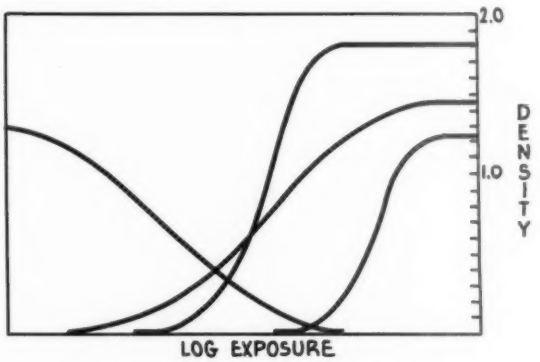


Fig. 1. Characteristic curves of papers of various types.

Presented at the Annual Conference, Rochester, N.Y., 8 October 1958. Received 19 November 1958.

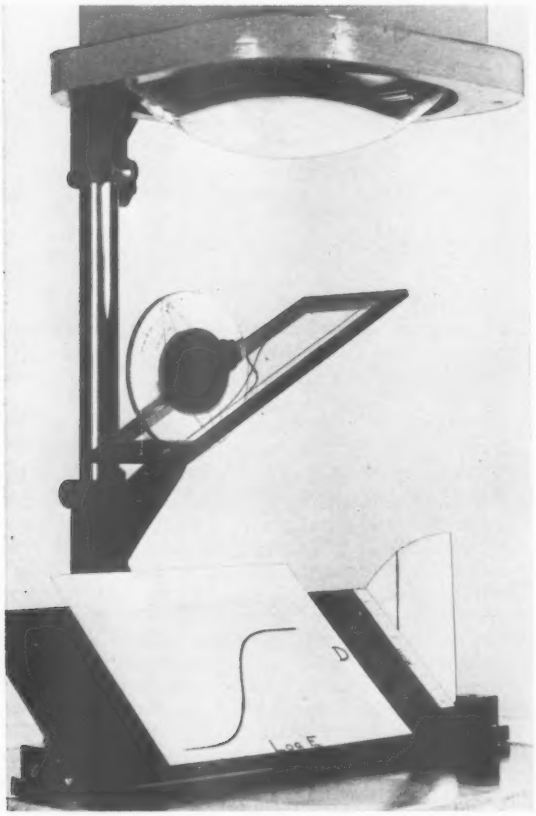

Fig. 2. Projector for evaluating D-log E curves.

vice (Fig. 2) can be simply described. A lens projects a parallel beam of light onto the curve to be evaluated. In the beam is placed a transparency containing a master curve. By rotating the master curve, its projected image can be expanded or shrunk in one direction (horizontally). By adjusting the angle of the graph easel, the curve can be expanded or contracted in the other direction. Lateral movement of the graph sheet may be required to bring the projected image of the master curve into coincidence with the graph to be evaluated.

The curve is placed in the projector so that the midpoint is on the axis of rotation of the master. The

TABLE I

| Grade Number | Log ES |
|---|---|
| 6.0 | 0.37 |
| 5.0 | 0.45 |
| 4.0 | 0.56 |
| 3.0 | 0.69 |
| 2.0 | 0.84 |
| 1.0 | 1.02 |
| 0.0 | 1.25 |
| −1.0 | 1.54 |

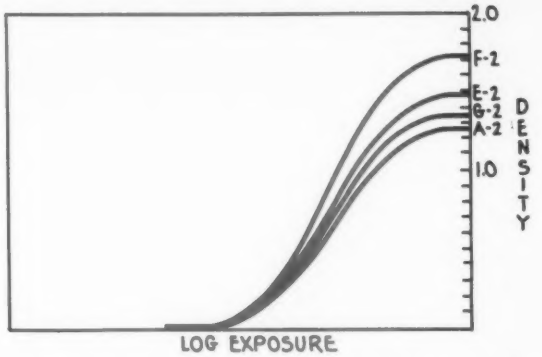


Fig. 3. Characteristic curves for papers of different surfaces but of the same grade number.

zero density ordinate of the graph to be evaluated must be exactly in the axis of rotation of the easel. The grade number scale is calibrated from the projected image of two points on the master curve, one of which is at 0.1 maximum density, the other at 0.9 maximum density. The log exposure scale (Log ES) between these two points can be checked and the linear relationship between log exposure scale and grade number used (see Table I). Maximum density is read from a scale attached to the easel.

The above relationship between Log ES and Grade Number is one which has been used for several years within the Paper Service Division of the Eastman Kodak Company for production release testing. It was originally derived empirically from measurements made on the D-log E curves of all Kodak papers of the same nominal grade number and whatever surface.

It was surprising as well as gratifying to the designers of this equipment to find how closely this one master curve could be made to simulate the characteristics of a wide variety of characteristic curves. The original intent was to use a variety of masters of basically different characteristics for various classes of photographic products. This solution is, of course, still available at some sacrifice in simplicity. Even the reversal curves can be matched by simply rotating the master curve to the other side.

Papers of different surface characteristics but the same grade number produce curves like those shown in Fig. 3. These represent a family of surfaces of Kodabromide Grade 2. Analysis of these curves with the optical projector shows that the principal difference is one of proportionality in the vertical direction. One might say that the curves have the same basic shape but differ chiefly in one parameter. For convenience we refer to this as the D-max parameter, even though the surface characteristics influence all of the curve, not simply the maximum density. This can be thought of as a new definition of Equivalent D-max, based on the characteristics of the curve as a whole rather than on the highest density only. This new definition will be identical with the conventional one for D-max when the curve shape of the projected image coincides with that of the actual

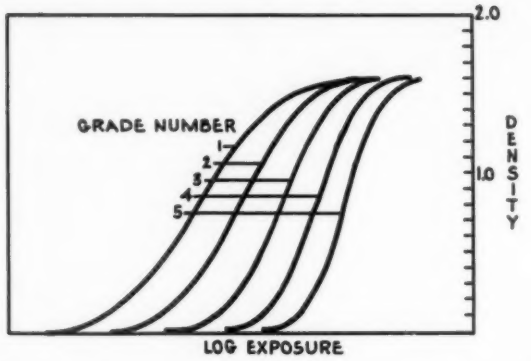


Fig. 4. Characteristic curves for papers of the same surface, but of different contrast grades.

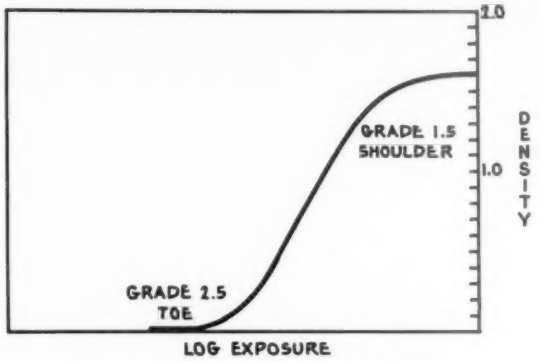


Fig. 5. Curve for paper of abnormal characteristics.

curve. When they do not coincide, the new definition has some advantage over the old in that it is based on the characteristics of the curve as a whole and not on the highest density only, which is usually not reached in the printing of negatives.[3]

Papers of the same surface, but differing in contrast grade number, produce curves like those in Fig. 4. The horizontal separation between the curves is indicative of speed difference. The difference in contrast grade number is indicated by the steeper slope of the high contrast papers. Adjustment of the angle of the master curve is all that is required to match the curves in this example. The scale on the master curve can be calibrated in terms of grade number. Characteristic curves selected at random will normally differ from each other in both D-max and Grade Number. In fact, these two modes of variation separately control the visual impression of contrast.

The speed determination made in this way has the advantage of basing speed on the characteristics of the whole curve, thereby avoiding the old argument as to whether speed should be based on toe, shoulder, middle densities, highlights, etc.

This optical projection method has been applied to a large number of characteristic curves of papers of various manufacturers, and works in many cases using only the three adjustments described. However, even in cases where it is not possible to match the curve exactly, further valuable information can be derived. In the first place, the very fact that a given paper has characteristics which cannot be matched by this master curve, while most papers can, is an indication that this is a paper of unusual curve-shape characteristics, such as in Fig. 5. No setting of the three controls will make the projected image match the curve shape. However, it is possible to form an independent match of the upper and lower halves of the curve and report a contrast independently for the two halves. We would say that this paper has a D-max of 1.6, a toe of Grade Number 2.5, and a shoulder of Grade Number 1.5.

Some curves are found which cannot be matched even by this method. In cases where the projected image is not identical with the curve to be evaluated, and yet the difference is judged by the quality control engineer to be unimportant, it is proposed that, for control purposes, the recorded parameters be those of the projected image. This procedure obviously is not completely objective, relying as it does on the experience of the quality control engineer to decide when the match is close enough for practical purposes. It may be found desirable to establish control limits about the master curve. In other words, for control purposes, a curve will be described by the parameters of the projected master curve which best matches the real curve, even though the match is not perfect.

The characteristics of the master curve were determined originally by averaging the standard character-

TABLE II
Definition of Master Curves

| Log E | Curve No. 1 Density | Curve No. 2 Density |
|---|---|---|
| 0.00 | 1.00 | 1.00 |
| 0.10 | 1.00 | 1.00 |
| 0.20 | 1.00 | 1.00 |
| 0.30 | 1.00 | 0.99 |
| 0.40 | 1.00 | 0.98 |
| 0.50 | 1.00 | 0.965 |
| 0.60 | 1.00 | 0.945 |
| 0.70 | 1.00 | 0.915 |
| 0.80 | 0.99 | 0.88 |
| 0.90 | 0.98 | 0.835 |
| 1.00 | 0.945 | 0.78 |
| 1.10 | 0.88 | 0.71 |
| 1.20 | 0.78 | 0.64 |
| 1.30 | 0.64 | 0.57 |
| 1.40 | 0.50 | 0.50 |
| 1.50 | 0.365 | 0.44 |
| 1.60 | 0.25 | 0.37 |
| 1.70 | 0.145 | 0.31 |
| 1.80 | 0.075 | 0.245 |
| 1.90 | 0.03 | 0.195 |
| 2.00 | 0.01 | 0.15 |
| 2.10 | 0.00 | 0.105 |
| 2.20 | 0.00 | 0.08 |
| 2.30 | 0.00 | 0.055 |
| 2.40 | 0.00 | 0.04 |
| 2.50 | 0.00 | 0.02 |
| 2.60 | 0.00 | 0.01 |
| 2.70 | 0.00 | 0.00 |

istic curves of all types of Kodak papers, averaging density values at selected Log E positions. The resulting average curve was then ratioed to a D-max of 1.0, because the adjustment of the easel can increase the D-max but not reduce it. A second curve can be added to facilitate measuring high contrast materials. This curve is the same as the first, but multiplied by a constant factor in the Log E direction so the master transparency does not have to be tipped at such a great angle. The master curve was then adjusted empirically after comparing the projected image with each individual standard curve.

Anyone wishing to experiment along this line will find the characteristics of our master curves useful. They may be described from the data in Table II giving the densities at 0.10 Log E intervals on the master curves.

This method of evaluation has a number of advantages which we hope are obvious from what has been said so far. In addition, some other advantages are that a testing laboratory can evaluate a characteristic curve by this means, then communicate the resulting three settings to other interested parties at remote locations. If the latter have a similar optical projector, they can adjust their projector and immediately see the curve shape of the material under consideration. Another advantage of this method is that one can quickly observe whether the differences between two materials are the result of proportional D-max variation or of variation in the log exposure scale, that is grade number, direction. If the variation is one of Grade Number rather than D-max, the implication is that the materials were designed for use with negatives of different density scales.

## References

1. Morrison, C. A., *J. Franklin Inst.*, 243: 55 (1947).
2. Bayer, B. E., Simonds, J. L., and Williams, F. C., "Vector Parameters: A New System for Sensitometric Comparison of Related Emulsion Coatings," presented at the Annual Conference of the SPSE, Rochester, N.Y., Oct. 8, 1958. (To be published in *P S & E.*)
3. Jones, L. A., and Nelson, C. N., *J. Opt. Soc. Am.*, 32: 558 (1942).

PHOTOGRAPHIC SCIENCE AND ENGINEERING
Volume 3, Number 3, May-June 1959

# Some Observations on the Reproduction of Flesh Colors

C. J. BARTLESON, *Research Laboratories, Eastman Kodak Company, Rochester, N.Y.*

**The colors of a limited number of optimum or preferred pictorial reproductions of flesh colors are found to be significantly different from the actual color of average natural flesh, but have essentially the same hues and saturations as the mean abstract memory-color for flesh.**

In theoretical discussions of the quality of photographic color reproduction, it is frequently assumed that the objective of the photographic process is to reproduce exactly the chromaticities of the original objects. This assumption most often has been made because of the lack of experimental evidence to the contrary. It has often been recognized that chromatic fidelity may not be necessary or even desirable, but no quantitative evidence can be called upon to supply an adequate alternate objective.

Some consideration has been given to this problem as it relates to the reproduction of flesh colors. W. R. J. Brown measured twenty-five reproductions which were considered to be excellent representations of flesh and found that their chromaticities were significantly different from those of natural flesh.[1] These included oil paintings, pastel chalk drawings, Carbro prints, Kodak Flexichrome Prints, and Kodak Dye Transfer Prints. Three of these media offered the possibility of controlling all chromaticities, including those of flesh areas, independently, which would imply that limitations inherent in any given process were not necessarily highly influential in the choice of the resultant chromaticities. MacAdam has reported similar work with comparable results.[2]

These investigations indicated that the preferred reproduction colors for flesh tended to be somewhat warmer or yellower than the colors of actual flesh.

It is perhaps significant that two investigations in which the abstract memory-colors for flesh were determined indicate a mean memory-color also significantly more yellow than natural flesh.[3,4] The mean memory-color determined by Bartleson[4] is compared with the chromaticity of average natural flesh (from Buck and Froelich[5]) in Fig. 1. Examination of the variability of judgments and the MacAdam color-matching ellipses[6] about these points indicate that the actual color and the memory-color are significantly different in chromaticity. The vector distance between the two means is approximately equal to $16\frac{1}{2}$ chromaticity JND's, according to the MacAdam ellipses.

Color photographs typically are not compared directly with original scenes, especially in amateur photography. Instead, the photographer must rely on his memory of the colors of objects in the original scene. Apparently, most people have rather consistent memory references or memory-colors for objects or substances with which they have frequent visual experiences. Flesh or, more precisely, complexions certainly constitute a familiar object-color category. It would seem that if the reproduction is not to conflict with one's memory, it should agree reasonably well with the memory-color.

The present experiment was designed to determine the relationship of flesh-reproduction chromaticities to the memory-color chromaticities, and to previous measurements of optimum reproduction chromaticities, when observers are allowed to choose among a series of prints in which only the flesh colors are systematically varied.

## Procedure

Since the chromaticity of flesh areas only was to be varied, it was necessary to choose a reproduction process in which such singular variations could be effected. For this reason, the Kodak Flexichrome Process was chosen as a means for producing sample prints. The subject matter of the prints was chosen to represent as simple a configural pattern as possible. A reproduction of the subject is shown in Fig. 2.

Twelve 4 × 5-in. prints were produced in which the chromaticities of the flesh areas were systematically varied around and between the chromaticities for average natural flesh and the corresponding mean memory-color. Figure 3 shows the relationship of a 52% luminous reflectance area on each print to the natural and the memory-color. The co-ordinates are those of MacAdam's $u$, $v$ transform[7] from the CIE system. The $u$, $v$ diagram is a more nearly uniform chromaticity metric than the usual CIE chromaticity diagram and therefore presents a somewhat better

Communication No. 1993 from the Kodak Research Laboratories. Received 25 November 1958.

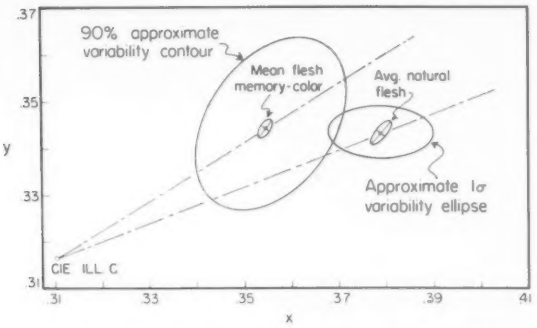


**Fig. 1. CIE Chromaticity co-ordinates of natural and memory-color flesh. Small ellipses are for color-matching variability after the method of MacAdam.**

graphical representation of the visual differences between sample prints.

The prints were viewed in a $2\frac{1}{2} \times 4 \times 4$-ft viewing booth with neutral gray walls of approximately 18% reflectance. A simulated daylight illuminant which would affect appearance specifications in essentially the same manner as CIE Illuminant C supplied approximately 100 ft-c at the viewing plane.

Ten observers were used; each had moderate to advanced technical knowledge of color photography.

Each of the observers performed 51 paired comparisons, representing an incomplete comparison block. They were asked to indicate which print of each pair they preferred. After the paired comparison evaluations were completed, each observer was shown one print at a time, in random order, and asked to indicate whether or not he considered the print "acceptable." Acceptability was defined as that condition in which the observer evidenced no displeasure when evaluating the reproduction.

## Results

The preference and acceptability data were analyzed after the manner of Guilford.[8] This data reduction located the prints along a scale of relative quality, but did not indicate absolute quality or acceptability. Acceptability values were generated by combining the relative quality figures with data from the acceptance judgments; a linear transformation* from the relative quality to acceptability was established. The response scale thus established passes from positive to negative through zero as the prints become generally unacceptable, with zero representing the psychological level of indifference. The response ratings for each of the chromaticity points are shown in Fig. 3.

Seven of the prints may be considered to have chromaticities that lie essentially along a line joining average natural flesh and average memory-color flesh in the $u$, $v$ diagram. Their departures from this line are indicated by the darkened areas in Fig. 3. It will be noted that the other five prints, lying at some distance from this vector, all have response ratings less than zero. The response ratings for the seven prints along the noted vector are plotted against relative vectorial location in Fig. 4. Those prints having chromaticities closest to the memory-color received the highest ratings.

The chromaticity of a 52% luminous reflectance area in the most highly preferred print is very close to that of Bartleson's mean memory-color which has a luminous reflectance of 57%. The CIE chromaticity co-ordinates for the print were $x = 0.3558$, $y = 0.3440$, and the memory-color co-ordinates were $x = 0.3548$, $y = 0.3441$. However, the mean memory-color is uniform while areas of flesh reproduction in the print vary in luminance. Actually, the mean luminous reflectance of complexion areas in the print was approximately 30%. The chromaticity co-ordinates for a flesh area of 30% reflectance in this print were computed to be approximately $x = 0.3700$, $y = 0.3600$. The difference in chromaticities arises from the fact that when dye concentrations vary in the print, both luminance and purity vary together.

In the chromaticity diagram of Fig. 5, then, point $d$ represents the average color of the best print in the series and its chromaticity co-ordinates are located at some distance from those of the mean memory-color. This figure illustrates the chromaticity relationships between average natural flesh and both

**Fig. 2. Illustration of subject matter used in sample prints.**

* of the form $y = ax + b$, where $a = 1$, and $y$ and $x$ are normal deviates.

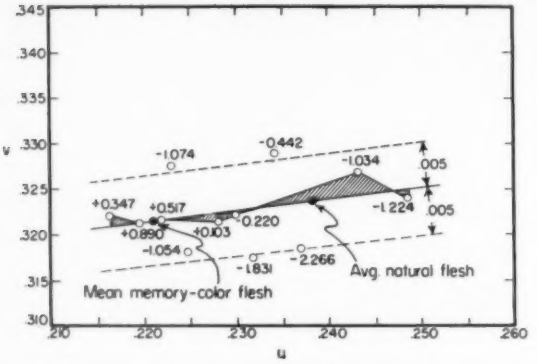


Fig. 3. Chromaticity co-ordinates of 52% luminous reflectance areas in Flexichrome prints used for judgments; shown in MacAdam's u, v diagram (approximately uniform chromaticity). Acceptability ratings are shown for each point.

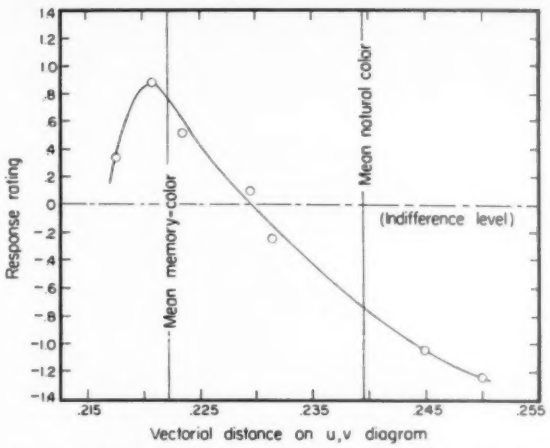


Fig. 4. Relative response ratings for prints having chromaticity co-ordinates closest to the vector connecting memory and natural flesh-colors in MacAdam's u, v diagram.

Newhall and Pugh's[3] and Bartleson's[4] mean memory-colors for flesh. In addition, points corresponding to the average of Brown's[1] optimum reproduction data and Buck and Froelich's[5] measurements of the chromaticities of photographic and photomechanical flesh reproductions are shown. The values of *Y* for each of these points are listed in the figure.

It will be noted that the chromaticities of the reproduction colors (*a*, *b*, *c*, and *d*) all lie at some distance from those of the two memory-color determinations (1 and 2). However, the dominant wavelengths and purities derived from CIE chromaticity points corresponding to colors of widely dissimilar reflectances do not correlate well with the visual attributes of hue and saturation. The relationship of hues and saturations of the points in Fig. 5 may be estimated more easily by reference to appearance specification data where it will be seen that the actual hues and saturations of these points are more similar than might be inferred from the CIE co-ordinates of Fig. 5.

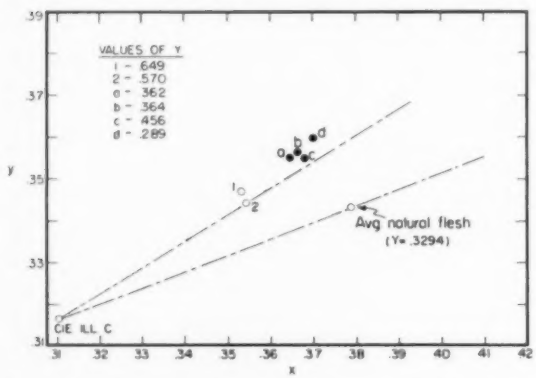


Fig. 5. Relationship of memory, natural, and reproduction flesh-colors in CIE diagram.
(1) Mean flesh memory-color according to Newhall
(2) Mean flesh memory-color according to Bartleson
(a) Mean forehead chromaticity of Brown's reproductions
(b) Mean chromaticity of Buck and Froelich's photographic reproductions
(c) Mean chromaticity of Buck and Froelich's photomechanical reproductions
(d) Mean chromaticity of preferred print in present investigation

Hue and saturation, considered without regard to the intensity of the stimulus, are referred to as the "chromaticness" of a color. Figure 6 shows a locus of constant chromaticness in the region of the color space corresponding to the reproduced and the memory flesh colors. The CIE specification for the mean memory-color is shown as a solid circle, and the open circle is the specification for the preferred reproduction-color. It may be seen that both these points fall on the same chromaticness locus.

The relationship of chromaticness for all the flesh reproductions, as well as the natural and memory-colors of Fig. 5, is illustrated in Fig. 7. The co-ordinates of Fig. 7 are those of the Munsell notation which is essentially a uniform visual metric. Therefore, identical chromaticnesses will be coincident in such a graph. In Fig. 7, the points for Bartleson's mean memory-color and the optimum print determined in the present experiment are coincident; they are therefore of the same chromaticness.

## Conclusions

There is some evidence that preferred flesh-reproductions may be of virtually the same hue and saturation (*vide*, chromaticness, above) as the abstract memory-color for flesh and, futher, that the reproduction preference tends to be more yellow than actual flesh. However, these conclusions should be considered qualitative rather than quantitative. The data on which they are based are rather limited. In the case of the present experiment, for example,

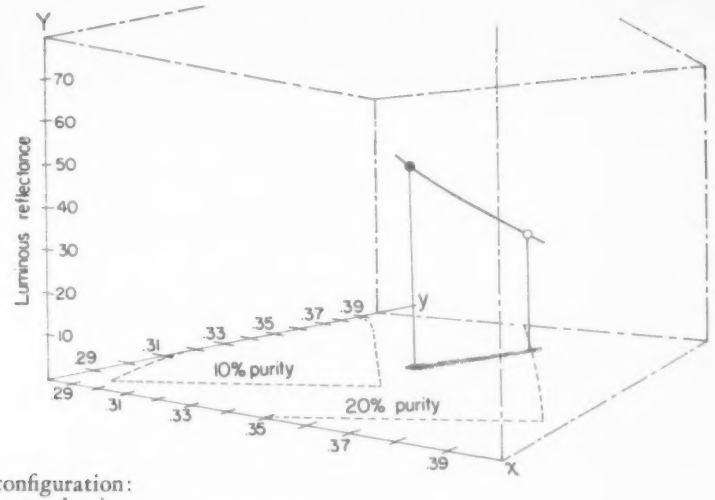


Fig. 6. Locus of chromaticity specifications for constant chromaticness in flesh-color region as it appears in CIE coordinate space. It may be seen that the locus of constant chromaticness represents the function of purity vs. luminance for which saturation remains constant.

there was only one very simple image configuration: a simple portrait. Undoubtedly, more complex images, smaller areas of flesh, variations in viewing and adaptation conditions, and variations in the luminances and chromaticities of surrounding image areas, to name only a few factors, will exhibit an influence on the choice of optimum flesh reproduction.

Within the limitations of the present experiment, then, it seems significant that the average chromaticnesses of preferred flesh-reproductions are essentially equal to those of two independent determinations of the mean flesh memory-color. For the present, this is an encouraging suggestion that there may be some general, systematic relationships between object-colors and their preferred reproductions which ultimately may lead to a sensible psychophysical method of evaluating the quality of color reproduction.

## References


1. Given in MacAdam, D. L., *Proc. IRE, 42:* 166 (1954).
2. MacAdam, D. L., *J. Soc. Mot. Pic. TV Engrs., 56:* 487 (1951).
3. Newhall, S. M., Burnham, R. W., and Clark, J. R., *J. Opt. Soc. Am., 47:* 43 (1957) (Supplementary Experiment 3 by Newhall and Pugh).
4. Bartleson, C. J. (to be published).
5. Buck, G. B., and Froelich, H. C., *Illum. Eng., 43:* 27 (1948).
6. MacAdam, D. L., *J. Opt. Soc. Am., 33:* 18 (1943).
7. *Ibid., 27:* 294 (1937).
8. Guilford, J. P., *Psychometric Methods*, 2nd ed., McGraw-Hill Book Co., New York, 1954, Chap. 7.


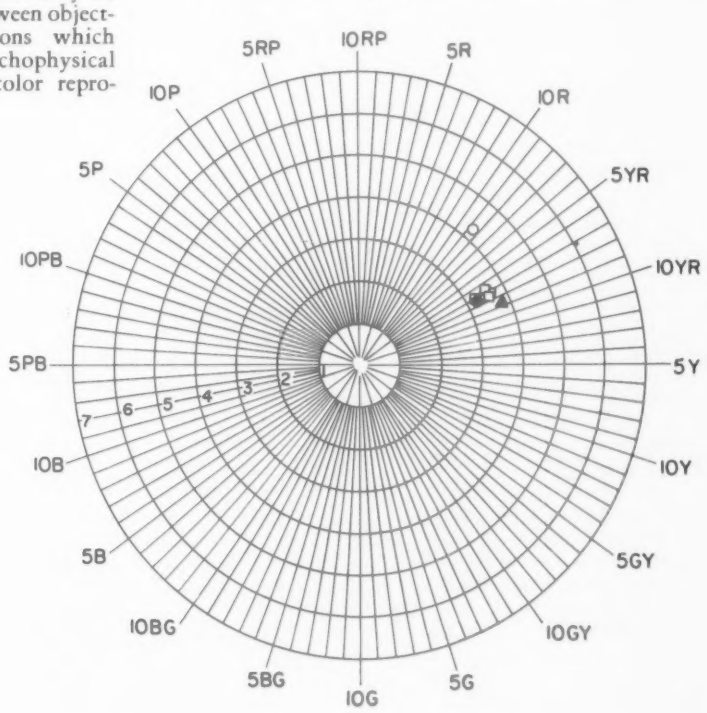


Fig. 7. Chromaticness of average natural flesh, memory-color flesh, and several reproductions of flesh (shown in Munsell coordinates).
Open circle (○), natural color
Closed circle (●), Bartleson's memory-color
Closed triangle (▲), Newhall's memory-color
Squares (□), reproductions of Fig. 5

PHOTOGRAPHIC SCIENCE AND ENGINEERING
Volume 3, Number 3, May-June 1959

# Image Illuminance Levels in Night Photography

WILLIAM G. CIBULA, *Task Engineer, WCLRDS, Aerial Reconnaissance Laboratory, Wright Air Development Center, Wright-Patterson Air Force Base, Ohio*

**Factors which determine the image illuminance levels for night photography under various ambient conditions are discussed. Incident light levels alone are not sufficient to determine the amplification required at the plane of the photoamplifier. Scene brightness, lens aperture, haze, and lens flare factor must also be considered. Typical values of exposure input in meter-candle-seconds are computed for several scene types at f/1.0 and an exposure of 0.2 sec.**

Much interest is being shown in the development of light amplifiers for low-light-level photography. If an amplifier is to be used for night photography, it must amplify the imaged light which falls upon it to a level which is capable of producing usable exposures on today's photographic emulsions. This paper will attempt to give an approximation of the image illuminances that can be expected under various night ambient conditions.

A good approximation of the image illuminance at a point in the focal plane of a lens system can be obtained through a consideration of the following:

1. Incident light falling upon the scene
2. Scene brightness
3. Haze
4. The relationship between object luminance and the corresponding image illuminance as a function of the aperture (*f*/stop) of the lens.
5. The flare factor of the lens and its effect in modifying the theoretical values for image illuminance computed in No. 4 above.

## Incident Illumination

The ambient light present at night is open to much more variation than is found in daylight. Under clear conditions, the major factor affecting the illumination on a given scene in daylight is the altitude of the sun above the horizon. An additional factor arises when moonlight is considered. This is the phase angle of the moon. A full moon has a phase angle of 0°, while a new moon has a phase angle of 180°. A phase angle of 90° represents either the first or last quarter.

It would seem on first thought that the incident light received from the moon in either the first quarter or the last quarter would be one-half that received from full moon. Actually, the incident illumination is only one-ninth that of a full moon. This results from the position of the moon relative to the sun and earth, which causes shadows from both mountains and pebbles, obscuring areas which are in full sunlight when the moon is full. As a result of this rapid reduction in light on either side of the full moon, the illumination changes markedly from night to night. The maximum light received (with the moon 90° above the horizon) would be:

| | | |
|---|---|---|
| Full moon | Phase Angle = | 0° is $3.5 \times 10^{-2}$ ft-c |
| ±1 day | = | ±12° is $2.63 \times 10^{-2}$ ft-c |
| ±2 days | = | ±24° is $1.86 \times 10^{-2}$ ft-c |
| ±3 days | = | ±37° is $1.5 \times 10^{-2}$ ft-c |
| ±7 days | = | ±85° is $3.85 \times 10^{-3}$ ft-c |

In addition to the variation as a result of phase angle, there is also an hour-to-hour variation resulting from the change in lunar angle with respect to the horizon. This function of altitude is the same as that for sunlight, and results from the moon's light traversing more of the earth's atmosphere as it approaches the horizon. Figure 1 shows this variation of illumination for various phase angles versus altitude of the moon.

The curves in Figs. 1 and 2 show the change in intensity of moonlight on a plane normal to the incident radiation as the moon's elevation changes. There are several reasons for using this particular orientation of measurement rather than some other in this paper. Jones and Condit[1a] have shown that the concept of the volume density of luminous energy (therein denoted by $V_t$ representing the total amount, with $V_d$ as the contribution from sunlight and $V_s$ as the contribution from skylight) gives a more reliable measure of minimum scene luminance than other methods of incident light measurement. A comparison of their data for $V_t$ as a function of solar altitude shows that its dependence upon solar elevation is of the same form as the variation in intensity for sunlight normal to a plane when measured in the same manner. Also, the ratio $V_d/V_s$ is constant except for very low elevations.

From measurements made of scene luminances from a large number of outdoor scenes,[2] several scene groups were obtained. For the groups that were in sunlight, a ratio of the luminances of each point in the scene

Presented at the Annual Conference, Rochester, N.Y., 8 October 1958. Received 15 October 1958.

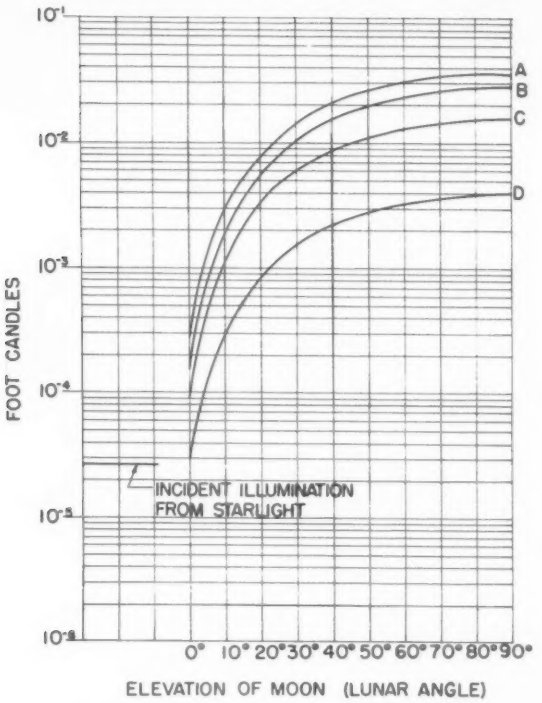


Fig. 1. Incident illumination from the moon for its various phase angles. The intensity is measured on a plane perpendicular to the direction of light. The abscissa shows the relationship of incident light for the elevation of the moon at several of its phases.

In the figure —

A — full moon, phase angle 0°

B — intensity one day before or after full moon, phase angle ±12°

C — three days before or after full moon, phase angle ±37°

D — one week before or after moon is full. Here the moon is in first or last quarter; the corresponding phase angle is ±85°

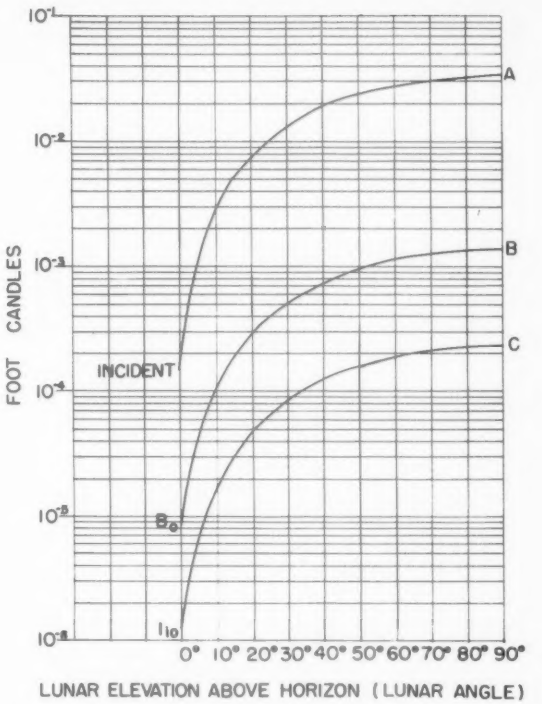


Fig. 2. Relationship between incident illumination, average scene brightness, and image illuminance from an average landscape for an f/1.0 lens under a full moon as a function of the moon's elevation above the horizon (perpendicular to direction of radiation).

A — incident illumination from the full moon as a function of moon's elevation above horizon.

B — incident illumination from an average moonlighted landscape as a function of the moon's elevation.

C — illumination present from an average landscape under a full moon at film plane for an f/1.0 lens.

when compared with incident sunlight could be obtained.

Since moonlight is not radically different from sunlight in spectral quality[3] it would seem reasonable that the same relationship between scene elements would hold under moonlight as under sunlight if the moon were in the same position in the sky as was the sun when the measurements were taken. Data collected by the author show that the ratio of scene luminances from various scene elements agrees well with the ratio between the same scene elements when the scene is in full sunlight. On the basis of these criteria, then, the measurement of moonlight on a normal plane will give a good approximation of actual values encountered when this value is multiplied by the appropriate ratio between corresponding scene brightness and the incident light present.

The lowest level of incident illumination possible on a clear moonless night is that which comes from starlight alone. It is approximately $2.8 \times 10^{-5}$ ft-c.[4]

## Scene Brightness

This will vary considerably from point to point in a scene and also from scene to scene. An average landscape (with no snow or other large areas of highly reflective materials) illuminated by a point source (sun or moon) will have an average reflectance of 4%. This percentage represents the average light entering an optical system from the scene.

For purposes of this discussion, we will consider scenes of two types, representing two different conditions that may be expected in night aerial photography. Other types may be encountered in practice, but it is felt that these will fall, in most cases, between the two described here. One represents a winter landscape condition and the other a summer landscape condition. It must be remembered that the moon does not approach a 90° elevation in the temperate latitudes during the summer months. The moon is at zenith in the tropics at least once during the year, and excepting for areas near either the Tropic of Cancer

or Tropic of Capricorn, overhead twice during the year.

#### *Type I — Snow Covered Landscapes*

This type will probably be the most commonly encountered when reconnaissance missions are made at night in the polar regions. Under a full moon the maximum brightness will be snow illuminated by the moon 50° to 60° above the horizon. The minimum brightness will probably be from shadow areas or small objects which are not snow covered. The over-all average illumination will be closer to the upper limit of the brightness scale than to the lower limit. Where $I$ is the incident illumination and $B_0$ is the scene luminance, we can write:

$$B_0\text{max} = 0.6 \times I$$
$$B_0\text{av} = 0.2 \times I$$
$$B_0\text{min} = 0.04 \times I$$

#### *Type II — Summer Landscapes*

Here the over-all reflectance is much lower than in Type I. The highest reflectance will probably be from light-colored wood, sand, concrete, etc. The average reflectance will be from foliage, grass, and earth. The areas of least reflectance will be represented by deep shadows. For this type of scene then:

$$B_0\text{max} = 0.45 \times I$$
$$B_0\text{av} = 0.4 \times I$$
$$B_0\text{min} = 0.006 \times I$$

This will correspond to scenes in Group I of Mees.[2] Values for $B_0$av under full-moon conditions are shown in Fig. 2.

Illumination from starlight will correspond to a heavy overcast condition when brightness ranges are considered. Unlike the previous case, where most of the light flux came from a point source, the incident illumination from starlight comes from the entire sky; $2\pi$ steradians. As expected, shadows will be practically nonexistent and the brightness range will be that of heavily clouded (no ground fog) conditions under either sunlight or moonlight. This type of lighting reduces the contrast of a scene when compared to either sunlight or moonlight, and as a result, the differences between $B_0$min and $B_0$max will not be nearly as great. The scene brightness will depend almost entirely on the reflectivity of the objects in the scene.

For a Type I scene we would expect:

$$B_0\text{max} = 0.6 \times I$$
$$B_0\text{av} = 0.3 \times I$$
$$B_0\text{min} = 0.04 \times I$$

while for Type II:

$$B_0\text{max} = 0.45 \times I$$
$$B_0\text{av} = 0.08 \times I$$
$$B_0\text{min} = 0.02 \times I$$

Since Type I scenes have a much wider difference of reflectivities, the difference between moonlight and starlight with respect to these coefficients will not be as great as found in Type II scenes.

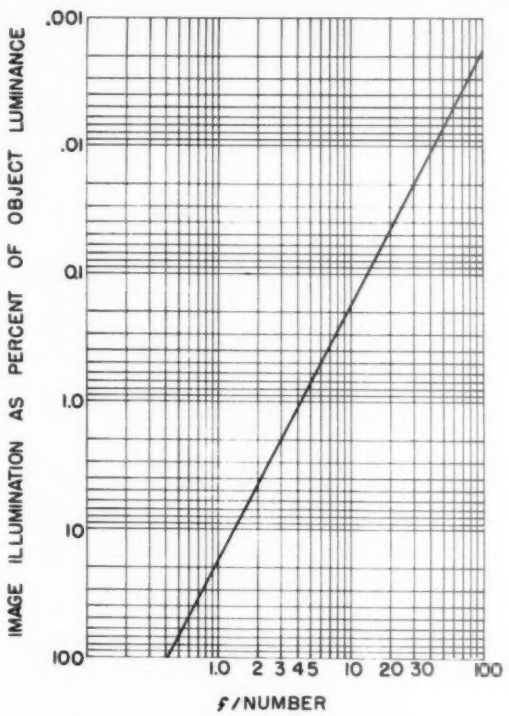


**Fig. 3. The relationship between object luminance and image illumination as determined by the lens aperture (f/stop).**

## Haze

The effect of haze is to reduce contrast. Haze results from scatter and tends to raise the values of $B_0$min discussed above. There is a negligible change in $B_0$max. The effect of haze increases as the altitude of the photo-reconnaissance aircraft increases up to approximately 20,000 ft; however, this relationship is not linear. At very low altitudes (1000 ft) the change due to haze will be small unless the haze condition is extreme. At higher altitudes, haze will increase the value of $B_0$min.

## Image Illuminance

If the scene brightness is known, the corresponding image brightness can be determined for a particular $f$/number. The relationship used by Jones and Condit[1,5,6] is:

$$I_{i0} = B_0 \frac{\mathbf{F}^2}{4V^2 f^2} \times \cos^4 \theta \times H \times T_a$$

where

$I_{i0}$ = image illuminance at focal plane (foot-candles)
$B_0$ = object luminance (foot-lamberts)
$V$ = image distance
$d$ = diameter of stop

$\mathbf{F}$ = focal length of lens
$f$ = $\mathbf{F}/d$, aperture ratio
$\theta$ = angle of image point off lens axis
$T_g$ = transmission factor due to reflection and absorption by glass
$H$ = transmission factor at points off lens axis due to vignetting by the lens barrel

For aerial photography, $\mathbf{F} = V$, since the object is effectively at infinity and the terms $\cos^4 \theta$ and $H$ can be ignored since we shall consider $I_{i0}$ on the axis of the lens. This gives:

$$I_{i0} = B_0 \cdot T_g / 4f^2$$

By setting $B_0 = 100$ and assuming a value fot $T_g$ of 0.7, we get the percentage by which $B_0$ must be multiplied in order to obtain $I_{i0}$ for that object.

The following computations are shown graphically in Fig. 3.

For an $f/1.0$ lens, $I_{i0} = 17.5\%$, $B_0 = 1.7 \times 10^{-1} B_0$
For an $f/2.0$ lens, $I_{i0} = 4.38\%$, $B_0 = 4.4 \times 10^{-2} B_0$
For an $f/3.5$ lens, $I_{i0} = 1.42\%$, $B_0 = 1.4 \times 10^{-2} B_0$
For an $f/5.6$ lens, $I_{i0} = 0.55\%$, $B_0 = 5.5 \times 10^{-3} B_0$

From the above, it will be seen that very fast optics are necessary if image illuminances are to even approach object luminance in intensity.

## Flare Factor

The image illuminance will be affected by dispersed light coming from the optical system.[1b] This dispersed light, which is not imaged light, reaching the focal plane of the lens is termed flare. As a result, the total image-forming light $I_i$ can be written as:

$$I_i = k \cdot B_0 + I_{if}$$

where $k = \dfrac{T_g}{4f^2}$ and $I_{if}$ = the flare light

In logarithmic form, this will be:

$$\log I_i = \log (k B_0 + I_{if})$$

If a camera lens produces a perfect reproduction of the luminance ratio of the scene, the equation would be the form: $\log I_i = \log k B_0$.

This, when plotted with $\log B_0$ as the abscissa and $\log I_i$ as the ordinate, will be a straight line with a slope of unity.

In practice, a graph of the function which involves flare departs from the straight line of $\log I_i = \log k B_0$ as the lower values of $B_0$ are reached. As a result, the effect of flare is most pronounced in values of $I_{i0}\text{min}$ and can be neglected for values of $I_{i0}\text{max}$.

To a first approximation, $I_i$ equals $I_{i0}\text{min}$ times the flare factors of the lens under consideration for values of $B_0\text{min}$. In the highlight areas $I_i \sim I_{i0}$.

## Conclusions

From the foregoing discussion, it will be seen we can write for image illuminance:

$$I_i\text{min} = (b \times B_0\text{min} \times k) + I_{if}$$

or

$$I_i\text{min} = k \times B_0\text{min} \times k \times F$$

where:

$b$ = factor by which $B_0\text{min}$ in high altitude photography is altered as a result of haze
$B_0$ = object luminance
$k$ = $T_g/4f^2$, which for an $f/1.0$ lens = $1.7 \times 10^{-1}$
$F$ = flare factor of lens

and

$$I_i\text{max} = k\, B_0\text{max}$$

Below, computations have been made giving the exposure in mcs where a lens of $f/1.0$ aperture is used at $\frac{1}{5}$ sec. The relationship to give the exposure $E$ is:

$$E = k \times I \times R \times t$$

where $R$ is the reflectivity coefficient of an object in a scene. This equation can be reduced to:

$$E = kB_0t$$

**TABLE I**

Lens: $f/1.0$ Exposure Time: $\frac{1}{5}$ sec

| Scene Type | Ratio, $\frac{B_0}{I}$ | Exposure, mcs | Image Illuminance, $I_{i0}$, ft-c |
|---|---|---|---|
| Type I, full moon at approximately 90° elevation | $B_0\text{max} = 0.6$ | $7.7 \times 10^{-3}$ | $3.6 \times 10^{-3}$ |
| | $B_0\text{av} = 0.2$ | $2.5 \times 10^{-3}$ | $1.2 \times 10^{-3}$ |
| | $B_0\text{min} = 0.04$ | $5.1 \times 10^{-4}$ | $2.4 \times 10^{-4}$ |
| Type I, starlight | $B_0\text{max} = 0.6$ | $6.2 \times 10^{-6}$ | $2.9 \times 10^{-6}$ |
| | $B_0\text{av} = 0.3$ | $3.0 \times 10^{-6}$ | $1.4 \times 10^{-6}$ |
| | $B_0\text{min} = 0.04$ | $4.1 \times 10^{-7}$ | $1.9 \times 10^{-6}$ |
| Type II, full moon at approximately 90° elevation | $B_0\text{max} = 0.45$ | $5.7 \times 10^{-3}$ | $2.7 \times 10^{-3}$ |
| | $B_0\text{av} = 0.04$ | $5.1 \times 10^{-4}$ | $2.4 \times 10^{-4}$ |
| | $B_0\text{min} = 0.006$ | $7.7 \times 10^{-5}$ | $3.6 \times 10^{-5}$ |
| Type II, starlight | $B_0\text{max} = 0.45$ | $4.3 \times 10^{-6}$ | $2.0 \times 10^{-6}$ |
| | $B_0\text{av} = 0.08$ | $7.9 \times 10^{-7}$ | $3.7 \times 10^{-7}$ |
| | $B_0\text{min} = 0.02$ | $2.0 \times 10^{-7}$ | $9.5 \times 10^{-8}$ |

The factors of $b$ and $\mathbf{F}$ have not been included with values of $B_0\text{min}$ in the computation of this table. The value for $b$ depends upon the altitude and the atmospheric conditions, and $\mathbf{F}$ depends upon the lens being used.

Where qualitative results are desired, these factors must be taken into consideration.

## References


1. a. Jones, Loyd A., and Condit, H. R., *J. Opt. Soc. Am.*, *38:* 123–78 (1948).
   b. *Ibid.*, pp. 127, 128–31.
2. Mees, C. E. K., *The Theory of the Photographic Process*, rev. ed., the Macmillan Company, New York, 1954, pp. 932–36.
3. WADC Night Ambient Light Reconnaissance Seminar, 6/26–27/57 WADC, published October 1957.
4. Brown, Dayton R. E., USN, *Natural Illumination Tables*, Bureau of Ships, Code 374.
5. Jones, Loyd A., and Condit, H. R., *J. Opt. Soc. Am.*, *39:* 125 (1949).
6. ———, *J. Opt. Soc. Am.*, *31:* 651 (1941).

PHOTOGRAPHIC SCIENCE AND ENGINEERING
Volume 3, Number 3, May-June 1959

# Hypersensitization of X-Ray Films

YOSHITADA TOMODA, *Government Chemical Industrial Research Institute Tokyo, Hiratsuka, Kanagawa Pref., Japan*

**It is well known that the sensitivity of ordinary photographic emulsions to light can be increased by treatment with silver salt solutions such as silver nitrate or silver tungstate solutions. This treatment, however, was found to decrease the x-ray sensitivity of x-ray emulsions. The x-ray or γ-ray sensitivity of x-ray emulsions was increased by a treatment with thallium nitrate solutions, and the effect of hypersensitization was larger in the higher exposure region, so that the treatment increased the contrast of x-ray or γ-ray images. The thallium hypersensitization also stabilized the latent images formed by x-rays and γ-rays.**

The sensitivity of photographic materials can be increased by immersion in weakly alkaline solution or in solutions of silver salts, gold salts, reducing agents, etc. In our early studies,[1] it was shown that the effect of hypersensitization by silver salts appears principally in the region of inherent sensitivity of the silver halide. The present work extends those studies to the effect of silver, lead, and thallium salts on x-ray sensitivity.

## Experimental Procedure

Two no-screen-type emulsions used for industrial radiography were employed: Film N-2, a medium- to large-grain emulsion, and Film N-3, a large-grain emulsion of somewhat higher sensitivity. Strips of each film were immersed for 5 min at 20°C in solutions of silver nitrate (0.005–0.05%), silver tungstate ($Ag^+$ = 0.01%), lead nitrate (0.5%), or thallium nitrate (0.01–1%), then dried quickly with alcohol. The effect of the treatment was examined for exposure to light, to x-rays from a 30-kv source, and to γ-rays from a Cobalt-60 source.

## Silver and Lead Salts

Silver nitrate and silver tungstate produced effective hypersensitization only for exposure to light. Both the silver and lead salts decreased the sensitivity to x-ray and γ-rays. Table 1 shows the results obtained for Film N-3. The inefficacy of the treatment with these metal salts is indicated.

## A Thallium Salt

Treatment of the emulsions with a thallium nitrate solution decreased the light sensitivity as shown by the characteristic curves in Figs. 1 and 2. According to the results shown in Fig. 1, the desensitizing effect is greater the higher the concentration of thallium nitrate.

In contrast to the results obtained with light exposure, the thallium nitrate treatment increased the sensitivity to x-rays. Figure 3 shows the effect of a 0.05% solution on Film N-3. Development was by Kodak Developer D-19b for 2 or 5 min. Figure 4 shows the influence of the thallium nitrate concentration on the hypersensitization of Film N-3 for x-ray exposure. The film was developed for 5 min in D-19b. The relative log exposure values for the five curves are 1.3, 1.7, 2.0, 2.3, and 2.5, based on the same scale as used for Fig. 3. These results indicate that 0.1% is the optimal thallium concentration for hypersensitization.

The x-ray sensitivity of Film N-2 also was increased by the thallium nitrate treatment. Figure 5 shows results for samples developed for 2 and for 5 min in Kodak D-19b at 20°C.

**TABLE I**
**Inefficacy of Treatment of X-Ray Film N-3 with Silver or Lead Salts**

| Hypersensitization | Densities for Gamma-Ray Exposures* (Distance from source) 50 cm | 79 cm | 125 cm | 200 cm | fog |
|---|---|---|---|---|---|
| None | 3.23 | 1.61 | 0.81 | 0.47 | 0.13 |
| $AgNO_3$ 0.01% | 2.20 | 1.10 | 0.52 | 0.32 | 0.16 |
| $Ag_2WO_4$ | 2.21 | 0.99 | 0.56 | 0.17 | 0.17 |
| **Hypersensitization** | **Densities for X-Ray Exposures** 30 sec** | 20 sec | 10 sec | 5 sec | 2 sec | fog |
| None | 3.10 | 2.43 | 1.46 | 0.83 | 0.41 | 0.13 |
| $Pb(NO_3)_2$ 0.5% | 1.93 | 1.53 | 0.92 | 0.57 | 0.34 | 0.16 |

* Cobalt-60 source; after exposure, film was developed in Kodak D-19b for 5 min at 20°C.
** 30-kv source; development same as above.

Presented at the Annual Conference, Rochester, N.Y., 9 October 1958. Received 12 September 1958.

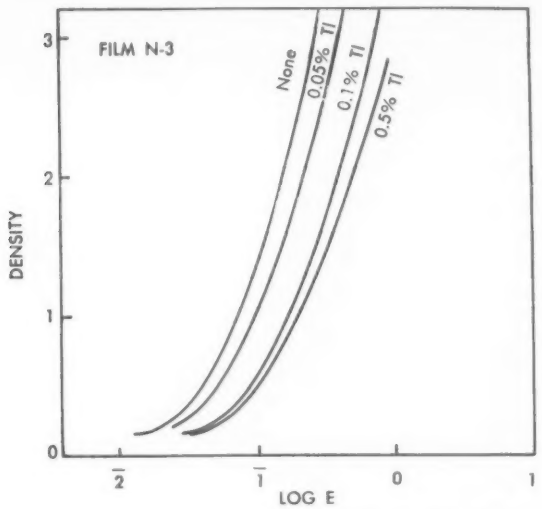


Fig. 1. Desensitizing action of thallium nitrate for the light exposure on Film N-3.

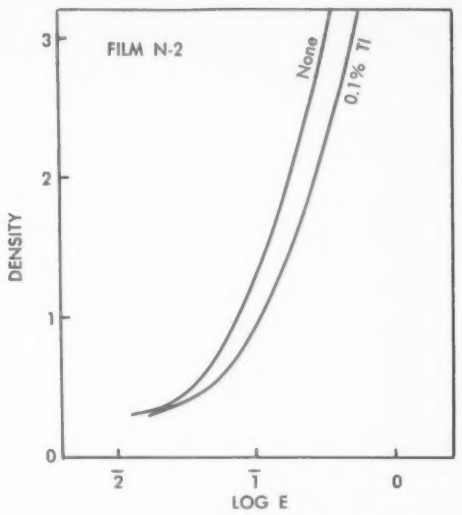


Fig. 2. Desensitizing action of thallium nitrate for the light exposure on Film N-2.

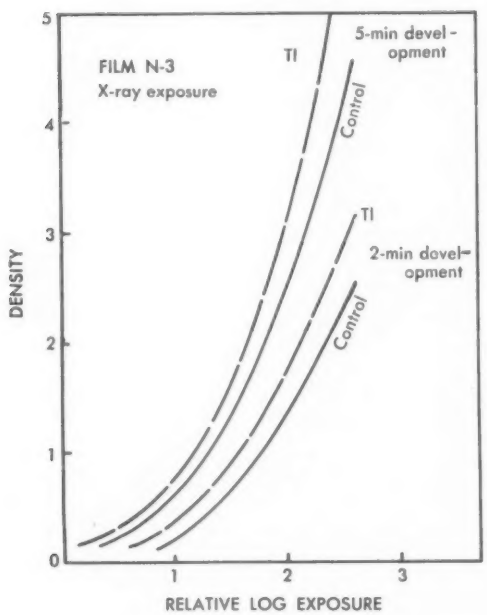


Fig. 3. Thallium hypersensitization of Film N-3, x-ray exposure, in Kodak D-19b development.

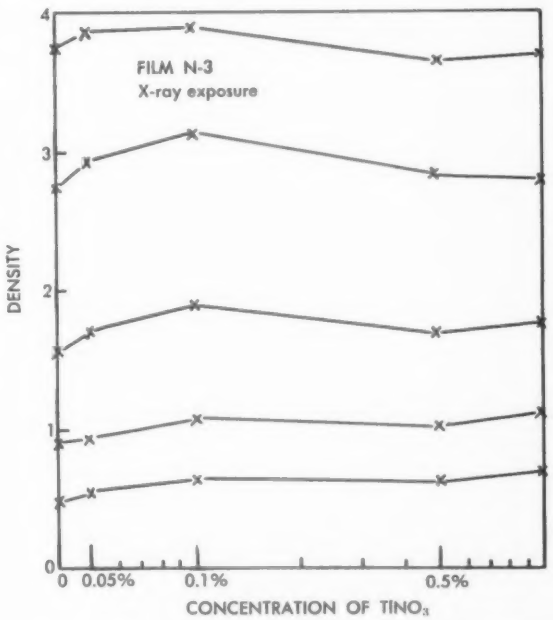


Fig. 4. Influence of thallium concentration on the sensitizing effect on Film N-3, x-ray exposure.

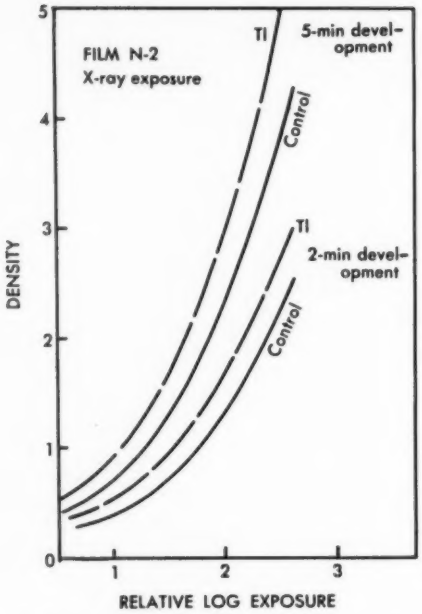


Fig. 5. Thallium hypersensitization of Film N-2, x-ray exposure, in Kodak D-19b development.

Thallium hypersensitization was examined for gamma-ray exposures. Results for the two films are shown in Figs. 6 and 7. The sensitizing action of the thallium was not as marked as before, but the effect was still obtained to some degree.

## Stability of Latent Image After Hypersensitization

In our recent studies,[2] we found that the latent image formed by gamma radiation in emulsion N-3 fades when it is stored in an atmosphere of 69% RH at 30°C. The stability of the latent image in emulsions subjected to thallium hypersensitization was examined in the same way. Prior to describing the results of the fading test, the stability of the emulsion containing the thallium salt must itself be considered. After hypersensitization, Film N-3 was stored under the same conditions used in the fading test, and fog densities were determined by development with D-19b (without exposure). The results in Fig. 8 show that use of a 0.01% solution is desirable to keep fog formation low.

The emulsion with or without thallium treatment now was exposed to γ-rays, stored, and then developed in D-19b after 4, 8, and 18 days. The fading curves of Fig. 9 were obtained. The ordinate of Fig. 9 shows the relative decrease of density due to fading of the latent image on storage. It is evident that the stability of the latent image is considerably better in the thallium-treated emulsion.

The stability of the latent image against chemical

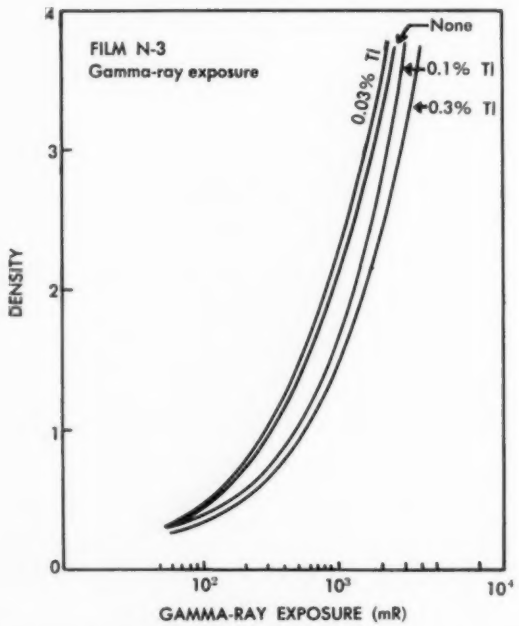


Fig. 6. Effect of thallium nitrate on Film N-3, gamma-ray exposure.

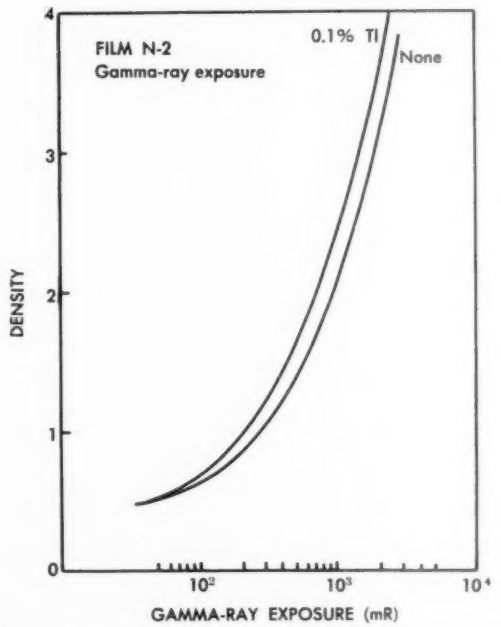


Fig. 7. Effect of thallium nitrate on Film N-2, gamma-ray exposure.

**TABLE II**
**Stability of Latent Image after Thallium Treatment**
**(Developed in a glycin developer)**

| Film | Hypersensitization | Bath after exposure | Densities formed by x-ray exposures of | | | | | |
|---|---|---|---|---|---|---|---|---|
| | | | 2 sec | 5 sec | 10 sec | 20 sec | 30 sec | fog |
| N-3 | none | water | 0.35 | 0.60 | 0.97 | 1.34 | 1.62 | 0.15 |
| | Tl, 0.05% | | 0.36 | 0.58 | 0.89 | 1.28 | 1.49 | 0.15 |
| | none | $K_3Fe(CN)_6$, 0.003%, 3 min | 0.31 | 0.46 | 0.65 | 1.02 | 1.31 | 0.14 |
| | Tl, 0.05% | | 0.34 | 0.56 | 0.90 | 1.34 | 1.67 | 0.16 |
| | none | $K_3Fe(CN)_6$, 0.006%, 3 min | 0.25 | 0.36 | 0,57 | 0.85 | 1.09 | 0.16 |
| | Tl, 0.05% | | 0.37 | 0.56 | 0.88 | 1.27 | 1.51 | 0.16 |
| N-2 | none | $K_3Fe(CN)_6$, 0.003%, 3 min | 0.43 | 0.60 | 0.76 | 1.07 | 1.16 | 0.30 |
| | Tl, 0.05% | | 0.76 | 1.16 | 1.58 | 2.12 | 2.41 | 0.33 |

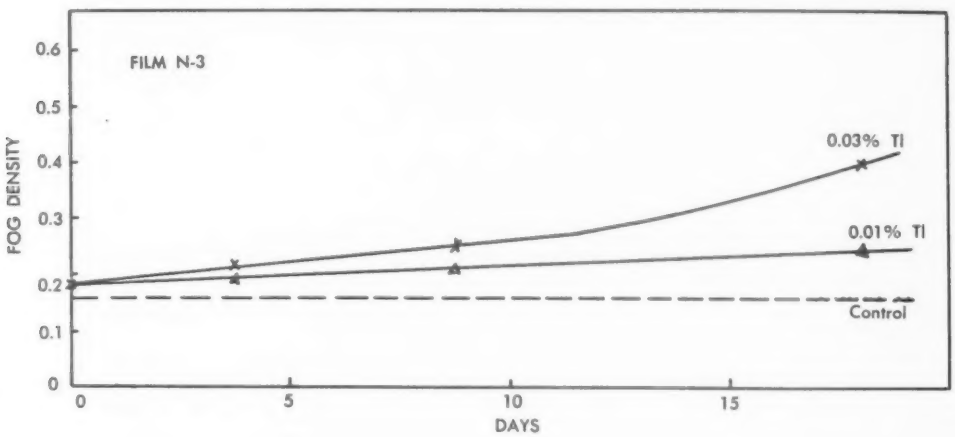


Fig. 8. Increase of fog density in Film N-3, stored at 30°C, 69% RH.

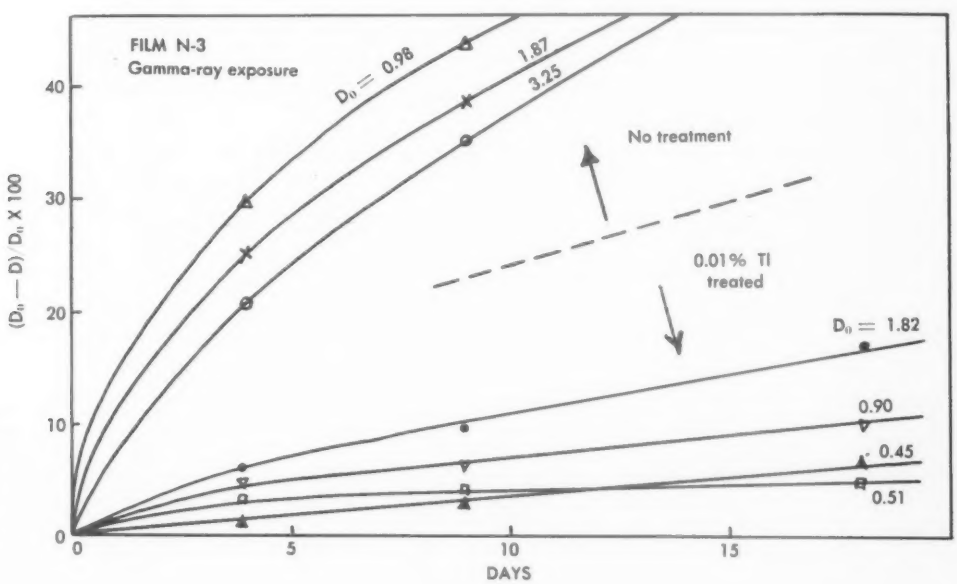


Fig. 9. Fading of latent image in thallium-sensitized or non-sensitized Film N-3, gamma-ray exposure, stored at 30°C, 69% RH.

oxidation is shown in Table II. The two emulsions were treated with thallium and then exposed to x-rays and developed in a *p*-hydroxyphenylglycine developer without sulfite. In both emulsions, it is seen that thallium hypersensitization makes the surface latent image more stable against oxidation by potassium ferricyanide.

## Discussion

It is well known that the x-ray sensitivity of silver halide emulsions can be increased by the addition of lead, thallium, or aurous salts to the emulsion.[3,4,5] In the case of hypersensitization, the present studies show that thallium nitrate is effective to increase the x-ray or γ-ray sensitivity, but silver and lead salts are ineffective. Maximum sensitization is obtained with a thallium nitrate solution of 0.05–0.1%. A more concentrated solution has a fogging action.

We conclude that one of the features of thallium hypersensitization is stabilization of the latent image formed by x-ray or γ-ray exposures. We assume that the hypersensitizing treatment leads to the adsorption of thallous ions on the silver halide crystals in the emulsion, and that this facilitates the formation of stable latent image, principally on the surface of the crystals.

## References

1. Tomoda, Y., *J. Chem. Ind. Japan*, *53:* 108 (1950).
2. ——— and Nakamura, N., *J. Soc. Sci. Phot. Japan*, *21:* 16 (1958).
3. Koslowsky, R., and Mueller, F. W. H., *Bibl. Sci. & Ind. Reports*, *873.PB:* 70053 (1936).
4. Mueller, F. W. H., *J. Opt. Soc. Am.*, *39:* 494 (1949).
5. Hoerlin, H., and Mueller, F. W. H., *ibid.*, *40:* 246 (1950).

PHOTOGRAPHIC SCIENCE AND ENGINEERING
Volume 3, Number 3, May-June 1959

# Effect of Derivatives of Thiourea and Related Compounds on Zeta-Potential of Silver Bromide

SHIN SUZUKI AND TOORU KATAOKA, *Department of Applied Chemistry, Faculty of Engineering, University of Tokyo, Japan*

**Effects of derivatives of thiourea and related compounds on the electrophoretic behavior of silver bromide at pH 3 and 11 were studied with a sol prepared in the presence of excess bromide. The effects of 1-methylthiourea, 1,3-dimethylthiourea, and 1,1,3-trimethylthiourea were nearly the same as that previously reported for thiourea. Addition of a small quantity of any of these compounds to the acidic sol caused marked changes in the zeta-potential and the stability of the sol. Addition of a sufficient quantity changed the zeta potential from negative to positive. This reversal was not obtained in the basic sol. However, the addition of 1,1,3,3-tetramethylthiourea to either acidic or basic sol caused the change to a positive potential. Addition of urea, 1,1-dimethylurea, or S-methylisothiourea hydroiodide did not cause a reversal of the potential. The results can be explained in terms of adsorption or chemical reaction of the addenda.**

A knowledge of the colloid-chemical behavior of silver halide sols is important to a fundamental understanding of the action of photographic addition agents, such as chemical sensitizer, antifoggant, and others. The authors have used several physicochemical methods in studies of this subject, among them an electrophoretic method which yields information about the charge on the silver halide surface. The results obtained by this method have usually been consistent with those obtained by other methods, and analysis of the detailed mechanism of the interaction of addition agents with the silver halide surface has been possible.

In the previous paper Suzuki and Oishi[1] reported the electrophoretic behavior of silver bromide sol containing thiourea, or urea, or benzimidazole. The addition of thiourea to silver bromide sols at low pH and high pAg caused a shift of the zeta-potential from negative to positive, whereas the addition of the same compounds at high pH and pAg did not cause such a change. These phenomena were explained by the adsorption or chemical reaction of thiourea with silver bromide, and the mechanism agreed well with the results obtained by James and Vanselow.[2] Independently Lu Valle and Jackson[3] reported similar results.

In this paper the authors describe the electrophoretic behavior of the derivatives of thiourea and of related compounds such as 1-methylthiourea, 1,3-dimethylthiourea, 1,1,3-trimethylthiourea, 1,1,3,3-tetramethylthiourea, urea, 1,3-dimethylurea, and S-methylisothiourea hydroiodide. More detailed information regarding the mechanism of interaction of thiourea with silver bromide are described.

Presented at the Annual Conference, Rochester, N.Y., 9 October, 1958. Received 12 September 1958; revised 19 December 1958.

## Experimental Procedure

The electrophoretic apparatus used for this study was quite similar to that previously described[1] (a moving boundary type — see Fig. 1 of Ref. 1). The electrophoresis was carried out under an electric potential gradient of 5.00 v/cm. for 15 min at 10 – 16.5° C.

The silver bromide sols of 0.008 mol solid AgBr per liter were prepared by pouring 0.1 *N* silver nitrate solution into a potassium bromide solution containing 5% excess bromide with mechanical stirring. The sols were allowed to stand for 24 hours and were diluted with distilled water after the addition of saccharose, pH controlling reagent, and desired addendum. The saccharose was added in order to obtain sharp boundaries. The experiments were carried out at pH 3 or 11. The pH controlling reagent used for pH 3 was nitric acid solution and that for pH 11 was sodium hydroxide solution. The composition of the final sol was:

| | |
|---|---|
| AgBr | 0.004 mol solid AgBr per liter sol |
| $KNO_3$ | 0.004 M |
| Saccharose | 2% (wt) |
| $HNO_3$ or NaOH | 0.001 M |
| Addendum | 0∼0.1 mol per mol AgBr |

The specific surface area of silver bromide before the addition of saccharose, pH controlling reagent, and addendum was $2.3 \times 10^5$ sq cm/gram AgBr, measured by the adsorption of 1,1′-diethyl – 2,2′-cyanine iodide (absorption maxima, in solution, 522 mμ and 490 mμ) and 3,3′-diethyl-9-methyl-thiacarbocyanine bromide (absorption maxima 540 mμ and 504 mμ). In this calculation, the areas covered by the former dye and the latter dye on a silver bromide surface were both assumed to be 79 sq A per molecule.

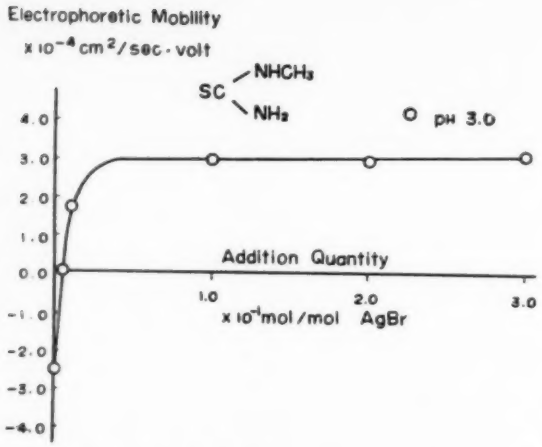


Fig. 1. Effect of 1-methylthiourea on zeta-potential of silver bromide (pAg 9).

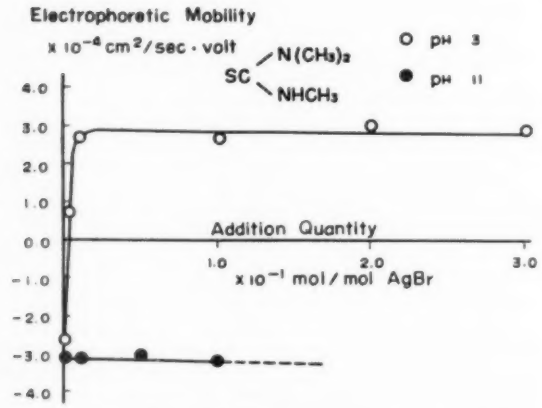


Fig. 3. Effect of 1,1,3-trimethylthiourea on zeta-potential of silver bromide (pAg 9).

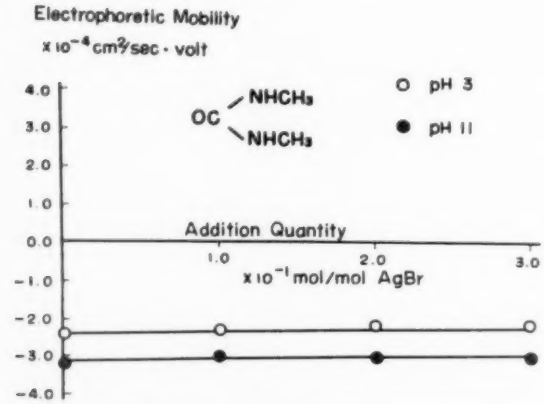


Fig. 5. Effect of 1,1-dimethylurea on zeta-potential of silver bromide (pAg 9).

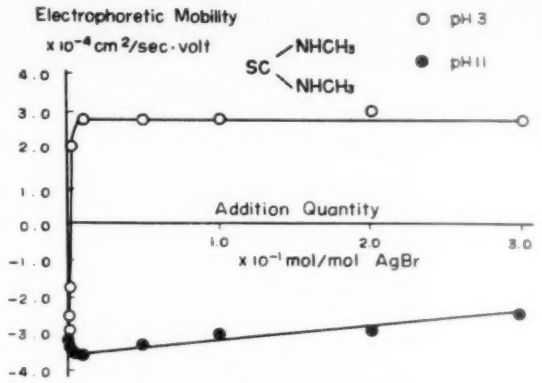


Fig. 2. Effect of 1,3-dimethylthiourea on zeta-potential of silver bromide (pAg 9).

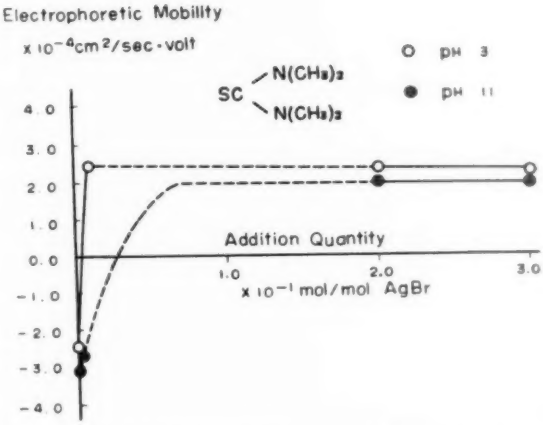


Fig. 4. 1,1,3,3-tetramethylthiourea on zeta-potential of silver bromide (pAg 9).

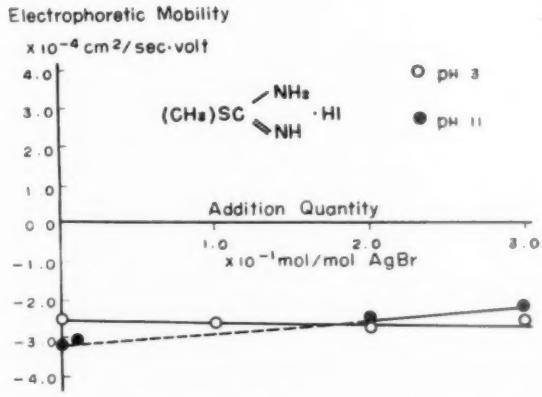


Fig. 6. Effect of S-methylisothiourea on zeta-potential of silver bromide (pAg 9).

Besides the addenda, the pH, pAg, electrolytes, and saccharose affect the electrophoretic behavior of silver bromide. These effects were studied thoroughly by the authors. The effects of pH and pAg were reported previously.[1] The change of zeta-potential of silver bromide sol with pH was minute at pAg 9. The addition of a large quantity of electrolyte caused the sol to be unstable, following the Schulze-Hardy rule. Therefore the quantity of added electrolytes must be limited to some lower value. The common buffer solutions were not used to control the pH in these experiments. The addition of saccharose also accelerated the precipitation of the sol in the presence of electrolytes. A suitable amount of pure saccharose must be used.

The zeta-potential is given by

$$\zeta = \frac{1}{f(\kappa\alpha)} \cdot \frac{4\pi\eta}{D} \cdot m$$

where $\zeta$ is the zeta-potential; $f(\kappa\alpha)$ the Henry's factor; $\eta$ the coefficient of viscosity of the medium; $D$ the dielectric constant of the medium; and $m$ the electrophoretic mobility.

Introducing the numerical values at 12° C. in the above equation, the zeta-potential equation to be obtained from a value of electrophoretic mobility $m$ (sq cm/sec/volt) is as follows:

$$\zeta = 22.1 \times 10^4 \cdot m$$

where $\zeta$ is in millivolts.

## Results

The effects of 1-methylthiourea, 1,3-dimethylthiourea, and 1,1,3-trimethylthiourea on the zeta-potential of silver bromide sol were, as shown in Figs. 1, 2, and 3, nearly the same as that already reported for thiourea.

The zeta-potential of silver bromide was initially negative at pAg 9.0 (nearly −55 mv). On the addition of a small quantity of any one of these compounds to the acidic sol, the zeta-potential shifted towards the positive direction from the negative potential. With the addition of around $2 \sim 5 \times 10^{-3}$ mol/mol AgBr, the curves crossed the zero axis of zeta-potential and near this isoelectric point the sol promptly flocculated. However, when the quantity added was increased to 0.01 mol/mol AgBr or more, the potential attained a constant value of approximately +60 mv.

Such a reversal or marked change of zeta-potential did not occur in the basic sol. However, a brown coloration of the sol was observed. When the amount of addendum was increased, the color changed to black and the sol became unstable. Zeta-potential measurements were difficult in the sol which contained 0.1 mol or more of 1,1,3-trimethylthiourea per mol AgBr because of instability of this sol. Alkaline sols containing 1-methylthiourea were not measured, but the authors assume that the results of such measurements would be nearly the same as those for thiourea, 1,1-dimethylthiourea and 1,1,3-trimethylthiourea.

The zeta-potential of a silver bromide sol containing a large quantity of 1,1,3,3-tetramethylthiourea was positive in the acid sol, just as in the case of thiourea and the other derivatives. However, the electrophoretic behavior of the basic sol containing the same compound was peculiar, when compared with that containing thiourea and the other derivatives. The zeta-potential changed from negative to positive in spite of high pH (Fig. 4), and the color was not brown but white. However, the addition of a sufficiently large amount of compound made the sol turbid and unstable, especially at high pH. Reproducibility of the experiments was not so good.

The addition of urea or 1,3-dimethylurea did not affect the zeta-potential of either the acidic or basic silver bromide sol and also did not cause any color change (Fig. 5).

The addition of S-methylisothiourea hydroiodide did not cause a marked change of the zeta potential in either acidic or basic solution. (Fig. 6). However, the addition of the compound caused the sol to change color. The color was not brown or black, but yellowish green. In the range of addition of $0.05 \sim 0.10$ mol/mol AgBr to the basic sol, the sol became unstable and yellowish green precipitates were produced.

## Discussion

In the previous paper,[1] Suzuki and Oishi attributed the phenomenon of the shift of the zeta-potential of silver bromide sols caused by thiourea at low pH and high pAg, to the adsorption of thiourea in the following ionized form

$$NH_2{-}\underset{\underset{S}{\|}}{C}{-}NH_2 + H_2O \rightleftharpoons NH_2{-}\underset{\underset{S}{\|}}{C}{-}NH_3^+ + OH^-$$

The authors also attributed the brown coloration of the silver bromide sol by thiourea at high pH and pAg to the formation of silver sulfide on the silver bromide surface, following James's mechanism.[2]

$$2AgBr + NH_2{-}\underset{\underset{S}{\|}}{C}{-}NH_2 \rightarrow Ag_2S + NH_2{-}C{\equiv}N + 2HBr$$

It was reported that the zeta-potential of a silver bromide sol containing silver sulfide is the same as that of a silver bromide sol.[1]

The authors can extend the same considerations to the explanation of the results obtained here.

Thus the results for 1-methylthiourea, 1,3-dimethylthiourea, 1,1,3-trimethylthiourea in acidic sol and 1,1,3,3-tetramethylthiourea in acidic and basic sols are explained by the fact that these compounds are adsorbed on the silver bromide surface, if they retain a proton. It is considered that the substitution of methyl radicals for hydrogen atoms of the amino groups increases the proton affinity by the negative induction effect of this radical towards a nitrogen atom. Therefore the result for 1,1,3,3-tetramethylthiourea is not so remarkable. The results for

1,3-dimethylthiourea and 1,1,3-trimethylthiourea in the basic sol are explained by the fact that these compounds chemically reacted with silver bromide, forming silver sulfide on the surface of the silver bromide.

The authors conclude that the results for urea and 1,3-dimethylurea indicate that these compounds are not adsorbed on silver bromide nor do they react chemically with it, because no zeta-potential change and no color change occur in either acidic or basic sols.

Regarding S-methylisothiourea, it is not clear whether adsorption or chemical reaction did occur, but the authors assume that the compound may react with silver bromide. Some discussion will be given later.

The results of the present work and that previously reported[1] are tentatively summarized in Tables I and II.

Table I seems to allow a decision as to what kind of group, thioketo or amino, is effective in the adsorption of thiourea on silver bromide. If the thioketo group is important, the results for all compounds which involve this group should be nearly the same. For example, the results for thiourea, 1-methylthiourea, 1,3-dimethylthiourea, 1,1,3-trimethylthiourea, and 1,1,3,3-tetramethylthiourea should be same. If, on the other hand, the amino group is important, the results for the compounds which involve this group should be nearly the same. For example, the results for thiourea, 1-methylthiourea, and urea should be the same.

Table I clearly indicates that the former case is true. A comparison of the result for 1,3-dimethylthiourea with that for 1,3-dimethylurea also indicates that the methylamino group is not very important in the adsorption.

S-methylisothiourea possibly is not adsorbed on silver bromide because there is no reversal of zeta-potential of the silver bromide sol containing this compound. However, it may have reacted with silver bromide, since a coloration was observed. The reaction products were not investigated, but they may be silver iodide or silver methylmercaptide or both. Silver iodide may result from the reaction of

TABLE I

Summary of Results (Acidic Sol)

| Addition Agent | $R_1$ $R_2$ $R_3$ | $-NH_2$ $=NH$ [HI] | $-NH_2$ $-NH_2$ | $-NH(CH_3)$ $-NH_2$ | $-NH(CH_3)$ $-NH(CH_3)$ | $-N(CH_3)_2$ $-NH(CH_3)$ | $-N(CH_3)_2$ $-N(CH_3)_2$ |
|---|---|---|---|---|---|---|---|
| $S=C(R_1)(R_2)$ | E | — | Reversal | Reversal | Reversal | Reversal | Reversal |
| | C | — | No change | No change | No change | No change | No change |
| | I | — | Adsorption | Adsorption | Adsorption | Adsorption | Adsorption |
| $O=C(R_1)(R_2)$ | E | — | No reversal | not tried | No reversal | not tried | not tried |
| | C | — | No change | | No change | | |
| | I | — | No adsorption | | No adsorption | | |
| | | | No reaction | | No reaction | | |
| $CH_3S-C(R_1)=R_3$ | E | No reversal change | — | — | — | — | — |
| | C | (Yellow-green) | — | — | — | — | — |
| | I | Reaction (?) | — | — | — | — | — |

E — Electrophoretic behavior of the sol containing the addition agent.
C — Color change when the addition agent was added into the silver bromide sol.
I — Presumed interaction of the addition agent with silver bromide.
Reaction — Chemical reaction (forming silver sulfide or the other compounds).

TABLE II

Summary of Results (Basic Sol)

| Addition Agent | $R_1$ $R_2$ R | $-NH_2$ $=NH \cdot HI$ | $-NH_2$ $-NH_2$ | $-NH(CH_3)$ $-NH_2$ | $-NH(CH_3)$ $-NH(CH_3)$ | $-N(CH_3)_2$ $-NH(CH_3)$ | $-N(CH_3)_2$ $-N(CH_3)_2$ |
|---|---|---|---|---|---|---|---|
| $S=C(R_1)(R_2)$ | E | — | No reversal | not tried | No reversal | No reversal | Reversal |
| | C | — | Change (Brown) | | Change (Brown) | Change (Brown) | No change |
| | I | — | Reaction | | Reaction | Reaction | Adsorption |
| $O=C(R_1)(R_2)$ | E | — | No reversal | not tried | No reversal | not tried | not tried |
| | C | — | No change | | No change | | |
| | I | — | No adsorption | | No adsorption | | |
| | | | No reaction | | No reaction | | |
| $CH_3-S-C(R)=R_3$ | E | No reversal change | — | — | — | — | |
| | C | (Yellow-green) | — | — | — | — | |
| | I | Reaction (?) | — | — | — | — | |

See Table I for key.

silver bromide with the hydrogen iodide of the S-methylisothiourea complex. Silver methylmercaptide may be the product of reaction of silver bromide and the decomposition products of S-methylisothiourea. It is well known that S-methylisothiourea is likely to decompose to urea and methylmercaptan. Recently Kasida[4] showed in his experiments with paper chromatography that this compound may be decomposed in ammonia-alkaline solution. He also obtained the methylmercaptan-like smell when S-methylisothiourea was titrated with a sodium hydroxide solution.

From the comparison of the result for thiourea with that for S-methylisothiourea, it may be concluded that the thioketo sulfur is effective for adsorption, but thioether sulfur is not.

Table II suggests that the hydrogen atom of the thiol form of thiourea or its derivatives is important in the chemical reaction with silver bromide. The evidence is this: All thioureas which contain a hydrogen atom reacted chemically with silver bromide, whereas the compound 1,1,3,3-tetramethylthiourea, which involves no active hydrogen atom, was only adsorbed on silver bromide and did not react chemically with it. This agrees with the consideration of James.[2]

The remarkable instability of the basic sol containing 0.1 mol or more of 1,1,3-trimethylthiourea per mol AgBr in comparison with the case of thiourea or 1,3-dimethylthiourea, may be explained by the following mechanism: The substitution of electron donor groups such as methyl for the hydrogen atoms of the amino groups decreases the rate of chemical reaction at high pH,[2] and also causes an increase in the proton affinity, which results in a shifting of the charge sign of the sol from negative to zero. When the quantity of the added compound is small, the compound is adsorbed on silver bromide and then immediately reacts with the latter, forming silver sulfide. As a result, the sol still keeps the negative charge. Undoubtedly, this means a stable sol. However, as the quantity added increases, the supply of 1,1,3-trimethylthiourea on the silver bromide surface increasingly competes with the rate of decomposition of the compound to silver sulfide. The amount of the sol which adsorbs the compound, but has not yet reacted with it, increases gradually. Thus the sol approaches the neutral point and becomes unstable.

The instability of the basic sol containing small amounts of 1,1,3,3-tetramethylthiourea also may be attributed to a similar mechanism. In this case, only the adsorption rate of this compound is considered to be a determining factor, since this compound does not react with silver bromide. Because of the lower adsorption rate in the low concentration region, passing through the isoelectric point requires much time, giving a chance for silver bromide particles to aggregate. Thus the sol may become unstable.

The results for urea and its derivatives indicate that the ketone radical is not effective for adsorption.

## Acknowledgment

This work was supported by the Tachibana Research Fund of the Society of Scientific Photography of Japan, contributed by Sennosuke Sugiura, to whom the authors are grateful. The authors also wish to express their gratitude to Dr. Yosihiko Kasida, Department of Pharmacy, Faculty of Medicine, Tokyo University, and Dr. Yasushi Hishiki, the Scientific Research Institute, for offering many kinds of addition agents or optical sensitizing dyes, to Prof. Shumpei Oka, Department of Applied Chemistry, Faculty of Engineering, Tokyo University, for his guidance in this laboratory, and to the research group on the colloid chemistry of silver bromide emulsions whose members are Prof. Hiroshi Nozaki, Dr. Kenichi Honda, Yasushi Oishi, Yuji Hamano, all of the Institute of Industrial Science, Tokyo University, and Dr. Tamio Nishimura, the Kitasato Institute, for their cordial discussions in this group. The authors also especially must thank Dr. T. H. James, Eastman Kodak Co., for giving them his special interest and friendly suggestions by letter.

## References

1. Suzuki, Shin, and Oishi, Yasushi, *Photo. Sci. & Eng., 1:* 56 (1957).
2. James, T. H., and Vanselow, W., *J. Photo Sci., 1:* 133 (1953).
3. Lu Valle, James E., and Jackson, Juanita M., *J. Phys. Chem., 61:* 1216 (1957).
4. Kasida, Yosihiko, private communication.

PHOTOGRAPHIC SCIENCE AND ENGINEERING
Volume 3, Number 3, May-June 1959

# Fungicidal Rinses for Processed Color Films

E. S. MACKEY AND C. E. JOHNSON, *Ansco Research Laboratories, Binghamton, N.Y.*

**Techniques for the prevention of image deterioration due to fungus growth are discussed, with particular emphasis on fungicidal rinse treatments. The evaluation of a number of different aqueous rinses for their fungicidal activity is presented.**

The use of color film has greatly increased in recent years. A few years ago only professional and advanced amateurs were using color film. Today, with the advent of higher speed color film and relatively inexpensive cameras, the casual photographer is now taking color pictures and getting prints. Naturally, it is desirable for these results, be they the family picnic, the vacation spot, or perhaps some valuable record, to remain in good physical condition for years to come.

Storage conditions,[1] particularly temperature and humidity, have a significant effect on the stability of photographic images. Warm temperatures and high humidities favor chemical reactions harmful to the photographic image. They also provide an ideal environment for the growth of fungi and other organisms in the photographic layer. This paper is primarily devoted to a discussion of techniques for the prevention of image deterioration due to fungus growth, with particular emphasis on fungicidal rinse treatments.

Fungus growth can manifest itself on black-and-white negatives where numerous fungus colonies appear as blotches or patches, and on color transparencies or prints which have the same filamentary pattern as the black-and-white negatives, but also show a change in color density in areas adjacent to the fungus filaments.

The fungus filaments which are the active part of the fungus are of microscopic thickness, and known collectively as mycelia. Fresh mycelia arise by the growth of existing mycelia or by the germination of spores which are usually capable of undergoing a resting stage. These spores are found in the air regardless of temperature and humidity, and are of many varied types. When the spores come to rest on a material, they will grow if the material is nourishing and the temperature and humidity are conducive to germination.

Photographic films with their gelatin emulsions provide an excellent "soil" for the seeding of fungus spores. This is equally true of both unprocessed and processed films. In order for the spores to germinate, a relative humidity of at least 60% is required.[2] Elevated temperature is an additional aid to germination and as a result fungus growth in tropical zones is an extremely serious problem. The coastal regions of the United States and especially the warm humid Southeastern states are areas for accelerated deterioration of color films by fungus growth.

Most film today is distributed in a vaportight package which prevents fungus growth until the seal is broken. In areas of potential fungus growth, loaded cameras and films without vapor barriers should be kept in airtight containers. The airtight container should be kept below 60% RH. Various desiccating agents such as activated silica gel[2] can be used to reduce and maintain proper relative humidity, although it is necessary to regenerate these desiccating agents from time to time by drying. Heated cabinets[2] can be used to store processed film satisfactorily in the more temperate zones but might prove harmful in tropical areas where relatively high temperatures would be necessary to reduce the relative humidity below 60%. As mentioned earlier, the combination of heat and humidity can have a severe detrimental effect on the color image dyes and should be avoided whenever possible.

Some commercial products are on the market which claim to impart protection to clothing and luggage from mold and mildew growth. Photographers should note the chemical composition of these mildew preventatives before storing color films and loaded cameras in luggage containing these products. Some products contain paraformaldehyde crystals whose fumes have a severe detrimental effect on speed and color balance of unprocessed color film.

Another approach to the problem of fungus growth in photographic film is the subject of a U.S. Patent,[3] in which the fungicide is incorporated in the film during manufacturing. In some cases, films can be successfully manufactured incorporating such ingredients.

A very effective yet simple method for prevention of fungus growth on processed photographic film is the application of a fungicidal rinse. This can be applied during processing after the final wash or in a separate step after the films and prints have been dried. We have evaluated a number of different rinses for their fungicidal activity. A general description of test procedures and the evaluation of results follow.

Presented at the Annual Conference, Rochester, N.Y., 6 October 1958. Received 6 January 1959.

## Testing Procedure

Compounds were tested for possible fungicidal effect in photographic film after being screened for such properties as solubility, toxicity, photographic inertness, and effect on stain and image dye quality under fresh or accelerated aging conditions.

This screening process eliminated many compounds in spite of their excellent fungicidal protection. A partial list of some of these compounds, indicating the reason for rejection as a photographic fungicidal rinse is shown in Table I.

TABLE I

Compounds Rejected as Fungicidal Rinses for Color Film and Prints

| Compound | Reason for Rejection |
|---|---|
| Magnesium silico fluoride | Turned film red |
| Thiourea | Excellent fungicide for color films, but may contaminate developer by carryover from film holders |
| Glycol bori-borate | Excellent fungicide for color film, but increased film brittleness |
| Sodium metaborate | Caused scum on film |
| Dehydro acetic acid | Caused stain |
| Borax | Caused scum on film |
| Copper sulfate | Caused stain |
| Polyglycol amine | Caused stain |

The actual screening procedure consisted of soaking 2-in. strips of processed 35mm black-and-white and color film material in various fungicidal rinse baths for 3 min at 68°F. The treated strips were then dried and placed in a mold chamber which contained a predominance of the Aspergillus Ochraceus fungi and bacteria. The mold cell was maintained at a relative humidity of at least 90% and a temperature of 71°F. During a 4-week period the samples were examined periodically to determine the amount of fungus growth, if any. Table II shows the rating system used to determine the magnitude of the growth.

TABLE II

Codes Used in Designating Fungus Growth of Processed Color Film Treated with Fungicidal Rinses

| | |
|---|---|
| 0 | No growth |
| + | Single area of growth |
| ++ | Several areas of growth |
| +++ | Heavy growth |

The fungicidal activity of phenol is well known. Kanagy, Charles, and Abrams,[4] working with leather, have shown that the fungicidal power of phenol is greatly enhanced by introducing into the ring a chlorine or nitro group. Both the OH group and chlorine appear to be necessary for effective protection from fungus attack. As a result, water-soluble chlorinated phenols were tested along with other compounds. The test results of these selected compounds are given in Table III.

As may be seen in Table III, and as was shown in many other of our screening tests, the 0.1% pentachlorophenol sodium salt rinse bath was the most effective fungicidal rinse of the solutions tested. In addition, its low effective concentration makes the bath an economical one to use and worth the protection it provides color film slides and prints from fungus growth.

TABLE III

Fungus Growth Resistance of Processed Color Film Treated with Various Aqueous Rinse Baths

| Final rinse composition | Days Exposure 7 | 14 | 21 | 28 |
|---|---|---|---|---|
| Control | 0 | + | ++ | +++ |
| 0.5% Formalin | 0 | 0 | + | ++ |
| 0.1% Pentachlorophenol sodium salt | 0 | 0 | 0 | 0 |
| 0.1% Diethyl cetyl hydroxy ethyl ammonium chloride | 0 | 0 | + | ++ |
| 0.5% Salicylamide | 0 | 0 | + | ++ |
| 3% Boric acid | 0 | 0 | + | ++ |
| 3% Sodium carbonate | 0 | 0 | + | ++ |
| 0.1% 2,4,5 trichlorophenol — Sodium salt | 0 | 0 | + | ++ |
| 3% Urea | 0 | + | ++ | +++ |
| 7% Poly glycol formal | 0 | + | ++ | +++ |
| 3% Sodium propionate | 0 | 0 | + | ++ |

See Table II for code.

In addition to the chlorinated phenol, an effective fungicide for color film and prints is the Ansco* 955 Stabilizing Rinse. This bath is also recommended for stabilizing the color image dyes of transparencies made with Anscochrome* Color Film and color prints made from Anscochrome Printon* Color Print material against deterioration due to natural aging processes. Since the 955 rinse contains metal salts which leave a residue on cine films, it is necessary that such films be washed on the base side to remove the residue.

The results of the application of the Ansco 955 Stabilizing Rinse, with and without an after-wash, are shown in Table IV.

TABLE IV

Fungus Growth Resistance of Processed Color Film Treated with Ansco 955 Stabilizing Rinse and 0.1% Pentachlorophenol Sodium Salt

| Fungicidal Rinse Composition | Days Exposure 7 | 14 | 21 | 28 |
|---|---|---|---|---|
| Control | 0 | + | ++ | +++ |
| 0.1% Pentachlorophenol sodium salt | 0 | 0 | 0 | 0 |
| 955 Stabilizing Rinse (followed by 10-sec water rinse) | 0 | 0 | 0 | 0 |
| 955 Stabilizing Rinse (followed by 5-min water rinse) | 0 | 0 | 0 | + |

See Table II for code.

* Registered trade mark of General Aniline and Film Corporation.

The formulation of the Ansco 955 Stabilizing Rinse in liquid form and in powdered form for export is shown in Table V.

**TABLE V**

| | | |
|---|---|---|
| 955 Stabilizing Rinse (liquid form) | Water to | 750.0 cc |
| | Solidogen* LT 13 | 30.0 cc |
| | Zinc Acetate $.2H_2O$ | 10.0 grams |
| | Igepal* CO 630 | 0.5 cc |
| | Water to make | 1.0 liter |
| 955B** Stabilizing Rinse (powdered form), for bulk mixing) | Water to | 750.0 cc |
| | Renex 25*** | 0.95 grams |
| | Solidogen* WF | 9.5 grams |
| | Zinc Acetate $.2H_2O$ | 9.5 grams |
| | Water to make | 1.0 liter |
| To make: | Add the ingredients in the above order to 750.0 cc of warm (90°F) water. Then add water to make 1 liter of working solution. Working pH should be maintained at 6.2 ± 0.5 with 10% $NH_4OH$ or 10% acetic acid if necessary. | |

* Registered trade mark of General Aniline and Film Corporation.
** The powdered formula packaged by Ansco is similar but not identical to the 955B formula.
*** Registered trade mark of Atlas Powder Company.

Table VI illustrates the technique of using the 955 Bath with Anscochrome Film or Anscochrome Printon material.

**TABLE VI**

| | | |
|---|---|---|
| Treatment of Anscochrome Film (non-NC-type) | Wash — Part I | 5 min, 63°–68°F |
| | Stabilizing Rinse 955 or 955B | 3–5 min, 66°–70°F |
| | Wash — Part II | 3–5 min, 63°–68°F |
| | Ansco 954 Rinse | 30 sec, 66°–70°F |
| | Dry | |
| Treatment of Anscochrome Printon Prints | Wash | 10 min, 63°–68°F |
| | Stabilizing Rinse 956 or 955B | 2 min, 66°–70°F |
| | Water Rinse | 10 sec, 63°–68°F |
| | Dry | |

## Summary

Of the solutions tested, a 0.1% aqueous solution of pentachlorophenol sodium salt available as Dowicide G† was the most effective rinse for prevention of fungus growth on black-and-white film and color transparencies and prints. It had no harmful effect on black-and-white or color images. Another almost equally effective fungicide is the Ansco 955 Stabilizing Rinse which is a component of the Processing Kits for Anscochrome Printon.

## Acknowledgment

The authors wish to thank T. Nightingale, C. Whittemore, and W. Wike of these Laboratories for their contributions of data.

## References

1. Mackey, E. S., *PSA Jour., 15:* 682 (1949).
2. Kodak Pamphlet 22, *Prevention and Removal of Fungus Growth on Processed Photographic Film*, Eastman Kodak Company, Rochester, New York, 1958.
3. U.S. Patent 2,762,708 (E. S. Mackey to General Aniline and Film Corporation), 1956.
4. Kanagy, J. R., Charles, A. M., and Abrams, E., *Jour. American Leather Chemists Assoc., 43:* 14 (1948).

## Discussion

*Anonymous:* Can the treatments described be used with other manufactured color products?

*Mr. Johnson:* These treatments were used successfully with other color films such as Kodachrome and E-2 Ektachrome.

*Walter Clark (Eastman Kodak Co.):* In tests conducted by the Kodak Tropical Research Laboratories in Panama, a discoloration of black-and-white paper prints was noted when treated with a 0.25% Dowicide G solution. In addition, the Dowicide G solution became discolored when exposed to sunlight. (Authors' Note: This paper describes the use of 0.1% Dowicide G formula. No tests were conducted with black-and-white prints although the solution was used on color prints with no ill effects.)

*Dr. Clark:* Do you know if the zinc salt is the active fungicidal ingredient in the 955 bath?

*Mr. Johnson:* Yes, the zinc salt is the active fungicide.

† Registered trade mark of the Dow Chemical Company.

PHOTOGRAPHIC SCIENCE AND ENGINEERING
Volume 3, Number 3, May-June 1959

# Photographic Developing Agents: I. Pyrimidines

R. W. Henn and Sue V. Carpenter, *Research Laboratories, Eastman Kodak Company, Rochester, N.Y.*

**Developing properties were displayed by pyrimidines substituted by two or more adjacent amino and hydroxy groups. Further substitution by methyl groups or additional functional groups increased activity. The amino-substituted agents were more active than those containing only hydroxy groups, which were very pH-dependent. Activity was increased by combination with hydroquinone or 1-phenyl-3-pyrazolidone. However, the activity of the combinations was lower than that of Elon*-hydroquinone, and they gave less emulsion speed and more fog. Two of the agents were oxidized with silver ammonium nitrate and found to form two atoms of silver per mole of developing agent.**

## 1. The Nature of Pyrimidines

The pyrimidine ring comprises two nitrogen and four carbon atoms. It has considerable biological and pharmaceutical importance, since it is a component part of the purines and of the barbiturates. Oxygen-substituted pyrimidines are written with either a keto or an enol structure, that is saturated or unsaturated, according to the nature of the reactions which they undergo.

Written in the classical keto form, barbituric acid and 5-aminobarbituric acid (uramil) appear as

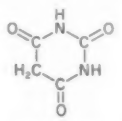

I. Barbituric Acid

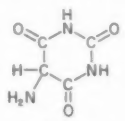

II. Uramil

The carbonyl groups indicated by these formulas undergo typical reactions, such as the formation of hydrazones and oximes.

Alternatively, however, the structures may be written in the enol form as

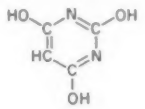

Ia

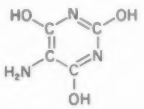

IIa

The hydroxy groups react to form metal salts and to give colored compounds with ferric chloride. Often the pyrimidines react as if they were only partially enolized.

Uramil, with its adjacent hydroxy and amino groups, might be expected to be more reactive than barbituric acid. It was found that, when solutions of uramil and barbituric acid were made alkaline with sodium hydroxide, the uramil strongly developed Velox paper, but the barbituric acid produced no image. When the alkalinity of the solution was reduced to about 10.0, the uramil developed only a trace of an image. However, on the addition of a small quantity of 1-phenyl-3-pyrazolidone, which is itself a weak developer but a powerful accelerator under these conditions of test, a strong image was again produced.

Communication No. 2004 from the Kodak Research Laboratories. Received 12 February 1959.

* Elon Developing Agent is the Eastman Kodak Company trademark for *p*-methylaminophenol sulfate.

## 2. Spot Tests

A spot-test technique described under "Experimental Procedures" was used to examine a number of pyrimidines substituted by oxygen (or hydroxy) and amino groups. Those giving positive results are listed in Table I. In each case, the oxygen is written in the hydroxy form. Compound I is barbituric acid, II is uramil, III is 5-aminouracil (5-amino-2,4-dihydroxypyrimidine), IX is dialuric acid, and X is 5,6-diaminouracil (5,6-diamino-2,4-dihydroxypyrimidine). All of these represent samples of commercial materials. The other eight compounds were specially synthesized. They may be named by their structures, as follows:

IV. 5-Amino-4,6-dihydroxypyrimidine
V. 2,4,5-Triaminopyrimidine
VI. 6-Methyl-2,4,5-trihydroxypyrimidine
VII. 2-Amino-4,5-dihydroxy-6-methylpyrimidine
VIII. 4-Amino-5,6-dihydroxy-2-methylpyrimidine
XI. 2,5-Diamino-4,6-dihydroxypyrimidine
XII. 2-Thiouramil
XIII. 2,5-Dihydroxy-4,6-dimethylpyrimidine

The enol form of the structures of uric acid, alloxantin, and murexide are as follows:

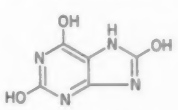

XIV. Uric Acid

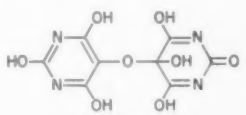

XV. Alloxantin

**TABLE I**
**Spot Tests of Substituted Pyrimidines**

| Compound No. | 2 | 4 | 5 | 6 | With NaOH (W) | With sodium sesquicarbonate: Alone (A) | With sodium sesquicarbonate: +PP* (B) |
|---|---|---|---|---|---|---|---|
| I | OH | OH | H | OH | 0, 0 | — | — |
| III | OH | OH | $NH_2$ | H | +, 0 | 0, 0 | 0, 0 |
| IV | H | OH | $NH_2$ | OH | ++, + | 0, 0 | +, 0 |
| V | $NH_2$ | $NH_2$ | $NH_2$ | H | +++, 0 | ++, 0 | ++, tr |
| VI | OH | OH | OH | $CH_3$ | ++, + | 0, 0 | +, 0 |
| VII | $NH_2$ | OH | OH | $CH_3$ | +++ > +++ | tr, 0 | ++, 0 |
| VIII | $CH_3$ | $NH_2$ | OH | OH | +++ > +++ | +++, 0 | ++, 0 |
| IX | OH | OH | OH | OH | ++, ++ | 0, 0 | ++, 0 |
| II | OH | OH | $NH_2$ | OH | +++, +++ | tr, 0 | ++, 0 |
| X | OH | OH | $NH_2$ | $NH_2$ | +++ > +++ | 0, 0 | +, 0 |
| XI | $NH_2$ | OH | $NH_2$ | OH | +++ > +++ | +++, 0 | ++, + |
| XIV | Uric Acid | | | | +, tr | 0, 0 | 0, 0 |
| XV | Alloxantin | | | | ++, + | 0, 0 | +, 0 |
| XVI | Murexide | | | | tr, 0 | 0, 0 | 0, 0 |
| Hq | Hydroquinone | | | | +++, ++ | tr, 0 | ++, 0 |
| XII | SH | OH | $NH_2$ | OH | + > + | 0, 0 | — |
| XIII | OH | $CH_3$ | OH | $CH_3$ | 0, 0 | 0, 0 | 0, 0 |

* 1-Phenyl-3-pyrazolidone

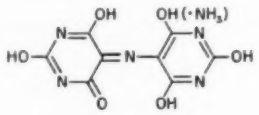

XVI. Murexide

Following common convention, ring carbon atoms are not noted.

The approximate degree of development is indicated by the system of "+'s" employed in Table I. These ratings are as follows:

| | |
|---|---|
| +++ | Strong, complete development |
| ++ | Intermediate |
| + | Clearly visible |
| tr | Trace |

The first value entered in each column is for the image; the second, for the fog. The "+" value given by the 1-phenyl-3-pyrazolidone (PP) blank has been subtracted from the values entered under "B" to give the net due to the pyrimidine, so a "++" represents maximum black.

In addition to the compounds of Table I, alloxan, violuric acid, 2-aminopyrimidine, thiobarbituric acid, caffeine, theobromine, and xanthine were tested with negative results.

## 3. Developing-Rate Tests

Where the initial spot test was encouraging and sufficient quantity of the material was available, the developing activity of the compounds was determined for a pH of 10.0. The pyrimidines were employed at 0.02 molar concentration; (1) alone; (2) + 0.02 molar hydroquinone; and (3) + 0.0025 molar phenylpyrazolidone (PP). Density data from these tests are entered in Tables II and III.

**TABLE II**
**Relative Activity (pH = 100.; 68°F)**
(Kodak Fine Grain Positive Film)

| Agent No. | Net Densities: 4 Min $D_3$ | 4 Min $D_9$ | 4 Min Fog | 32 Min $D_3$ | 32 Min $D_9$ | 32 Min Fog |
|---|---|---|---|---|---|---|
| III | 0.00 | 0.00 | 0.00 | 0.22 | 0.04 | 0.00 |
| VI | 0.00 | 0.00 | 0.00 | 0.08 | 0.00 | 0.00 |
| VII | 0.19 | 0.00 | 0.00 | 3.66 | 1.14 | 0.08 |
| VIII | 1.54 | 0.42 | 0.03 | — | — | — |
| II | 0.33 | 0.07 | 0.00 | 3.64 | 1.20 | 0.13 |
| X | 0.04 | 0.00 | 0.00 | 1.96 | 0.49 | 0.01 |
| XI | 1.94 | 1.05 | 0.58 | — | — | — |
| Elon | 2.70 | 0.98 | 0.08 | — | — | — |
| Hq | 0.05 | — | — | 3.49 | — | — |
| PP | 0.43 | — | — | 1.22 | — | — |

**TABLE III**
**Relative Activity — Combinations of Agents (pH = 10.0)**
(Kodak Fine Grain Positive Film — 4 min at 68°F)

| Agent No. | With Hydroquinone $D_3$ | With Hydroquinone $D_9$ | With Hydroquinone Fog | With Phenylpyrazolidone $D_3$ | With Phenylpyrazolidone $D_9$ | With Phenylpyrazolidone Fog |
|---|---|---|---|---|---|---|
| III | 0.94 | 0.28 | 0.01 | 1.29 | 0.28 | 0.02 |
| VI | 0.20 | 0.04 | 0.01 | 1.76 | 0.59 | 0.05 |
| VII | 0.82 | 0.17 | 0.01 | 2.08 | 0.81 | 0.08 |
| VIII | 2.24 | 0.59 | 0.10 | — | — | — |
| II | 0.96 | 0.27 | 0.01 | 2.01 | 1.12 | 0.19 |
| X | 0.72 | 0.17 | 0.01 | 1.58 | 1.48 | 0.06 |
| Elon | 3.39 | 1.16 | 0.09 | 2.76 | 1.06 | 0.10 |

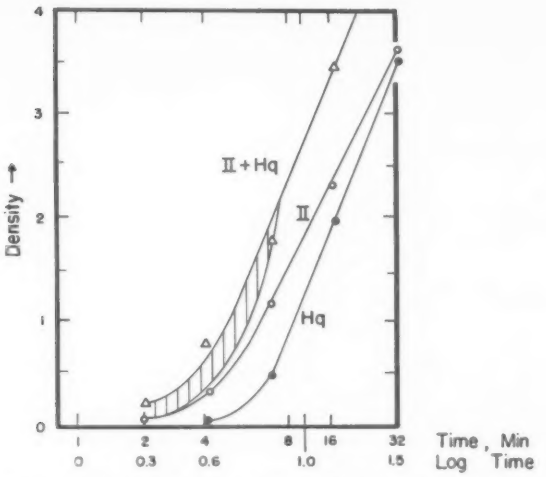


Fig. 1. Density:log time curves for uramil (II), hydroquinone (Hq), and the combination. The shaded area indicates the extent of superadditivity, in which the density given by the combination exceeds the sum of the densities given by the separate agents.

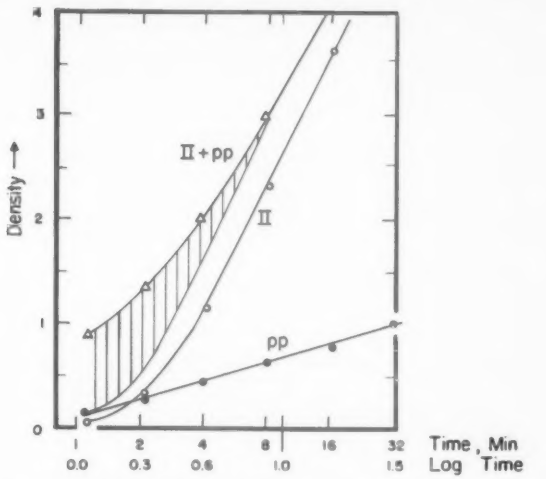


Fig. 2. Density:log time curves for uramil (II), 1-phenyl-3-pyrazolidone (PP), and the combination. The area of superadditivity is shaded.

These results will be seen to be generally consistent with those obtained in the spot tests. Those agents which are weak in caustic solution fail to develop in carbonate solution except when the time is greatly prolonged. The agents containing three functional groups and a hydrogen (III, IV) are weaker than those containing the three functional groups and a methyl (VII, VIII). Those containing four functional groups are active, but VIII is surpassed only by XI. The compound with three amino groups, V, is exceptionally active, while those with only hydroxy groups, VI and IX, are very pH-dependent, and XIII failed to develop, although it did reduce alkaline silver nitrate. However, VI and IX are active in the presence of the PP. Alloxantin, XV, is reported to be largely dissociated to dialuric acid, IX, and alloxan, XVII, in solution; development may, therefore, be due to the dialuric acid obtained. Murexide, XVI, hydrolyzes readily in alkaline solution to dialuric acid and uramil and the weak development indicated in Table I, which was quite variable from test to test, may be due to these hydrolysis products.

In every case, combinations of the agents with hydroquinone were superadditive to some extent; that is, the combinations produced greater image density than was obtained by adding the density produced by hydroquinone to that produced by the pyrimidine, at least for short times of development, as in the 4 min selected for the tests of Table II. A better idea of the effect over the complete time range is given in Fig. 1, which applies to uramil and hydroquinone. This shows that, while the combination is more active than either constituent alone, over the entire time range, superadditivity (shown by the shading) is confined to the first 10 min.

The development of all the weaker agents was markedly accelerated by the addition of PP, whose strong effect in accelerating development by weakly charged agents has been reported in other papers.[1] It will be noted that the effect of the PP on Elon, which is already developing actively, is very slight. The large effects on the pyrimidines would indicate that they are developing as negatively charged ions. Figures 1 and 2 give the complete time-density picture for the systems, uramil + hydroquinone, and PP + uramil. The superadditive effects are strong for short times of development but disappear as the time is extended.

## 4. Sensitometric Data

The data in Table IV apply to three emulsions: the positive film of the rate tests; the very high speed emulsion, Kodak Royal X Pan Film; and an experimental coating of a simpler negative emulsion. The pyrimidines proved relatively less active, compared to Elon-hydroquinone, on the negative emulsions than

TABLE IV
Sensitometric Data

| Developer | Time (min) | Density (3rd step) | Gamma | Relative Speed (Log 1/E) | Fog |
|---|---|---|---|---|---|
| 1. *Kodak Fine Grain Positive Film* | | | | | |
| DK-50 | 5.0 | 2.90 | 2.18 | 0.84 | 0.03 |
| VIII + Hq | 6.4 | 2.88 | 2.35 | 0.70 | 0.09 |
| 2. *Kodak Royal-X Pan Film* | | | | | |
| DK-50 | 5.0 | 1.31 | 0.88 | 3.53 | 0.09 |
| II + PP | 14.0 | 1.32 | 0.41 | 3.54 | 0.73 |
| VIII + PP | 10.0 | 1.33 | 0.76 | 3.43 | 0.31 |
| VIII + Hq | 10.0 | 1.32 | 0.86 | 3.43 | 0.10 |
| 3. *Bromoiodide Emulsion* | | | | | |
| DK-50 | 5.0 | 1.29 | 0.77 | 2.57 | 0.06 |
| VIII + Hq | 10.0 | 1.27 | 0.80 | 2.27 | 0.22 |

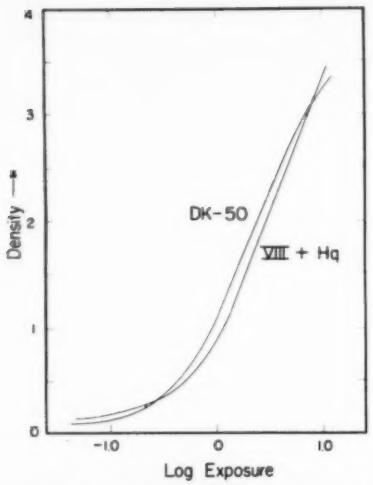


**Fig. 3. Characteristic curves comparing Kodak Developer DK-50 containing Elon and hydroquinone, with a combination of 4-amino-5,6-dihydroxy-2-methylpyrimidine (VIII) and hydroquinone. Kodak Fine Grain Positive Film at 68°F; DK-50, 5 min.; VIII + Hq, 7 min.**

on the positive film. The combination of VIII (4-amino-5,6-dihydroxy-2-methylpyrimidine) with hydroquinone proved the most promising. It showed one half to possibly two thirds the activity of the Elon-hydroquinone developer, Kodak Developer DK-50 (which has similar pH and developing agent concentrations), but gave appreciably higher fog and lower emulsion speed. Surprisingly, it appeared to work well with the very complex Royal X emulsion. Sensitometric curves for the positive emulsion are reproduced in Fig. 3.

## 5. Oxidation: Silver Equivalence

Hydroxy- and amino-substituted benzenes are oxidized to the corresponding quinones and quinonimines

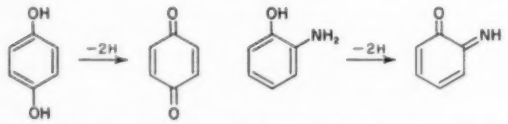

Hydroquinone Quinone *o*-Aminophenol *o*-Benzoquinonimine

An analogous type of oxidation might be expected for the pyrimidines. This is borne out for the aerial oxidation of dialuric acid where alloxan is formed over a wide range of conditions.[2]

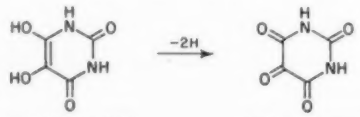

IX. Dialuric Acid XVII. Alloxan

In this case, the keto form has been employed in writing the equation, since it is always employed for alloxan, and it illustrates a simple oxidation around the ene-diol group HO—C=C—OH.

Uramil has been reported as oxidized by silver oxide to murexide, XVI.[3] This would correspond to the loss of only one hydrogen, and the murexide could be considered roughly analogous to quinhydrone. Similarly, the intermediate oxidation product of dialuric acid is alloxantin (XV); but, although this has been reported as an oxidation product in some reactions, it apparently does not occur on aerial oxidation.[2]

An idea of the nature of the product formed during development may be obtained by determining the silver equivalence. This was done for two of the agents, by using a technique employed by Tarassenkof for the analytical determination of hydroquinone.[4] A silver ammonium nitrate solution was added to a hot aqueous solution of the developing agent and, after reaction, the solution was filtered and the silver weighed. Since this reaction was slightly on the acid side (pH = 4), the filtrate was made slightly alkaline with ammonium hydroxide (pH = 8 to 9), heated again, and any further deposit of silver was collected.

As indicated in Table V, an exact equivalence of 2.00 atoms of silver was obtained for each molecule of hydroquinone. The two pyrimidines also gave values close to 2.0. Agent VII gave a low value on the first assay, but a very good equivalence when the second precipitate of silver was collected. The value given by the uramil was almost exactly 2.0.

**TABLE V**
**Silver Equivalence**

| Agent | Weight Taken (mg) | Silver Found (mg) | Equivalence (atoms/mole) |
|---|---|---|---|
| Hydroquinone | 110 | 216 | 2.00 |
| VII | 141 | 190* | 1.75 |
| | | 221† | 2.04 |
| II | 143 | 215* | 1.99 |
| | | 218† | 2.01 |

* Acid precipitation
† Acid + alkaline precipitation

The equivalence of two atoms of silver per mole would indicate that two functional groups were oxidized in each case. Presuming these to be in adjacent positions, the oxidation products would be:

2-Amino-4,5-diketo-6-methylpyrimidine Alloxanimine

Alloxanimine is formed as an intermediate in one preparation of uramil. It is not difficult to cleave the pyrimidine ring under slightly stronger oxidizing conditions, but this seems less probable here.

## 6. Literature

Reducing properties have been reported for a great number of pyrimidines. Thus, dialuric acid, uramil, aminouracil, and diaminouracil are known to reduce ammoniacal silver nitrate. Dialuric acid has been employed in chemical reductions. Knott reports on the examination of some twenty-six reducing pyrimidines, using iodine as an oxidizing agent for a system of identification.[5] His pyrimidines contain amino or hydroxy groups in the 5-position, and amino, hydroxy, or mercapto groups in the 2-position. This gives an idea of the great number of reducing agents in this ring system.

The use of pyrimidines containing amino and hydroxy groups in the 2- and 5-positions as photographic developing agents is the subject of a twenty-year-old patent.[6] This patent describes four compounds: the diaminouracil, X; 6-hydroxy-2,4,5-triaminopyrimidine; 2,4,5,6-tetraminopyrimidine; and 2,5-diamino-6-methylpyrimidine. This patent relates the developing activity to the "para" (2,5) positioning of the functional groups. However, we found that 2,5-dihydroxypyrimidine (XIII) was too weak to produce an image. Neither the patent nor Knott's paper describes compounds containing only adjacent functional groups such as IV, VIII, and XII of Table I. The patent mentions fine-grain developing properties which we did not confirm; although agent VIII in combination with hydroquinone produced a warm-toned image and a loss in emulsion speed, characteristics possessed by many fine-grain developers, no reduction in graininess was obtained. Saunders has described the use of dialkylamino pyrimidines as color developers.[7]

## 7. Experimental Procedures

(*a*) *Spot Testing*. The solutions used in making these tests comprised, per milliliter:

| | W | A | B |
|---|---|---|---|
| Substituted pyrimidine | 10.0 mg | 5.0 mg | 5.0 mg |
| Sodium sulfite, desiccated | 25.0 mg | 25.0 mg | 25.0 mg |
| Sodium hydroxide | 25.0 mg | — | — |
| Sodium sesquicarbonate | — | 75.0 mg | 75.0 mg |
| 1-Phenyl-3-pyrazolidone (PP) | — | — | 0.25 mg |
| Acetonitrile | 0.2 ml | 0.2 ml | 0.2 ml |
| Water | 0.8 ml | 0.8 ml | 0.8 ml |

The acetonitrile was included as a water-miscible solvent of polar and nonpolar properties. It was less necessary in these tests than in some others, since most of the pyrimidines were readily soluble in the alkaline solution. The large excess of sesquicarbonate buffered the solution at a pH level of about 9.7.

In making the test, half of a sheet of Kodak Velox F-4 Paper, chosen as representing a simple, rapid-developing chloride-type emulsion, was given a strong controlled exposure. The "developer" was streaked across the paper, along with control solutions, so as to cross from the exposed to the unexposed area, and allowed to stand 3 min at approximately 25°C. The paper was then rinsed, fixed, and washed.

(*b*) *Developing-Rate Measurements*. The solutions comprised:

| | No. 1 | No. 2 | No. 3 |
|---|---|---|---|
| | (Moles per Liter) | | |
| Experimental agent | 0.02 | 0.02 | 0.02 |
| Hydroquinone | — | 0.02 | — |
| 1-Phenyl-3-pyrazolidone, PP | — | — | 0.0025 |
| Sodium sulfite, desiccated | 0.20 | 0.20 | 0.20 |
| Sodium carbonate, monohydrate | 0.20 | 0.20 | 0.20 |
| Acetic acid to pH = | 10.0 | 10.0 | 10.0 |

The molar quantities amount to approximately 25 grams/liter of sodium carbonate and sodium sulfite, 2 to 5 grams/liter of the developing agents, and 0.4 gram/liter of the PP. Processing was at 68°F with high agitation, in small-scale sensitometric equipment.[8] The third step density selected for the primary measurements lies high on the sensitometric curve; the ninth step density, at 0.9 log E units less exposure.

(*c*) *Tests with the Negative Films*. The developer formulas were the same as used in the developing-rate tests with the exception that 0.004 mole (0.5 gram) of potassium bromide was added per liter to the combination of VIII + hydroquinone.

(*d*) *Analytical Procedure*. The silver-ammonium nitrate reagent comprised:

| | |
|---|---|
| Silver nitrate | 0.4 mole (67.6 grams) |
| Ammonium nitrate | 4.0 moles (322 grams) |
| Water to | 1.0 liter |

An 0.001 molar quantity of the developing agent was weighed out on an analytical balance and added to 80 ml of hot, air-free water. This was brought to a boil, and 12.5 ml of the silver-ammonium nitrate reagent (containing 0.005 mole of silver) were added slowly from a buret. The first additions had to be made very slowly, with strong stirring, to assure a coarse precipitate that would filter readily. The solution was then again heated, boiled for 5 min, and allowed to stand for 25 min, and then the precipitate was filtered off, washed thoroughly, dried, and weighed.

## Acknowledgment

We wish to acknowledge the large contribution of C. F. H. Allen and his co-workers, particularly G. A. Reynolds, for the synthesis of many of the compounds studied.

## References

1. James, T. H., *PSA Jour., Phot. Sci. Tech., 19B:* 156 (1953).
2. Richardson, G. M., *Biochem. J., 26:* 1959 (1932).
3. Piloty, O., and Einckh, K., *Ann. Chem., 333:* 87 (1904).
4. Tarassenkof, D., *Sci. ind. phot., 7M (Memoires originaux):* 40 (July 1927).
5. Knott, E. B., *J. Soc. Chem. Ind. (London), 60:* 313 (1941).
6. I. G. Farbenindustrie A.-G., Brit. Pat. 479,446 (1936).
7. Saunders, D. G., *J. Chem. Soc. (London):* 3232 (1956).
8. Henn, R. W., and Hughes, K. R., *Phot. Sci. & Eng., 2:* 81 (1958).

PHOTOGRAPHIC SCIENCE AND ENGINEERING
Volume 3, Number 3, May-June 1959

# The Calcium-Sequestering Properties of Organic Compounds in Photographic Developers

R. W. HENN, *Research Laboratories, Eastman Kodak Company, Rochester, N.Y.*

**The quantity of calcium sulfite held in solution in a photographic developer is used as the means of measuring the relative sequestering power of seventy-two organic compounds, of widely differing structures. Chelate rings are formed between a carboxy-, nitroso-, or nitro-primary group and an oxy-, hydroxy-, amino-, or olefinic-secondary group. Multiple chelation greatly enhances sequestration. Sulfonic acid groups show no activity, while mercapto groups are weak. These systems greatly increase the number of calcium-sequestering agents described, and have led to some practical photographic applications.**

Calcium reacts with certain constituents of photographic developers to produce calcium precipitates which are undesirable in processing. The source of the calcium is usually hard-water supplies and sometimes the photographic emulsion. The calcium precipitates as the sulfite, borate, or carbonate to form sludges in the developer, scum on the film, and scale on equipment. Studies of calcium precipitates have been made by Crabtree[1] and Crabtree and Henn.[2] The most common technique of overcoming the difficulty has been to complex the calcium in an unionized form in a sequestering agent such as a polyphosphate,[2,3] or an aminopolyacetic acid.[4–8] Further advantages are claimed by mixtures of sequestrants. Pyridine carboxylic acids have also been proposed.[9]

The available sequestering agents have offered some disadvantages when applied to the photographic processes. The polyphosphates slowly hydrolyze to the orthophosphates which form insoluble calcium precipitates, and the calcium polyphosphate complex dissociates slowly to release calcium which recombines to form scales and sludges. Ethylenediaminetetraacetic acid is the most powerful of the amino-acid sequestering agents and is capable of holding calcium in a much tighter complex than the polyphosphates. However, in the presence of iron, it promotes developer oxidation, but this can be prevented quite well by the addition of 8-hydroxyquinoline or its derivatives to the developer.[10]

Calcium forms few of the chelate rings characteristic of many of the heavier metals.[11] The discovery of the complexing ability of the aminopolyacetic acids has had great commercial importance, but even now few types of calcium-complexing agents have been described. Consequently, it seems worth while to summarize the results of this investigation, since it covers a large number of organic compounds of widely differing structures. The data are also significant because the various compounds have been studied in photographic developers, providing information of potential usefulness in the photographic field.

The data obtained have revealed some significant relationships between organic structure and calcium-sequestering ability, and have greatly extended the number of compounds known to complex calcium. The study has disclosed some compounds of practical interest, including the strongly complexing amino acid, 1,3-diaminopropanoltetraacetic acid, which does not promote developer oxidation.[5] The study has also resulted in the discovery of oxyacetic acid complexing agents, such as diglycolic acid, which, when used in conbination with a polyphosphate, produce a powerful sequestering system.[8]

## Experimental Procedure

The sequestering action of the compound was evaluated by its ability to prevent the precipitation of calcium sulfite in a developer and should apply to any moderately alkaline solution containing sulfite as the precipitating ion.

The compound, usually an acid, was added at several concentrations in the range of 0.01 to 1.0 *M* to the control developer, together with sufficient sodium hydroxide or sulfuric acid to maintain the pH. A series of calcium chloride concentrations was added to each of the modifications, using 0.01 or 0.1 *M* chloride solution. The resulting mixture was shaken to dissolve or disperse the precipitate formed and was then held for 5 min at 60°C. The concentration of calcium chloride at which the first precipitate was formed was noted. In the case of darkly colored solutions, and those containing suspended matter, it was sometimes necessary to filter and analyze the precipitate obtained. This was done by reprecipitating the calcium as the oxalate and titrating it with permanganate.

Communication No. 1413 from the Kodak Research Laboratories. Received 12 February 1959.

The developer formula employed in these tests, reduced to its simplest terms, comprised sodium sulfite, 0.5 *M;* sodium metaborate, 0.073 *M;* and sufficient acid to adjust the pH to 9.8. The precipitate formed in this case is largely the sulfite, although a calcium-sodium borate has been formed in the sludge formed in used developers. Measurements have also been made with a carbonate-containing developer, in which case the calcium is precipitated as the carbonate. The sequestering values are much lower in this case and may amount to as little as one-tenth of that obtained against sulfite precipitation. This formula was 0.12 *M* with respect to sulfite and 0.2 *M* with respect to carbonate and was effective at a pH of 10.2. The measurements obtained with this developer are not included in the table, but are referred to in the discussion.

The calcium-sequestering value was measured as the difference between the threshold value in the absence of the complexing compound, and that determined in its presence. In most cases, the net sequestering action of the addition agent was fairly proportional to its concentration, with somewhat greater-than-proportional values being obtained at high concentrations of the addendum. The results given in the accompanying table have been expressed in terms of millimoles of calcium chloride sequestered per mole of addendum and represent an average of the values obtained. A few exceptions to the linear relationship between concentration and sequestering action were obtained, and here the range of strength is noted. For example, in the case of citraconic acid, Compound No. 52 in the table, a 1 *M* concentration sequestered nearly 0.1 mole of calcium chloride, but a 0.25 *M* solution would sequester only 0.003 mole. Evan acid, No. 55, showed a similar concentration effect.

## Discussion of Results

On the basis of the sequestering values entered in the table, and from information with regard to chelate ring structures which appears in the literature, certain structural influences appear to be established. Since the experimental evidence is, however, largely limited to the determination of the values entered in the table, the influences deduced and structures derived are not suggested as the only possible interpretation of the data.

1. Two distinct types of groups are found in the successful sequestering agents: one yielding a primary, covalent, or acidic bond, such as the carboxy or nitroso group; and one yielding a secondary or coordinate link, such as the hydroxy or amino group. Compounds in which both groups are either primary or secondary, common as they are to chelation chemistry, have proved weak or unsuccessful in reducing the concentration of calcium ions in these aqueous, alkaline systems (e.g., Nos. 59–72). In some compounds, the "secondary" group may be functioning as an acid to a greater or lesser extent, for example, in the phenolic hydroxy groups of gallic acid, No. 23, but even so it cannot be replaced by the strongly acidic carboxy groups (as in pyromellitic acid, No. 63) without losing its sequestering potency.

2. These functions should be placed alpha to each other so as to form a 5-membered ring with the calcium atom, although weak sequestering is obtained with 6-membered rings and may be of supplementary benefit. Compare Nos. 14 and 29, 13 and 31. But the supplemental action of the 6-membered ring has made No. 22 stronger than No. 25, and No. 9 stronger than No. 10.

Multiple rings, acting through the same molecule, greatly extend sequestering action and, where two or more rings are drawn through the same bond, the stability appears to be further enhanced. The conditions for stable chelation of calcium, which has a coordination number of six, should be achieved with the five 5-membered rings of ethylenediaminetetraacetic acid (No. 1). The progressive effect of multiple chelation is indicated in the following series:

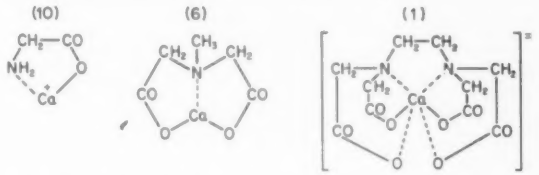


| *Sequestering (Millimoles per mole)* | | |
|---|---|---|
| To sulfite: | | |
| 4 | 180 | 1000 |
| To carbonate: | | |
| — | 25 | 800 |

The stability of the ethylenediaminetetraacetic acid–calcium complex and the repression of ionization are confirmed by both experimental and practical evidence. This evidence includes the high sequestering values noted, the titrations of Schwarzenbach and Ackermann,[12] long-term and high-temperature keeping tests, and the present commercial importance of this compound. Triglycin, or nitrilotriacetic acid, No. 4, while sequestering nearly as much calcium temporarily, holds it less stably than No. 1.

The sequestering properties of 1,3-diaminopropanotetraacetic acid, No. 3, are not far above those obtained by Schwarzenbach and Ackermann for 1,3-diaminopropanetetraacetic acid. However, the hydroxy group may also enter into ring formation in the manner shown here.

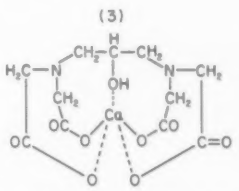


It is interesting to compare the values of Schwarzenbach and his co-workers, determined by titrating the acid both in the presence and in the absence of calcium, with the values obtained by the precipitation method just described.

## Calcium-Sequestering Power of Various Addenda in a Sulfite-Borate Photographic Developer

| No. | Compound | Sequestering (Millimoles Calcium Chloride per Mole) |
|---|---|---|
| | *Amino Carboxylic Acids* | |
| 1. | Ethylenediaminetetraacetic acid $(HOOCCH_2)_2NCH_2CH_2N(CH_2COOH)_2$ | 1000 |
| 2. | 1,2-Diaminocyclohexanetetraacetic acid $C_6H_{10}[N(CH_2COOH)_2]_2$ | 1000 |
| 3. | 1,3-Diaminopropanoltetraacetic acid $(HOOCCH_2)_2NCH_2CH(OH)CH_2N(CH_2COOH)_2$ | 740 |
| 4. | Nitrilotriacetic acid $N(CH_2COOH)_3$ | 700 |
| 5. | β-Alaninediacetic acid $(HOOCCH_2)_2NCH_2CH_2COOH$ | 200 |
| 6. | Methylaminodiacetic acid $CH_3N(CH_2COOH)_2$ | 180 |
| 7. | Anthranilic diacetic acid $2\text{-}[N(CH_2COOH)_2]C_6H_4COOH$ | 320 |
| 8. | Glutamic acid $HOOCCH_2CH_2CH(NH_2)COOH$ | 30 |
| 9. | Aspartic acid $HOOCCH_2CH(NH_2)COOH$ | 35 |
| 10. | Glycine $H_2NCH_2COOH$ | 4 |
| | *Hydroxy- and Oxy-Carboxylic Acids* | |
| 11. | Tartronic acid $(HOOC)_2CHOH$ | 200 |
| 12. | Diglycolic acid (α,α′-Oxydiacetic acid) $(HOOCCH_2)_2O$ | 170 |
| 13. | Ethylene bisglycolic acid $HOOCCH_2OCH_2CH_2OCH_2COOH$ | 130 |
| 14. | Pyruvic acid $CH_3COCOOH$ | 60 |
| 15. | Citric acid $HOOCC(OH)(CH_2COOH)_2$ | 120 |
| 16. | Tartaric acid $HOOCCHOHCHOHCOOH$ | 55 |
| 17. | Gluconic acid $CH_2OH(CHOH)_4COOH$ | 90 |
| 18. | Galacturonic acid $CHOH(CHOH)_3CH(COOH)$ (O) | 90 |
| 19. | Saccharic acid $HOOC(CHOH)_4COOH$ | 150 |
| 20. | Mucic acid $HOOC(CHOH)_4COOH$ | 60 |
| 21. | Quinone tetracarboxylic acid $C_6O_2(COOH)_4$ | 100 |
| 22. | Malic acid $HOOCCHOHCH_2COOH$ | 35 |
| 23. | Gallic acid $3,4,5\text{-}(HO)_3C_6H_2COOH$ | 40 |
| 24. | Oxalacetic acid (Ketosuccinic acid) $HOOCCH_2COCOOH$ | 90 |
| 25. | Glycolic acid $HOCH_2COOH$ | 6 |
| 26. | Lactic acid $CH_3CHOHCOOH$ | 6 |
| 27. | Mandelic acid $C_6H_5CHOHCOOH$ | 10 |
| 28. | Benzilic acid $C_6H_5C(OH)(C_6H_5)COOH$ | 12 |
| 29. | Levulinic acid $CH_3COCH_2CH_2COOH$ | 5 |
| 30. | Acetoacetic acid $CH_3COCH_2COOH$ | 20 |
| 31. | Tricarboxyethoxy propane $C_3H_5\text{-}1,2,3\text{-}(OCH_2CH_2COOH)_3$ | 30 |
| 32. | 4-Hydroxyphenoxyacetic acid $HOC_6H_4OCH_2COOH$ | 3 |
| | *Heterocyclics* | |
| 33. | Imidazole-4,5-dicarboxylic acid HOOC−C=C(COOH)N=CHNH (ring) | 170 |
| 34. | 2,5-Dicarboxy-3,4-dihydroxyfurane HOCC(COOH)OC(COOH)COH (ring) | 150 |
| 35. | Pyridine-2,6-dicarboxylic acid HOOC−C=N−C(COOH)=CH−CH=CH (ring) | 380 |
| 36. | Alloxan NHCONHCOCOCO (ring) | 75 |
| 37. | Parabanic acid NHCONHCOCO (ring) | 25 |
| 38. | Methylene citric acid $CH_2OC(CH_2COOH)_2C(O)O$ (ring) | 10 |
| 39. | Dehydroacetic acid $OCOCH(COCH_3)COCH=CCH_3$ (ring) | 25 |
| 40. | Dehydromucic acid HOOC−C=CH−CH=C−COOH (O ring) | 14 |
| 41. | Violuric acid NHCONHCOC=NOHCO (ring) | 10 |
| 42. | 3-Nitrophthalimide $3\text{-}NO_2C_6H_3\text{-}1,2\text{-}(CO)_2NH$ | 20 |
| 43. | Furoic acid HC=CHCH=C(COOH)O (ring) | 2 |
| 44. | Quinaldinic acid $C_6H_4N=C(COOH)CH=CH$ (ring) | 3 |
| 45. | 2-Hydroxybenzoxazole $C_6H_4OC(OH)=N$ (ring) | 2 |
| | *Nitro and Nitroso* | |
| 46. | Nitrosoresorcinol $1\text{-}NOC_6H_3\text{-}2,4\text{-}(OH)_2$ | 320 |
| 47. | Dinitrosoresorcinol $2,4\text{-}(NO)_2C_6H_2\text{-}1,3\text{-}(OH)_2$ | 400 |
| 48. | Picric acid $2,4,6\text{-}(NO_2)_3C_6H_2OH$ | 80 |
| | *Diazo* | |
| 49. | Diazomalonic acid $N_2CH(COOH)_2$ | 140 |
| | *Unsaturates* | |
| 50. | Maleic acid HOOCCH=CHCOOH | 20 |

Calcium-Sequestering Power of Various Addenda in a Sulfite-Borate Photographic Developer (Continued)

| No. | Compound | Sequestering (Millimoles Calcium Chloride per Mole) |
|---|---|---|
| 51. | Aconitic acid $HC(COOH)=C(COOH)CH_2COOH$ | 30 |
| 52. | Citraconic acid $HOOCCH=C(CH_3)COOH$ | 2–100 |
| 53. | Acetylene dicarboxylic acid $HOOCC\equiv CCOOH$ | 20 |
| *Mercapto-carboxylic* | | |
| 54. | Quinone tetrathioglycolic acid $C_6O_2(SCH_2COOH)_4$ | 140 |
| 55. | Evan acid $HOOCCH_2SCH(COOH)CH_2COOH$ | 4–150 |
| 56. | Hydroquinone tetrathioglycolic acid $C_6(OH)_2(SCH_2COOH)_4$ | 20 |
| 57. | Thioglycolic acid (Mercaptoacetic acid) $HSCH_2COOH$ | 0.5 |
| 58. | Thiodiglycolic acid $S(CH_2COOH)_2$ | 3 |
| *Double Acid Function* | | |
| 59. | Succinic acid $(CH_2COOH)_2$ | 2 |
| 60. | Glutaric acid $CH_2(CH_2COOH)_2$ | 2 |
| 61. | Cyanoacetic $CNCH_2COOH$ | 1 |
| *Lack Sequestering Action* | | |
| 62. | n-Butane-1,2,3,4-tetracarboxylic acid $CH_2(COOH)CH(COOH)CH(COOH)CH_2COOH$ | |
| 63. | Pyromellitic acid $C_6H_2$-1,2,4,5-$(COOH)_4$ | |
| 64. | Ethylenediaminetetraglycol $(HOCH_2CH_2)_2NCH_2CH_2N(CH_2CH_2OH)_2$ | |
| 65. | Urea $H_2NCONH_2$ | |
| 66. | Guanidine $H_2NC(NH)NH_2$ | |
| 67. | Melamine $NH_2C=NC(NH_2)=NC(NH_2)=N$ | |
| 68. | Diacetyl $CH_3COCOCH_3$ | |
| 69. | Acetylacetone $CH_3COCH_2COCH_3$ | |
| 70. | N,N′-Ethylenediaminetetramethylenesulfonic acid $(HSO_3CH_2)_2N$-$C_2H_4$-N-$(CH_2SO_3H)_2$ | |
| 71. | 1,3-Indanedione $C_6H_4COCH_2CO$ | |
| 72. | 1,2,3-Triketohydrindene $C_6H_4COCOCO$ | |

*Notes*

1. Although the acid form of the compounds is given, they were employed in alkaline solution. Carboxylic acids would therefore be present as ions or their sodium salts and enols and nitroso compounds would be present in their alkaline form.
2. The esters of Compounds Nos. 24, 30, and 31 were hydrolyzed in dilute alkaline solution by holding at 90° to 100°C for 10 to 60 min. The formation of the acid indicated (or its sodium salt) was not verified by isolation.
3. As noted in the text, the sequestering action of Compounds Nos. 52 and 55 was dependent on the concentration in which they were employed.
4. Compounds Nos. 3, 5, 7, 11, 21, 31, 35, 38, 40, 49, 54, 56, 58, 64, and 70 were prepared by C. F. H. Allen and his co-workers, of these Laboratories, to whom the author is greatly indebted. The remainder represent commercial samples, mostly Eastman Organic Chemicals.

| Compound | Sequestering (Millimoles Ca) (Henn) | Log Bildungs Konstant (Schwarzenbach et al.) |
|---|---|---|
| 1. Ethylenediaminetetraacetic acid | 1000 | 10.5 |
| 2. Diaminocyclohexanediacetic acid | 1000 | 12.44 |
| 3. Diaminopropanoltetraacetic acid | 740 | — |
| Diaminopropanetetraacetic acid | — | 7.12 |
| 4. Nitrilotriacetic acid | 700 | 6.41 |
| 5. Alaninediacetic acid | 200 | 5.05 |
| 6. Methyliminodiacetic acid | 180 | 3.75 |

The qualitative agreement is good and the same increasing effect of multiple chelation is indicated.

3. The oxygen-substituted acetic acids are closely parallel to the aminoacetic acids in their calcium-sequestering properties but this analogy seems to have received little attention in the literature. Thus, compounds of the oxygen series show the following effects of multiple chelation and alternate methods of achieving multiple ring structure:

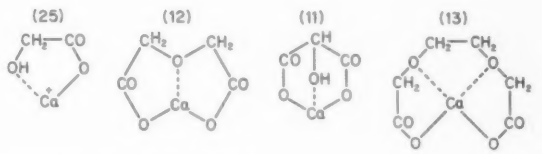


*Sequestering (Millimoles per mole)*

| | | | |
|---|---|---|---|
| To sulfite: | | | |
| 6 | 170 | 200 | 130 |
| To carbonate: | | | |
| 2 | 35 | — | 25 |

4. The chelating groups may be attached to aliphatic structures, as in the examples just given, or to a benzene ring, or they may form part of a cyclic compound. Compounds 23 (compare with No. 17), 46–48, and probably 7, illustrate the use of a benzene ring as an integral part of the chelate, whereas 27 and 28 illustrate benzene-ring substitution into an aliphatic compound (No. 25). Heterocyclics include Nos. 43 and 40, which are weaker than Nos. 25 and 12, respectively, but No. 34 is fairly powerful. The

dicarboxyimidazole, No. 33, compares well with its aliphatic analog, No. 6, while the dicarboxypyridine, No. 35, is more powerful. The heterocyclics, Nos. 36 and 37, are much more powerful than urea, No. 65. Placing the groups on the quinone ring appears helpful, tremendously increasing the potency of the weak thioglycolic acid (No. 54 vs. No. 57; see also No. 21 vs. No. 63).

5. The most potent of the primary groups is probably the nitroso, followed by the nitro and carboxy (see Nos. 46, 47, 48, and 23). Schwarzenbach, Ackermann, and Ruckstuhl report that the substitution of a phosphoric acid group for a carboxy group in No. 4 somewhat increased its calcium-sequestering action.[13] However, No. 70, in which the carboxy groups of No. 1 are replaced by sulfonic acid groups, proved inactive.

6. The secondary groups may be arranged in the following order of relative strength:

$$=O > -OH = -NH_2 > -C=C > SH$$

as demonstrated in the series No. 14 vs. No. 26, No. 10 vs. No. 25 vs. No. 57; also No. 9 vs. No. 22 vs. No. 50, and No. 12 vs. No. 6 vs. No. 58. In its lone example, No. 49, the diazo group appears exceptionally powerful (compare with Nos. 50, 9, and 22).

## References


1. Crabtree, J. I., *Amer. Phot.*, *12:* 126 (1918).
2. Henn, R. W., and Crabtree, J. I., *J. Soc. Mot. Pic. Engrs.*, *43:* 426 (1944).
3. Kieser, K., *Phot. Ind.*, *34:* 1166 (1936); *Brit. J. Phot.*, *84:* 232 (1937).
   ———, "Le 'Calcivore Lumière,' " *Rev. franç. phot. et cinémat.*, *18:* 76 (1937); *Brit. J. Phot.*, *84:* 184 (1937).
4. Munz, F., U.S. Pat. 2,240,957 (May 6, 1941).
5. Henn, R. W., and Piper, D. E., U.S. Pat. 2,656,273 (Oct. 20, 1953).
6. Miller, A., U.S. Pat. 2,172,216 (Sept. 15, 1939).
7. Henn, R. W., and Crabtree, J. I., U.S. Pat. 2,541,470 (Feb. 13, 1951).
8. Henn, R. W., U.S. Pat. 2,625,476 (Jan. 13, 1953).
9. Gevaert Photo-Producten N. V., Dutch Pat. 200, 654 (Sept. 22, 1955).
10. Henn, R. W., U.S. Pat. 2,691,588 (Oct. 12, 1954).
11. Diehl, H., *Chem. Revs.*, *21:* 39 (1937).
12. Schwarzenbach, G., and Ackermann, H., *Helv. Chim. Acta*, (a) *30:* 1798 (1947); (b) *31:* 1029 (1948). [These authors concede the hexadendate structure as logical.]
13. ———, ———, and Ruckstuhl, P., *Helv. Chim. Acta*, *32:* 1175 (1949).


# • Notes from the Editor

### *Editorial Staff Changes*

A valuable member of the Editorial Staff, Willard W. Van Allen, has found it necessary to relinquish his duties as Associate Editor of *P S & E*. Van served as Associate Editor of *Photographic Engineering* and continued in the same capacity for *P S & E* from the first issue until the present one.

Two new appointments have been made: N. A. Exley as Assistant Editor and S. C. Goddard as Feature Editor.

### *Mathematical Tables and Other Aids in Computation*

The Division of Mathematics of the National Academy of Sciences – National Research Council has announced that Harry Polachek, Technical Director of the Applied Mathematics Laboratory of the David Taylor Model Basin, has been appointed Chairman of the Editorial Committee for the quarterly journal *Mathematical Tables and Other Aids to Computation*, effective January 1959. This journal, founded in 1943, features original papers in numerical analysis, high speed computer methods, and other aids to computation, as well as short articles reporting upon the latest developments in these fields. Papers for publication should be addressed to: Harry Polachek, Editor, David Taylor Model Basin, Washington 7, D.C.

### *International Symposium*

An international symposium on scientific photography will be held at the University of Liège, September 14–19, 1959. Professor A. Hautot of that university is the General Chairman of the conference and Dr. H. Sauvenier is the Secretary. The conference is being organized to allow extended discussion of specific questions, and will be limited to the following subjects:

1. Factors in photographic sensitivity
   - A. Intrinsic sensitivity of crystals of silver halides (Professor Dekeyser, Chairman)
   - B. Influence of the binding agent, particularly gelatin (H. W. Wood and J. Pouradier, Chairmen)
   - C. Chemical sensitization (P. Faelens, Chairman)
2. Optical sensitization (B. H. Carroll, Chairman)
3. Nature of the exposure process
   - A. Fundamental processes of latent image formation (E. Klein, Chairman)
   - B. Reciprocity law failure (Professor J. Eggert, Chairman)

The program for the symposium is now substantially complete, and no additional papers will be accepted.

# • Book and Journal Reviews

## Simplified Satellite Prediction from Modified Orbital Elements

IGY Satellite Report Series Number 7, 1 January 1959, by L. N. Cormier, N. Goodwin, and R. K. Squires.

This booklet has been issued by the National Academy of Sciences—National Research Council, Washington, D.C., to enable those participating in the Phototrack and Moonbeam programs to make their own predictions as to when and where artifical satellites can be expected to pass near their stations. The authors point out that from a computation and communications standpoint the transmission of orbital elements offers the simplest method of supplying observers with the necessary data. Chief disadvantages to this method, however, are that many observers are not familiar with orbital elements, and for those who are, the required computation is extremely time-conconsuming. Chief advantage is that observers are able to receive up-to-date information in sufficient time for maximum usefulness The purpose of this booklet is to describe a prediction system of practical computation and communication which minimizes the disadvantages of using orbital elements.

The booklet contains all the computation forms, tables, and charts required to predict, from the orbital elements data, the precise time when the satellite will cross the observer's latitude circle, the longitude of the crossing, the satellite's height as well as the azimuth, elevation, and slant range of the satellite.

The modified orbital elements for a given satellite are communicated by the Smithsonian Astrophysical Observatory to participating volunteer observers by air mail postal card and by radio. The world-wide radio teletype channel is the IGY World Warning Agency which broadcasts the data in the SATOR code, explained in Appendix 2 of the booklet. Within the United States, Puerto Rico, and adjacent portions of Canada and Mexico, the data are broadcast by the Civil Air Patrol (CAP) voice communications network from a number of stations on Tuesday and Friday evenings. Special broadcasts are made nightly for a satellite with rapidly changing elements. A list of stations with their frequencies and times of broadcast is also given in Appendix 2.

Observers are cautioned by the authors that the time beyond orbital information for which a satellite's position can be predicted depends upon the stability of its orbit. For very stable orbits, satisfactory predictions can be made for a week or more in advance. For close-in orbits, predictions may be valid for only a few days in the future. During the terminal phase of a satellite's life, predictions may be reliable for no more than half a day. — *H. R. Condit.*

## Wissenschaftliche Photographie. Ergebnisse der Internationalen Konferenz für Wissenschaftliche Photographie Köln 24–27 September, 1956.

Verlag Dr. Othmar Helwich, Darmstadt, 1958. xviii + 723 pp., 7 × 10 in.

This volume contains 123 papers and discussion of the papers presented at the International Conference for Scientific Photography held at Cologne, Germany, in 1956. In the rather long interval between the Cologne meeting and the publication of the Proceedings, many of the Conference papers have been published elsewhere, either in full or as abridgments, and the information contained in certain others has been included in other publications by the authors. The amount of new material contained in the present volume, therefore, is relatively small. However, it is convenient to have these papers collected in one volume, and the publication, even though late, serves a useful purpose. The papers are published in either English, French, or German, with abstracts of each paper in the other two languages. The papers are grouped under the broad headings of photographic sensitivity, development, properties of photographic layers, photographic optics, and the theory of color photography. The paper, typography, and reproduction of figures are excellent. — *T.H.J.*

## Tekhnika Kino i Televideniya, October 1958

*Resumés by S. C. Goddard*

### *Use of Polymers in Cinematography*

P. V. Kozlov, pp. 1–9

As part of the drive to expand the plastics industry in the Soviet Union, attention is being paid to the more thorough-going use of plastics in the motion picture industry. The subject is surveyed with particular reference to the new polymers available for film base, the possibilities of producing plastic motion picture screens, the use of plastics in constructing studio sets, and the wider use of plastics in the structure of apparatus for cinematography.

### *An Infrared Reversal Film for Special Effects Cinematography with the Traveling-Matte Technique*

A. M. Churaeva, pp. 10–15

The new Russian-made infrared reversal film, Type 2, has its maximum sensitivity in the zone 805–810 mμ. It has three coatings, the lowest of which is a colloidal silver layer, with an optical density of at least 2, which intercepts any infrared radiation penetrating the base. The emulsion layer is coated on the silver layer, and a gelatin protective layer forms the

third. The actor is filmed against an infrared-reflecting screen with a double-exposure camera using color film (unaffected by infrared) and the masking film. The latter is reversal-processed to give a dark mask on a transparent background, and is then used over the still undeveloped color film to shoot the required background. The sensitometric properties of the film are discussed.

### *The Role of the Hydrodynamic Conditions in Accelerating the Processing of Black-and-White Films*

B. V. Valuiskii, pp. 36–47

Development is considered from the point of view of the diffusion processes and not of reaction kinetics. At normal temperatures of processing, the dependence of the rate of development in an axial flow on the Reynolds number is incomplete, indicating that the resistance of the emulsion layer to diffusion is high and that its importance increases as the resistance to diffusion in the developer solution falls (i.e., as the Reynolds number increases). The influence of the Reynolds number on the rate of development increases as the temperature is raised, and, at 80°C, the rate of development is determined only by the hydrodynamic conditions and not by the diffusion properties of the emulsion. At normal temperatures, fixation shows the same behavior as development, but at high temperatures the dependence on the Reynolds number decreases. The dependence of the rate of fixation on the Reynolds number becomes greater at high temperatures if the emulsion layer is made considerably thicker. Fixation is of a transitional nature, raising the temperature and lowering the thickness of the gelatin layer causing the process to pass from the field of diffusion to the field of reaction kinetics.

### *Influence of the Developer Formula on the Reproduction of Image Detail by a Photographic Material*

G. V. Derstuganov, pp. 47–51

It is shown experimentally that the reproduction of image detail by a photographic material depends on the composition of the developer used. In the comparison of seven different developers on Soviet-made AM motion-picture negative film, best results were obtained with Kodak Developer DK-20, SIZ-3 (a *p*-phenylenediamine–*p*-hydroxyphenylglycine developer without alkali), Kodak Developer SD-26 + 1 gram benzotriazole per liter, diluted 1:10, and the developer specified in the Russian standard GOST 2817-50 (a Metol-hydroquinone-carbonate developer), also diluted 1:10; while the worst results were given by SD-26 (full strength) alone or with the benzotriazole addition. For Soviet-made motion-picture negative film, Type B, four developers were compared: SD-26 + 1 gram benzotriazole per liter, diluted 1:10, the GOST 2817-50 developer, diluted 1:10, D-76, and NM-NIKFI. Preference was given to the last of these. The method of evaluation used for the developers can materially simplify the choice of the optimal developer for different motion-picture materials.

## Zhurnal Nauchnoi i Prikladnoi Fotografii i Kinematografii, Vol. 3, No. 5, Sept.–Oct. 1958

*Resumés by S. C. Goddard*

### *An Investigation into the Radiolysis of Silver Halide*

K. S. Bogomolov and I. F. Razorenova, pp. 321–22

In order to account for the difference between the energy requirements (6–8 ev) for the formation of one conduction electron in silver halide by ionizing radiation and the energy requirements (30–40 ev) for the formation of one atom of silver in the latent image, also by ionizing radiation, the dependence of the energy required for latent-image formation on three factors was studied: the grain size of the emulsion, the degree of ripening, and gold sensitization. Emulsions were irradiated with 61 kev electrons and the radiolytic silver was estimated by potentiometric titration. The energy consumption in the formation of one atom of latent image silver increased as grain size was decreased; it decreased as the time of ripening was increased; and it was not influenced by gold sensitization. Ripening had no effect on the energy required for latent-image formation by light ($\lambda$ = 436 m$\mu$). The difference between the action of light and of charged particles is ascribed to the expenditure of energy of the charged particles in "completing the structure of the lattice" (dostroïka reshetki). (See also paper by Bogomolov and Razorenova in "Photographic Sensitivity, Vol. 2, Tokyo Symposium," in English, reviewed in *Phot Sci. & Eng.*, 2: 234 (1958)).

### *Study of the Conversion of Primary Centers into Latent-Image Centers and Visible Blackening*

Zh. L. Broun, pp. 323–28

A silver bromide emulsion was digested for 10 min and for 2 hr to give Emulsions 1 and 2. The two emulsions were diluted to $^1/_{40}$ of the original concentration and coated for spectrophotometric examination by Kirillov's method. Some plates coated with Emulsion 1 were oxidized with chromate, and some coated with Emulsion 2 were exposed, some exposed and developed, and some exposed, developed, and fixed. By comparing the absorption spectra in the range 400–850 m$\mu$ for pairs of plates, each stage being compared with that immediately preceding, a set of absorption curves was obtained which could be ascribed to the separate processes taking place at each stage. The curves are interpreted as showing an agglomeration of primary centers during digestion, followed by an increase in their concentration on exposure, and a conversion of silver bromide to metallic silver to form a visible density during development. The induction stage in development with a developer containing sulfite and potassium bromide consists in the solution of the surface of the solid phase; only after this does the intensive formation of a new solid phase — free silver — begin. The spectrophotometric curves show a gradual agglomeration of silver impurity centers and their growth during digestion, the further increase in their concentration and dimensions

on exposure, and, after the induction period, a vigorous precipitation of silver during development. This gradual transition indicates the essential chemical unity of all stages of the photographic process.

### *Some Questions of Method in the Study of the Kinetics of the Photoconductivity of Emulsion Layers*

L. G. Gross and P. V. Meĭklyar, 329–34

Miller and Hamm showed that the photocurrent in photographic emulsion layers continued to grow after the cessation of the exposure, and later writers have taken this as evidence of exciton formation in the silver halide crystal. The effect has now been studied by exposing emulsion layers, previously kept in the dark over calcium chloride, to a light beam modulated to give a rectangular pulse. The sample in a holder with silver electrodes was placed in a hermetically sealed chamber with an internal relative humidity of 30%, and the photocurrent was fed into a three-stage amplifier, the output of which was recorded on a cathode-ray oscilloscope. Measurements were also made on samples of dried photographic gelatin. A delay of 0.5 sec was observed between the cessation of the exposure (0.5 sec) to white light and the maximum current flowing in the emulsion, but a similar delay was shown by the gelatin alone. It was found that the delay could be eliminated by reducing the input resistance to the amplifier. The delay effect was also reproduced with a photoelectric cell in combination with gelatin to provide the necessary resistance, or with an equivalent resister. A study of the equivalent circuit shows that the delay in reaching maximum conductivity is not related to processes occurring in the emulsion, but is a property of the input circuit.

### *Comparative Investigation of Different Methods of Photographic Emulsion Making*

V. L. Zelikman and E. I. Klyenkova, pp. 335–44

A standard silver iodobromide negative emulsion formula was used, involving two precipitations, the first with slow mixing of the solutions and the second, after 30-min ripening, with instantaneous addition of the silver nitrate. Ammonia was introduced in a number of different ways, or was omitted altogether. Five forms of precipitation were studied: ammoniacal, neutral-ammoniacal (ammonia added in the silver nitrate solution), neutral, partly converted, and with the ammonia added to the bromide solution. By using one method in the first precipitation and another in the second, a number of combinations were obtained. The quality of an emulsion is taken to be a function of its photometric equivalent (or covering power) and its maximum speed. The photometric equivalent was plotted against maximum speed for each method of emulsion-making, giving a straight line in each case. The covering power, $P$, is related to the maximum speed, $S$-max, by the equation, $P = (S\text{-max} - b) \tan \alpha$, where $\alpha$ and $b$ are constants for the given method of emulsion-making. It is shown that the advantages of any one method of preparation are not retained over the whole range of sensitivity, but must be considered in relation to a given sensitivity. In general, a change in the method of the second precipitation — a change in the quantity and method of introducing the ammonia into the emulsion — influences the grain size of the developed image to the same extent as a change in the method of the first precipitation. Photomicrographs of emulsions made with different combinations of first and second precipitation are reproduced.

### *Photographic Activity of p-Hydroxyphenylglycine in the Light of the Electrochemical Theory of Development*

Ya. M. Veprik and G. P. Faerman, pp. 345–50

The correctness of some conclusions drawn from the electrochemical theory of development could be tested for a single developing agent from measurements of the redox potential of *p*-hydroxyphenylglycine in the pH range 1.0–11.0. The predicted linear dependence of the optical density of the developed image over the straight-line portion of the characteristic curve on the pH of the developer and on the logarithm of the concentration of the developing agent was confirmed. It has been shown that Metol and *p*-hydroxyphenylglycine developers containing equimolecular quantities of developing agent at the same redox potentials give the same or very nearly the same results both in physical and in chemical development. *p*-Hydroxyphenylglycine in alkaline medium develops more slowly than Metol, but in acid it develops faster. These relations between the rates correspond to the relations between the redox potentials of the substances at different pH values. In the development of normal emulsions with *p*-hydroxyphenylglycine as a physical developer, the speed obtained is 6 to 10 times smaller, while the coefficient of contrast is 2.5 to 3.0 times greater than in development of the same material for the same length of time in a standard sensitometric Metol (chemical) developer. (*Translation of authors' abstract.*).

### *Sensitometry of Photographic Materials Used in Obtaining Images in Relief*

V. A. Veidenbakh and E. A. Karpovich, pp. 351–58

In the past a relationship has been obtained connecting the height of the relief image and the exposure for materials forming a relief image by differential tanning. No direct simple method of determining the height has been available, however, and the sensitometry of wash-off relief and similar materials has been carried out indirectly by measuring the density of pigment or dye in the layers. The method now described uses a microinterferometer adapted from a design by V. P. Linnik. A beam-splitting cube directs beams from a single source, one onto the step wedge and one onto a plane glass surface, and recombines them at the objective of a low-power microscope. With this apparatus, characteristic curves plotting the height of the image against log exposure have been obtained for bichromated gelatin and for a silver halide relief material. The bichromated-gelatin layers

gave curves showing no signs of a shoulder, but the silver halide curve showed the normal three parts.

***Influence of Hypersensitization by Silver-Halide Solvents on Low-Intensity Reciprocity Failure***

K. V. Vendrovskii and V. I. Sheberstov (Letter to the Editor), pp. 377–78

In an earlier work (*Zhur. Nauch. i. Priklad. Fot. i Kinematog.*, 3: 136 (1958)), it was suggested that the hypersensitizing action of amines was connected with their solvent action and the etching of the surface of the silver halide crystals. This has now been tested by studying the effect of other silver halide solvents — sodium thiosulfate, sodium sulfite, potassium thiocyanate, ammonium thiocyanate, potassium bromide, and sodium chloride. All noticeably reduce low-intensity reciprocity failure when used in a bath before exposure. Surface etching, particularly of the less sensitive grains, therefore has an important effect on reciprocity failure, but this does not exclude other additional effects produced by the individual silver halide solvents.

***The Mechanism of the Photographic Process***

V. N. Zharkov (Letter to the Editor), pp. 379–80

Values for the concentraton of interstitial silver ions in silver halide crystals, derived by extrapolation of Ebert and Teltow's equations to room temperature, do not give a true picture, as the actual concentration is strongly affected by the presence of divalent impurities which Berry has shown to be present in normal silver halide crystals. These increase the number of vacant silver-ion sites and, because of the mass-action effect, the concentration of interstitial ions falls by a factor of $10^3$-$10^4$ compared with the concentration predicted from extrapolation. It must be concluded that, at room temperature, the interstitial ions do not play as large a part as has been assumed.

***Sensitivity of Hypersensitized Nuclear Emulsions at the Temperature of Liquid Hydrogen***

K. S. Bogomolov, I. F. Razorenova, I. A. Ruditskaya, and A. A. Sirotinskaya (Letter to the Editor), pp. 380–81

An iodide-free silver bromide nuclear emulson, hypersensitized with triethanolamine, can be used for recording relativistic particles at liquid hydrogen temperatures. A hypersensitized iodobromide emulsion loses sensitivity at the low temperatures.

***The Rational Utilization of LN-3 Color Negative Film***

V. Ya. Mikhailov (Letter to the Editor), pp. 384–85

The Russian color negative film, Type LN-3, is intended for use with a light source of low color temperature (incandescent lamps). It can be used with sources of a higher color temperature without light filters if an alcoholic solution of iodine is added to the developer (0.06-0.08 grams iodine per liter). This has the effect of suppressing the extra blue sensitivity of the film and restores color balance.

***Review of the Properties of a Contemporary Assortment of Imported Photographic Papers of Miscellaneous Designations***

Ya. Z. Zaidenberg, pp. 390–94

The products surveyed were papers imported into the Soviet Union and produced in 1956 by the firms of Agfa, Gevaert, Forte, Kodak, and Ilford. An analysis of grades and surface finishes shows that the West European and American markets have a wider choice available than the Russian. The silver content, photometric equivalent, resolving power, density range, and energies of activation for the development of fog and image are tabulated.

***Development of Reversal Motion-Picture Film in the Field***

A. G. Sokolov, pp. 398–400

A formula for the development of reversal motion-picture film under field conditions, e.g. on an expedition, is based on the developer prescribed for use in processing laboratories for the (Russian) film, but used at one-tenth that concentration and with the content of Metol and potassium thiocyanate increased a little. With the dilute developer, the film is not very susceptible to changes in the time of development, and the stricter control available in the laboratory is not necessary. The necessary alterations in processing technique are outlined.

## Zhurnal Nauchnoi i Prikladnoi Fotografii i Kinematografii, Vol. 3, No. 6, Nov.-Dec. 1958

*Resumés by S. C. Goddard*

***The Kinetics of Regression of Photographic Latent-Image Centers***

B. I. Kazantsev and P. V. Meiklyar, pp. 401–06

Samples of film were exposed through a step wedge and then stored at a constant temperature in an air-tight container for various lengths of time up to 30 days before development. Parallel with these experiments, others were carried out in which the latent image was oxidized by immersion in a 0.01% solution of potassium dichromate or destroyed by red light (Herschel effect). From the characteristic curves, curves were constructed showing the relative number of silver atoms in the latent image as a function of the time of regression. The form of the curve is taken to show that the rate of destruction of latent image increases with time, and hence the stability of the latent image center decreases with size of the center; moreover, the process is neither monomolecular nor bimolecular, and hence is neither oxygen oxidation nor rebromination. An equation is derived for the kinetics of regression, and fitted to the data obtained for the two types of materials studied (lantern-slide plate and graphic-arts line plate). The oxidation experiments gave curves which are different in shape from those of regression on keeping. Destruction of the latent image by red light gave curves similar to those for regression and it is assumed that the mech-

anism is similar for the two processes, namely, the liberation of electrons by photoelectric action and thermal action, respectively.

### *A Study of the Relation Between Regression and the Energy of Particles Giving Rise to the Formation of Latent Images*

K. M. Romanovskaya and K. S. Bogomolov, pp. 407–09

Packs of several tens of emulsion layers, in all 400 $\mu$ thick, were equilibrated at 20° C and 58% relative humidity for 7 to 10 days after preparation and then exposed to a beam of $\pi$-mesons of energy 180 and 220 mev from a synchrocyclotron. After exposure, a coordinate grid was impressed on the emulsion by an x-ray exposure, and 12 to 14 hr later the seven upper layers were removed and developed from both sides. The emulsion layers were subsequently stuck to glass. At intervals, further batches of seven layers were removed and processed, the pack being kept at 20° C and 58% relative humidity before processing. Track densities were measured at various distances from the points of arrest of the mesons, and a regression factor was calculated. Regressions are tabulated for two different emulsions. Some small decrease in the amount of regression was observed with increase in the ionization produced by the particles. The weak dependence of regression on ionization is explained on the basis of Bogomolov's fluctuation theory of the effect of charged particles. With increasing ionization, within the limits of the experiment, it is not the energy consumed in the individual grains which increases but the number of grains experiencing the primary ionization, and the size of the latent-image centers depends but little on the energy of the charged particles.

### *Influence of the Activity of Gelatin on the Kinetics of Chemical Sensitization*

I. Malinovski and V. Pavlova, pp. 410–15

Experiments were carried out to decide between conflicting statements in the literature regarding the best stage in emulsion-making at which to add the more active gelatin. An emulsion formula previously described (*Z. wiss. Phot.*, *51:* 186, 200 (1956)) was used, but clumping of the grains was avoided by raising the excess of bromide and by the addition of a small amount of iodide. After the physical ripening state, the grains were precipitated with sodium sulfate and redispersed in the second gelatin for the chemical sensitization stage. Inactive gelatins were prepared from a production gelatin by an oxidation technique, with bromine, hydrogen peroxide, and potassium ferricyanide as oxidizing agents. Of these, the ferricyanide gave the most inert gelatin. The treated gelatins and the original untreated material were used in different combinations in the physical ripening (first gelatin) and chemical sensitizing (second gelatin) stages, respectively. If the first gelatin is more active than the second a high emulsion speed can be obtained, but the rate of chemical sensitization can be decreased by the influence of the lower activity of the second gelatin; if the latter is very inert the rate of sensitization may become extremely small. If the second gelatin is more active than the first, the latter has no influence on sensitization and on the final sensitometric properties of the emulsion.

### *Anti-Repellency Activity of Wetting Agents in the Coating of Photographic Emulsions*

### *II. Anti-Repellency Activity of Some Alkylphosphinic Acid Derivatives*

O. K. Smirnov, S. M. Levi, A. I. Rybnikova, and S. N. Kochneva, pp. 416–18.

The following alkylphosphinic acid compounds were studied for anti-repellency activity in emulsion coatings: disodium salts (**I**), monosodium salts (**II**), monoglycerides (**III**), and polyglycerides. Surface pressures of aqueous gelatin solutions of these substances are also tabulated. Anti-repellency activity is closely bound up with the chemical constitution of the compounds. In series **I** and **II** an alkyl group containing 8 or 9 carbon atoms is necessary. **III** show practically no action, whatever the length of the carbon chain. Polyglycerides with a polyester chain of from 6 to 20 molecules of glycerol begin to show activity when the carbon chain length of the alkyl reaches 18 atoms. With polyester chains exceeding 25 molecules in length, excellent anti-repellency is obtained when the alkyl group has 10 to 12 carbon atoms. Similar effects were obtained with octaglycerides with alkyl chains of 10-12 and 8-9 carbon atoms. These show high anti-repellency activity. No relation was established between anti-repellency, surface pressure, and kinetic wetting for the compounds studied.

### *The Photographic Properties of Some Symmetrical Carbocyanine Dyes with Different Alkyl Groups on the Heterocyclic Nitrogen Atoms*

I. I. Levkoev and E. B. Lifshits, pp. 419–26

A study was made of the photographic properties and absorption spectra in emulsions of a number of symmetrical carbocyanines with no substituents on the chain, but with different heterocyclic nuclei containing methyl, ethyl, or higher alkyl groups on the nitrogen atoms. Contrary to statements in the literature, the methoxides of a number of dyes (with indolenine, thiazoline, benzimidazole, and thiadiazole nuclei) show practically no difference among themselves in their sensitizing action, while, in other cases (thia-, oxa-, and 2-quinocarbocyanines) the N,N′-dimethyl derivatives are considerably less effective than the ethyl derivatives. Moreover, with regard to sensitization spectra, fogging action, desensitizing action, and also the basicity, the methoxides of all the carbocyanines studied came close to the corresponding ethoxides. A considerably smaller sensitizing action, in comparison with the ethoxides, is shown by the

methoxides of those carbocyanines which, contrary to the ethoxides, are adsorbed on the grains preferentially in the H-state. These states, as a rule, show such slight photochemical activity that the bands corresponding to them are not observed in practice in the sensitivity spectra. In a series of 1,1′-dialkyl-3,3,-3′,3′-tetramethylindocarbocyanines, the tendency to second-type sensitization increases on passing from the methoxide to the ethoxide, and especially to the *n*-propoxide. (*Translation of author's abstract.*)

### *A Characteristic for the Photographic Activity of Diffusing Couplers in Color Development*

B. A. Chartoriiskii and V. S. Chel'tsov, pp. 427–29

A fine-grain positive film was developed in a diethyl-*p*-phenylenediamine sulfate developer containing a color coupler. After destruction of the dye with acid hydrosulfite, the silver density was measured. Curves of gamma against time of development were plotted and the relations between gamma and the concentration of the coupler were obtained. The couplers studied were 2-chloro-1-naphthol, 2,4-dichloro-1-naphthol, 1-phenyl-3-methylpyrazol-5-one, acetoacetanilide, and acetoacet-2-chloranilide. The main reaction of the coupler would seem to be that of combining with the oxidation products of the developer, and this is confirmed by the increase in the rate of development with increase in coupler concentration. A straight-line relation was found by plotting the gamma of the silver image against the logarithm of the coupler concentration, and the slope of the line is a good characteristic for rating the photographic activity of the coupler.

### *Densitometric Studies*

### *I. The Scattering of Light by Developed Photographic Films*

Yu. N. Gorokhovskii and I. M. Davydkin, pp. 430–39 (A German-language version of this paper appeared in *Z. wiss. Phot.*, 53: 18–32, Dec., 1958.)

With the aid of a visual goniophotometer, the light-scattering values of densities, differing in their character, have been measured. The following rules were established: (a) Light-scattering by densities obtained by development to a given contrast increases with increase in the optical density. (b) Light-scattering by a given density is greater the higher the contrast. (c) Different photographic materials behave similarly in regard to their light-scattering properties, but sensitometrically comparable densities show some difference in light-scattering.

From the light-scattering values, values of the total diffuse densities have been calculated and compared with those obtained by direct experiment, and the relation between optical density and the solid angle of the light collector has been established. From this was obtained information on the practically allowable minimum dimensions of the solid angle of the collector in the measurement of total diffuse density. The Callier coefficient has been used in an analysis of the physical basis of a numerical light-scattering characteristic. It is shown that this quantity is not at all a strict measure of the light-scatter, in so far as it includes the absorption of light by the density.

Two new methods of numerical evaluation of the light-scatter by densities are proposed: (a) by means of a light-scatter factor, $q$, representing the fraction of the scattered light in all rays transmitted through the density, i.e. $q = 1 -$ antilog $(D_{\text{total diffuse}} - D_{\text{diffuse}})$, and (b) by the angle of scatter $2\alpha$ characterizing, to a known approximation, the form of the scatter index. (*Translation of authors' abstract.*)

### *The Influence of Silver Halide Concentration on the Scattering of Light in an Emulsion Layer*

Yu. Sh. Moshkovskii, pp. 440–42

The investigation was carried out with emulsion coatings of constant grain size (average 0.5 $\mu$) and weight of silver per unit area, but with a varying quantity of gelatin. The light scattering was determined by exposing plates to a striped test plate (contrast between stripes and background density was 1.73) in Burmistrov's resolving-power meter, which gives a reduction of $^1/_{25}$. The widths of the stripes in the photograph were 8, 16, 32, 40, and 84 $\mu$. After standard development, the densities were read on a microdensitometer. The maximum density of a stripe was found to depend on the logarithm of its width, $b$, that is, $D_m = D_o + \delta \log b$, where $\delta$ is a constant depending on the contrast coefficient of the photographic material, the contrast of the test plate, and the scattering properties of the layer. Comparison of the results with those obtained with a test plate with $D = 0.5$ showed that $\delta$ decreases as the contrast is reduced. Increasing the image contrast by lengthening development causes $\delta$ to increase. The quantity $P = \delta/\gamma$, was chosen as an index of light-scattering. With development times of 1 to 12 min., $P$ did not alter with $\gamma$. When $\rho$, the ratio of gelatin to silver in the emulsion is varied, $P$ falls to a minimum as $\rho$ is lowered to 1, and then increases. This is explained by the increase in absorption as the grains become crowded, but with $\rho < 1$, aggregation sets in.

### *Theory of the Threshold Characteristics of Photographic Apparatus*

### *I. The Role of the Optical System of the Apparatus in the Case of Separated Objects in the Field of View*

L. P. Moroz, pp. 443–51

Equations have been obtained to correlate the width of an isolated object, in the form of a band, in cases in which the object is placed in a field which is lighter or darker than the band itself, its contrast against the surrounding field, the contrast between a point on its axis and the surrounding field in the image formed by an aberration-free optical system with a circular pupil, the aperture of this system, and the wavelength of the illumination. With these equations, it is possible to solve problems which require finding the necessary, and, in part, threshold values

for each of the calculated quantities when the remaining quantities are given, in relation to the threshold of perception of contrast of the receiving element of the apparatus. The form of the equation varies, depending on whether the object is lighter or darker than the field, for a given contrast between object and field. The two cases are found to be connected. The method used to obtain the equations may be used for objects of different forms, optical systems with other properties, and also for image-receiving elements with scattering properties. On this account, some of the results have been generalized. (*Translation of author's abstract.*)

***A Study of the Possibility of Increasing Photographic Sensitivity During Development without Deterioration of Picture Quality***

G. A. Istomin and V. I. Sheberstov (Letter to the Editor), pp. 450–51

Several developers, tested with a Soviet cine-negative film, showed comparatively little difference in speed measured at a density of 0.2 above fog; when speed was measured by the smallest exposure necessary to give a resolving power of 7.5 lines/mm, marked differences became apparent. A dilute Metol developer with a low concentration of developing agent (0.2 gram Metol per liter) and a high alkalinity (pH > 10) gave the highest speed under these conditions, with a low gradient in the part of the characteristic curve corresponding to this speed, and a wide latitude consistent with registering of fine detail. Such low-concentration, high-alkalinity developers are suggested as a useful line of attack in obtaining higher speeds with good picture quality.

***The Work of Soviet Scientists in the Field of Photographic Emulsion Technology***

V. L. Zelikman, pp. 452–68

Reviewed are 223 published papers covering improvements in equipment and methods of emulsion making, classification and choice of emulsion gelatins, the conditions of emulsion making (e.g. excess of halide or silver ions), the photographic properties of cine film, aging of photographic materials, and technological aspects of emulsion making.

## Latent Image Fading in Nuclear Track Emulsions

The phenomenon of latent image fading in photographic emulsions was recognized well before the advent of nuclear track emulsions, and even some attempt had been made to account for fading on a quantitative basis. In recent years, the importance of fading in nuclear track emulsions has led to numerous investigations of latent image fading both in nuclear and other emulsion types. Several quantitative relations have been suggested, ranging from a simple exponential decay[1] (first-order law) to the relatively complex formulation due to Kazantsev and Meĭklyar,[2] covered elsewhere in this Review section. Another study published by H. W. Meier[3] deals with results of fading tests made on Agfa K2 emulsions, 50 $\mu$ thick, exposed to a radium-beryllium source. The emulsions were kept for various times at 20° ± 1 C after exposure, and then developed in an Amidol developer. Meier found that the percentage of fading, expressed as $y = 100\ D/D_0$, could be represented as a function of time with considerable accuracy by a linear combination of two simple exponential expressions:

$$y = A_1 e^{-(\ln 2/T_1)t} + A_2 e^{-(\ln 2/T_2)t},$$

where $D$ is the density at time $t$, $D_0$ is the initial density, $T_1$ and $T_2$ are "half-life" times, and $A_1 + A_2 = 100$. Meier interprets the agreement between the data and the exponential expression as indicating that a portion of the latent image fades by a first-order "short-life" process and another portion fades by a slower, also first-order, "long-life" process. The relative portions of latent image fading by each process varied according to experimental conditions. The percentage of "short-life" portion ($A_1$) increased linearly with increasing water content (volume percent) of the coating, whereas the percentage of "long-life" portion ($A_2$) decreased linearly with increasing water content.

Latent image fading has been variously interpreted by other workers as a destruction of latent image by oxidation and as an "evaporation" of electrons from silver atoms in a process which is the thermal equivalent of the Herschel effect. Meier suggests that these two mechanisms of latent image fading correspond to his "short-life" and "long-life" components, the oxidation of surface latent image being the short-life fading process.

In a later paper,[4] Meier states that the Herschel effect obtained by infrared exposure of Agfa K2 plates which had been exposed initially to the radium-beryllium source also can be represented by a linear combination of two exponentials representing short-life and long-life components. — T.H.J.

*Literature Cited:* 1. T. H. James, J. M. Blair, and F. E. E. Germann, *J. Phys. Chem.*, *38:* 1211 (1934). 2. B. I. Kazantsev and P. V. Meiklyar, *Zhur. Nauch. i Priklad. Fot. i Kinematog.*, 3:401 (1958). 3. H. W. Meier, *Z. wiss. Phot.*, 53: 46–59 (1958). 4. *Ibid.*, 53: 61–8 (1959).

PHOTOGRAPHIC SCIENCE AND ENGINEERING
Volume 3, Number 3, May-June 1959

# • Technicalia Photographica

FRANK SMITH

## • Cameras and Projectors

### *Optomechanisms Camera Shutter Tester*

Optomechanisms, Inc., 216 E. Second St., Mineola, N.Y., has announced a new instrument for measuring,

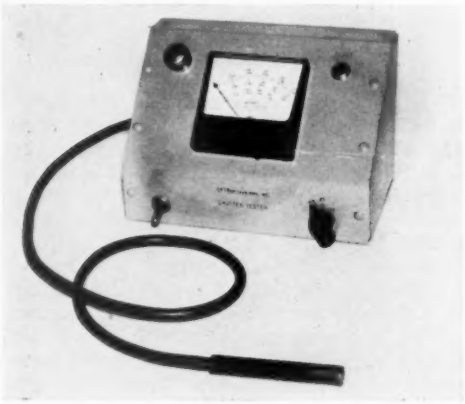

without disassembling the camera, the total time that a shutter is open.

Measurement is read directly on a meter by placing a probe containing a phototransistor at the film end of the camera and illuminating the lens by a flashlight or other light source. Accurate measurements are obtained independent of lens, aperture, or light illumination level.

### *Comapco OAR — Optical Automatic Ranging System*

A simple, rugged, continuously-operating electronic automatic focusing system suitable for use with motion picture, television, or still cameras has been developed by Comapco, Inc., 17071 Ventura Blvd., Encino, Calif.

The system is built around a rapidly oscillated "sensor" composed of a linked group of photoelectric cells. These cells monitor light as distributed within the focal area of a system of lenses or mirrors. Minute changes in the focal situation will produce definite alterations in both frequency and phase characteristics of the electric currents "reported" by the sensor device. These alterations give rise to commands that regulate servo-mechanisms to produce required changes in lens or mirror position, or to make other adjustments.

The servo system, in any case, restores the normal situation in which the midpoint of sensor oscillation falls on the plane of sharpest image definition (focal plane). Thus any change in distance from lens to object observed at the center of its field effects a corresponding resetting of focus. As a result, from a precalibrated lens or mirror system, the distance of the observed object can be ascertained. Distance determination within 2% of true value has been indicated in preliminary tests of OAR laboratory models, according to the company.

Focusing and ranging accuracy of OAR increases with the use of lenses of larger focal lengths and apertures, and with the use of light of shorter wavelengths.

The OAR system is suitable also for automatic determination of focal length, color characteristics, and optical symmetry of lenses or lens systems with magnification of less than unity. Thus it can serve as an automatic optical bench of advanced characteristics.

### *Traid Wide-Angle Lens Withstands 50 Gs*

A new motion picture wide-angle lens with a rugged GSAP mount designed to withstand accelerations as high as 50 Gs is now available from Traid Corp., Encino, Calif. The lens was designed for missile scoring systems, but is also suitable for installation in restricted quarters inside missiles or aircraft.

Designated the Traid 725, the new lens for 16mm cameras is manufactured by Pacific Optical Co., Inglewood, Calif. It has an aperture of $f/1.5$ and a 110° field of view. It forms a round image of 0.297 in. diameter in the film frame and has a focal length of 0.1655 in. or 4.038 mm. The lens has a fixed focus and is provided with filters and iris control.

In addition to the GSAP mounting, built to withstand acceleration or deceleration loadings of 50 Gs, a "C" mount is available.

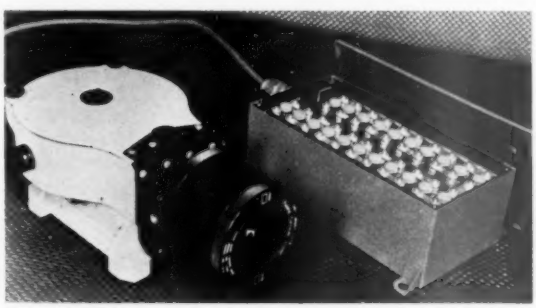

Official United States Navy Photograph

### *First Picture from Navy Weather Surveillance Rocket-Camera*

Tests of a new U.S. Navy Rocket-Camera Unit specifically designed to photograph high-altitude ocean cloud formations associated with hurricane and weather frontal systems are being conducted by the Office of U.S. Naval Research. The Rocket-Camera Unit will be utilized where there are no permanent weather stations.

Shown here is one of the first pictures obtained from a Project HUGO (High Unusual Geophysical Operations) Rocket which soared to an altitude of 86.25 miles during the first test flight on Dec. 5, 1958. The picture, a composite of five photographs, shows a frontal cloud formation over the Atlantic Ocean, starting about 200 miles off shore and stretching nearly 700 miles further seaward. This mosaic strip covers a distance of about 1000 miles, ranging approximately from the southern tip of Maine to mid-Florida.

The film was successfully recovered at sea from the nose cone of the Nike-Cajun rocket by the USS Leary (DDR-879). The rocket was fired from the National Aeronautics and Space Agency's Pilotless Aircraft and Research Station at Wallops Island, Va.

### *Linhof 4-by-5 Aero-Technika Camera*

A new aerial camera, the 4-by-5 Aero-Technika, using standard films and processing, has been developed by Linhof Precision Camera Works, Germany. It is being distributed in the United States by the Kling Photo Corp., 274 4th Ave., New York 10, N.Y.

While conventional aerial cameras use large film rolls requiring special processing, the Aero-Technika takes standard 4 by 5-in. film in regular holders, pack adapters, or magazines. It may also be used with a Polaroid back for picture-in-a-minute taking. With a wide choice of films, including infrared and all types of color materials available for the Aero-Technika, the camera permits taking as few, or as many shots as necessary for a given project with resulting operating efficiency and economy.

Lighter and more compact than traditional aerial cameras, the Aero-Technika has a streamlined body made of special corrosion-proof alloys, smoothly finished and anodized, with two adjustable hand grips. The revolving camera back permits taking horizontal or vertical views without changing the accustomed camera position. Lenses are protected by lens-shading cowlings fitted with a holder for standard 4 by 4-in. glass filters.

Six lenses with focal lengths ranging from the extreme wide-angle 75mm $f/4.5$ Carl Zeiss Biogon to the $10\frac{1}{2}$-in. $f/5.6$ Rodenstock Rotelar telephoto lens — all with built-in shutters — are instantly interchangeable to obtain the desired coverage in air-to-ground shooting from every altitude, or for optimum results in air-to-air work. An accessory focal plane shutter with speeds up to 0.001 sec may be added.

The camera is of particular interest to industry, land development or exploration companies, newspapers, private pilots, and professional photographers doing aerial work.

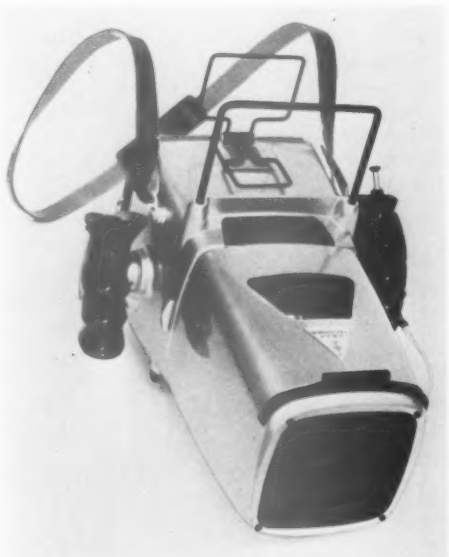

### *Pacific Laboratories Type M-35 Recording Camera*

A miniaturized 35mm interval and motion picture camera, introduced by Pacific Laboratories, 12808 Venice Blvd., Los Angeles 66, Calif., includes a turret lens mount, and demountable daylight loading magazines of 100, 200, 400 and 1000 ft capacities. Exposure rates can be varied from 10 frames/sec to elapsed time rates as slow as desired. Cine operation is possible at 16 or 24 frames/sec or 16 to 48 frames/sec with variable drive. Remote control circuits are included for automatic operation and automatic recording. Electric drives are available for 12 and 28-v d-c or 110-v 60 and 400-cycle a-c operation. Camera weight with 100 ft magazine loaded is 8 lb and the size is $4\frac{1}{2}$ in. wide, $6\frac{3}{4}$ in. high and 7 in. deep with 100-ft magazine.

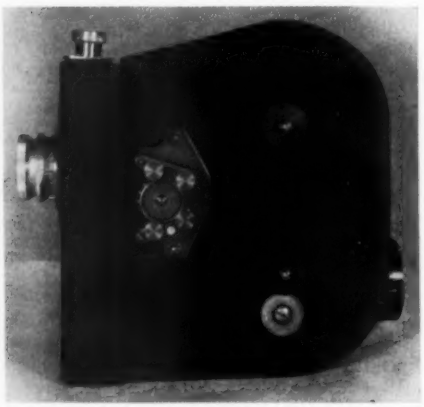

The M-35 camera is available in commercial, industrial, scientific and military types, with wide application to method and process analysis, police, press and document recording, scientific and test-laboratory event and data recording, and military airborne systems.

A significant feature, available on order, is the new composite 16-35mm panoramic frame size.

### *Traid 16mm Long-Run Camera*

A new, high-capacity 16mm motion picture camera, designed for filming rocket engine tests, is now available from Traid Corp., Encino, Calif. The camera holds 1200 ft of film and may be used for recording events up to 50-min duration.

Designated the Traid Model 805 Fototracer, the new 16mm camera is a rugged lightweight intermittent movement type. It was developed specifically for rocket engine testing, but is also suited for any applications requiring large film capacities or long running periods.

It operates at 16, 24, 32, and 64 frames/sec from a governor-controlled heavy-duty motor. A fail-safe device automatically stops the camera if the film breaks.

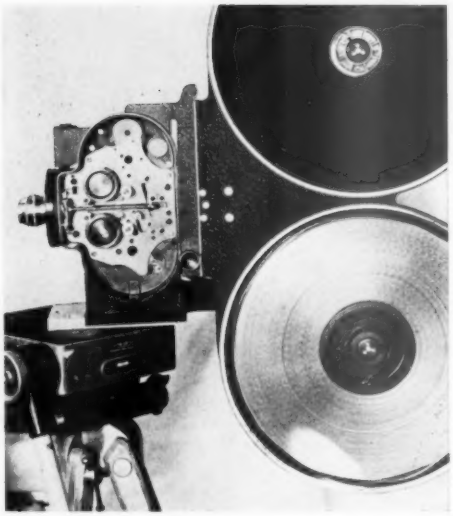

Extra large sprockets provide more teeth to engage the film perforations and provide extra pulling power on the 1200-ft roll.

Lubrication is of the metered oil-feed type, and is solenoid actuated when the camera is started. The camera has a heavy duty head and the cam shaft is fitted with ball bearings. A thick, heavy-duty plate mounts camera and motors as an integral unit for resistance to shock and vibration.

### *Fairchild's New Exposure Meter for High-Speed Cameras*

Fairchild Camera and Instrument Corp., Industrial Products Div., Syosset, N.Y., has announced a new exposure meter for high-speed cameras.

Called the HS 3201 Exposure Meter, the instrument is claimed to be the first and only reflectance-type

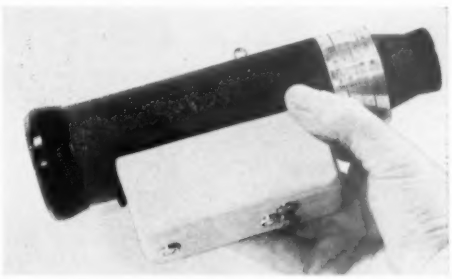

meter designed specifically for the high light levels associated with high-speed photography.

The meter is used as if it were a telescope, by sighting through the eyepiece, and aiming a black dot in the field at the subject. The narrow acceptance angle of 2° facilitates both pinpoint readings and better average readings.

### *70mm Camera for Instrument, Document, and Oscilloscope Recording*

A new 70mm camera has been developed by the Instrument Division of D. Shackman & Sons, Chesham, Bucks, England.

The camera uses daylight loading film cassettes which are available in 25, 50, 100, and 200-ft sizes. They are usable as "feed" and "take-up" cassettes, and it is possible to load the camera with 200 ft of film, and take off 25 ft or other lengths into any of the smaller sizes.

The camera may be operated automatically for shot-by-shot recording requiring only a single electrical impulse of 24 v to operate the focal plane shutter and transport the film for the next exposure. For continuously moving film photography, the film speed is infinitely variable between 40 in./sec and 1 in./sec, and the speed may be varied while the film is in motion.

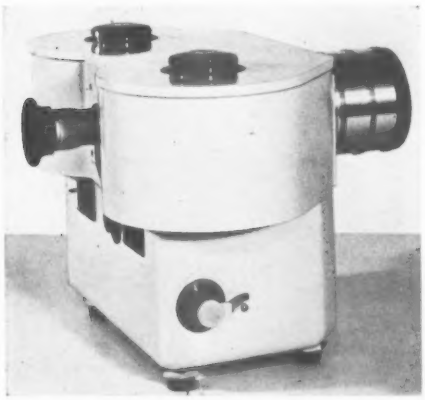

The focal plane shutter permits lenses of any focal length and aperture to be interchanged quickly. Exposure times are controlled by the duration of the applied electrical impulse and may therefore be varied over the wide range required by the many applications of this camera. Both single exposure counters and footage indicators are included, together with an indicator lamp circuit that tells when the film is being transported and when all the film has been used. "Foxing" switches prevent the camera being run for continuously moving film with the shutter closed.

The film is driven via the adjustable gearbox by a standard-current operated, capacitor-start, induction-type motor. Accessories available include guillotine, focusing magnifiers, intervalometers, data and number recording devices, etc. Overall dimensions (exluding lens) of the camera are 13½ by 7½ by 8 in. J. A. Maurer, Inc., 37-01 31st St., Long Island City, N.Y., are United States agents.

### *Optomechanisms Photo Instrumentation*

Optomechanisms, Inc., 216 East 2nd Street, Mineola, N.Y., has announced two recording cameras of advanced design for photographic instrumentation applications.

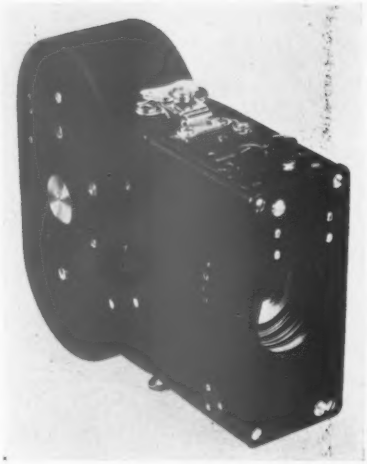

The first of these, the 35mm Sentinel Recording Camera, is a fully automatic electrically controlled pulse camera of rugged construction, especially designed for instrument and data recording.

The shutter opening and film advance can be controlled from a remote location, synchronized to any source, or manually operated with a push-button switch.

Selection of different shutter speeds and frame rates is provided by rotary wafer switches. The focal plane, solenoid operated shutter has a minimum time of 0.01 sec. Maximum speed is 6 frames/sec. All necessary adjustments are available on the camera body and are achieved with reliable transistorized circuits.

The camera is equipped for 100-ft spool loading and magazines of 50 and 100-ft capacity are available. The Sentinel Camera is 9½ in. long by 2⅝ in. high by 8½ in. wide, maximum. It is equipped with a

Schneider $f/2$, 50mm lens and is available for operation from 28-v d-c or 115-v a-c sources. A full line of accessories is available.

The other camera, Model 205A, is a 35mm recording pulse camera for photographing the images appearing on the face of a 5-in. cathode-ray tube through the optics of a periscope.

The camera is $7\frac{5}{8}$ by $2\frac{1}{4}$ in. and weighs $4\frac{1}{2}$ lb (plus $1\frac{1}{2}$ lb for periscope). The instrument uses 25mm $f/1.8$ or 40mm $f/1.5$ lenses with focus adjustable from 12 in. to infinity.

Film capacity is 60 exposures in a self-contained, 35mm ASA standard cassette. Frame rate is 1 pulse/sec. The camera uses 28-v d-c source; 115-v a-c types are also available.

## • Illumination

### *Westinghouse Sealed-Beam Projection Lamp*

Westinghouse Electric Corp., Lamp Div., Bloomfield, N.J., has announced a newly designed projection light source. The new lamp (shown at right in two sizes) is of the sealed-beam type, and is similar in principle to the sealed-beam headlamp used in autos (shown at left in illustration below).

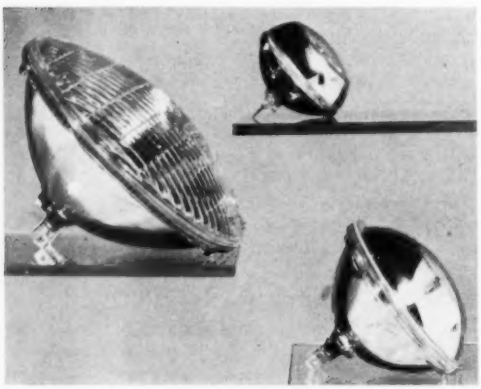

The lamp, which has an intensified controlled beam, is reported to produce about the same screen brightness as a conventional-type projection lamp, while using only about one-fourth the wattage. It is also said to produce greater screen brightness than recently introduced lamps which incorporate an internal reflector in a projection lamp of the ordinary type.

Because the sealed-beam lamp has a built-in optical system, it eliminates the need in the projector for the condenser lens and reflector. This permits the design of more compact projectors.

According to Westinghouse engineers, the lamp provides exceptional light uniformity as a result of the improved filament used. At the same time, the lamp provides extreme accuracy in directing the light produced, with the result that there is practically no stray light

It is expected that the new lamp will be made in various sizes and wattages for different types of slide and movie projectors. It may be a year before the lamps come into general use in projectors.

### *Sylvania Long-Duration Floodflash FF-33*

Sylvania has announced the development of a new high-intensity flashlamp—the Floodflash FF-33—for use with high-speed motion picture cameras.

The average flash duration of the new lamp is 1.75 seconds—more than 100 times longer than that of the popular miniature flashlamps used by amateur photographers.

The Floodflash lamp is $5\frac{1}{2}$ in. high, identical in size with the No. 3 flashlamp, the most powerful type manufactured. A single lamp will expose some 37 ft of motion picture film at 1000 frames/sec, or 75 ft at 2000 frames/sec. At slower camera speeds, several of the new lamps may be flashed in sequence at 1.75-sec intervals.

The Floodflash lamp provides a high-level light source without the heat that usually accompanies the use of flood lamps in such work.

### *GE Miniature Photoflash Lamp*

Development of a miniature photoflash lamp called the "All-Glass" flashlamp has been announced by General Electric Co., Photo Lamp Dept., Nela Park, Cleveland 12, Ohio. The new lamp has a grooved glass base for use in multi-lamp clips much like clips used in automatic pistols.

Although only one-quarter the size of present No. 2 flashlamps, the zirconium-filled "All-Glass" delivers the same light output, i.e., 7000 lumen-sec for the clear lamp and 4000 for the blue version. The baseless, all-glass lamp is about the width of a pencil and only $1\frac{1}{8}$ in. long. It is designed to work with all popular types of cameras, although its most widespread use is ex-

pected to be in both existing and future models of simple box cameras. It can be used with adjustable cameras having "F" or "X" synchronization at times as short as $\frac{1}{60}$ sec, and with Class M synchronized cameras at all shutter speeds.

GE engineers envision a flash-holder with a multi-lamp clip stored in its handle. Lamps would be advanced like film by means of a lever. After one lamp is fired, insertion of the second lamp would eject the first and reload. Such a flash-holder would be practical for existing cameras and would cost only slightly more than conventional flash-holders.

Also envisioned for more expensive cameras is lamp-changing and film-advancing by means of a single lever. Features of such a completely mechanized flash-holder might include a combination flash shield and used-lamp container which would eliminate hot lamp handling and disposal problems.

#### *Westinghouse Proximity Reflector Projection Lamp*

A new lamp for slide and movie projectors which has its own reflector sealed in the bulb has been developed by Westinghouse Electric Corp., Lamp Division, Bloomfield, N.J. It is known as the proximity reflector lamp, and is claimed to produce 20% more

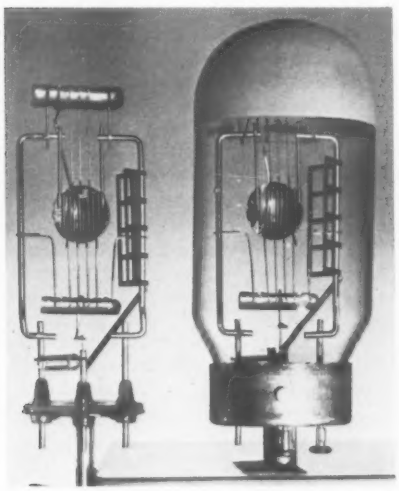

screen brightness than ordinary lamps. The additional brightness is the result of a spherical molybdenum reflector which is precision positioned immediately behind a concentrated tungsten filament. The $\frac{1}{2}$-in. reflector is said to greatly increase the efficiency of the projection lamp, since it reflects more light through the projector's optical system. In addition, the spherical shield reflects heat away from the rear of the bulb wall, thus reducing the usual blackening of that area, and resulting in cooler lamp operation and increased lamp efficiency.

The lamps will be available in 500 and 300-w sizes with four-pin wafer-stem "Focus-Lok" bases.

#### *Sylvania AGI Miniature Photoflash Lamp*

A new miniature zirconium-filled all-glass photoflash lamp no longer than an ordinary-sized paper clip provides the same light output as a lamp four times its size, says it developer, Sylvania Electric Products, Inc.

The AGI is $1\frac{1}{4}$ in. long and slightly thicker than a cigarette. Only one-fourth the size of the Blue-Dot M2 flashlamp, it supplies identical light ouput — 7000 lumen-sec from the clear lamp and 4000 lumen-sec from the blue. It reaches a peak light output in 15 msec.

The new lamp has a horizontal groove in its glass base for use in either a multi-lamp clip or the socket of an individual flashgun. It is reported that this flashlamp will make possible the design of completely automatic flash cameras in which the lamps are clip-loaded like bullets in an automatic pistol.

#### *Internal-Reflector-Projection Lamps*

J. M. Harris, *The Sylvania Technologist*, *12:12* (Jan. 1959)

The development of internal-reflector lamps for 8mm movie projectors is described. Two designs are discussed: one with a 115-v, 150-w filament providing screen illumination equivalent to that from a conventional 500-w projection lamp; the other with a 21-v, 150-w transformer-operated filament providing screen illumination equal to a conventional 750-w lamp.

#### *A New Development in Gas-Discharge Lamps*

*The British Journal of Photography*, in its Jan. 2, 1959 issue, reports on a new gas-discharge lamp by Philips of Holland. The lamp, Type SPP, for motion picture projection has a nominal rating of 800 w.

It consists of a quartz tube $3\frac{1}{8}$ in. in length and with a maximum diameter of $\frac{3}{16}$ in. The actual discharge takes place inside a thin capillary tube with an arc length of just over $\frac{5}{8}$ in. For film projection the lamp is driven by a pulsating direct current of 72 impulses/sec, or 3 pulses/picture. Light is produced only during these impulses of current; in the intervening periods the lamp is dark. The film is advanced during one of the dark intervals.

## • Processing Equipment and Techniques

#### *Fairchild Portable 35mm Film Processor*

A new, rapid 35mm processor, second in a line of portable film processors, has been announced by the Industrial Products Div., Fairchild Camera and Instrument Corp., Syosset, N.Y.

The "Mini-Rapid 35" will process 35mm film automatically. It is designed to operate at speeds up to 6 ft/min, to process 400 ft of film at one loading, to operate under daylight conditions, and to use any size of film spool. It weighs 120 lb and is 15 in. deep, 13 in. high, and 37 in. wide.

Principle feature of the unit is a patented plastic drive insert in each solution tank. This drive insert transports the film while at the same time providing

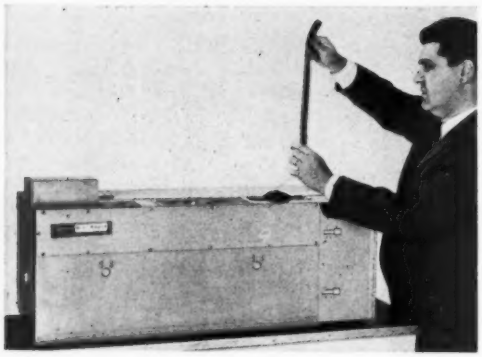

solution agitation and squeegee action. In normal operation six solution tanks — two developer, two fixer, and two wash — are used. The final wash tank is fitted for a circulating water wash, but the unit may be used without it when running water is not readily available.

Primary users of the new processor are expected to be military and civilian agencies engaged in missile tracking instrumentation, data recording, and general engineering photography.

#### *Consolidated Electrodynamics Oscillogram Processor*

A thermistor drum temperature control is one of several features which Consolidated Electrodynamics Corp., 300 N. Sierra Madre Villa, Pasadena, Calif., has incorporated in its new 23-109A Oscillogram Processor.

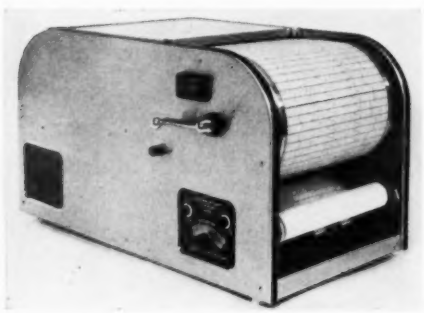

The processor is a completely self-contained portable motorized unit used at test installations for daylight processing of oscillograms. The control system consists of a sealed thermistor sensing unit and a transistorized control amplifier in the electrical compartment. It provides close control of the drum temperature and at the same time eliminates the maintenance required when open thermostats are used.

The new processor has a knob adjustment that varies the bath temperature. Such an adjustment has not been necessary in the past, but will be required in the near future because of anticipated new chemical processes.

Other features include a unitized drive assembly, a speed-control contact shoe that is wide enough to allow simultaneous processing of two narrow rolls, and a take-up spindle coated with Teflon to facilitate record removal.

The 23-109A affords the same portability, simple operating technique, and daylight operation as other Consolidated oscillogram processors. It is pointed out that no external water supply is needed for field use.

#### *Kodak Automatic Industrial X-Ray Film Processor*

The Kodak Industrial X-Omat Processor delivers dry, ready-to-read radiographs 13 min after the exposed film has been fed into it. A series of small, driven rollers, arranged in offset positions, transport each film independently through the solutions. No film hangers are required.

The processor is compact. Occupying approximately 27 sq ft of floor space, only about 22 in. of the processor's length extends into the darkroom. The remaining 9 ft of its over-all length are in the fully lighted working room.

The processor is versatile. Most standard sizes of Kodak Industrial X-Ray Film, Type AA or Type M, in sheets and rolls, may be handled without adjusting the system. Fed three at a time, $4\frac{1}{2}$ by 10-in. film may be processed at a rate of approximately 600 sheets/hour. Radiographs 14 by 17 in. will go through the processor at a rate of about 140 sheets (over 163 ft) per hour. Continuous lengths of film from 70mm to 17 in. wide may be fed through the system at 38 in./min.

A description of this general type of processor is given in *P S & E*, 3: 27 (1959).

## • Miscellaneous

#### *Digital Recorder for Test Data on Motion Picture Film*

A new digital recording device, developed by Magnavox Research Laboratories, has been incorporated in some 35mm motion picture cameras of the Traid Corp., 17136 Ventura Blvd., Encino, Calif.

The recording device produces a 96-bit matrix image on each frame of film thus correlating coded data with pictorial records in real time. The device, known as the Magnavox Digital Recorder, is expected to find immediate application in engineering tests, missile

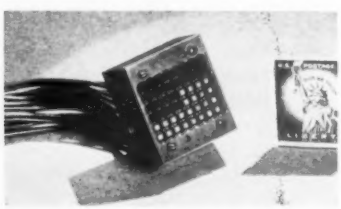

tracking, reconnaissance, flight tests, and microfilm document recording.

The unit may be used to record time, temperature, pressure, vibration, stress, deflection, shaft position, elevation, azimuth, and similar coded digital data. The camera can be operated at any frame rate desired up to 80 frames/sec. At 80 frames/sec, the Traid 75 camera can record 7680 bits of coded information per second.

The recorder uses two 48-lamp assemblies to form a 96-lamp array. A prism arrangement projects the matrix image onto film. Each lamp image measures 10 mils. The sub-miniature, 1-v incandescent lamps are designed for long life and may be easily replaced.

Traid Corp. will offer the device on its new 35mm Traid 75 Fototracker and on Bell & Howell Model 71 Eyemo cameras.

### Instrument for Thermal Photography

Robert W. Astheimer and Eric M. Wormser, *J. Opt. Soc. Am., 49:* 184 (1959).

This paper describes an instrument for taking thermal photographs utilizing infrared radiation passively emitted by objects at ambient temperature. The instrument consists of an 8-in. radiometer utilizing thermistor infrared detectors and an imaging attachment. A glow modulator forms a thermal photograph on Polaroid or conventional film.

Quantitative analysis of thermal photographs is described, and several examples of thermal photographs are given. Illus., 2 refs.

### *Recordak Lodestar Magazine-Load Microfilm Reader*

Coded rolls of microfilm, protected in plastic magazines and viewed in a high-speed reader, make possible rapid retrieval of information on microfilm. Recordak Corp., 415 Madison Ave., New York 17, has developed the Lodestar magazine-load microfilm reader for use with many types of material where frequent reference and speedy location of a document is required.

In the reader, code lines are exposed between document pages on the microfilm. A matching code scale on the reader guides the viewer to the proper document.

When looking up a document, the viewer merely locates the proper code number and film magazine from a master index, inserts the magazine in the reader and moves the control lever. Film can be viewed at speeds from a fraction of a foot per second to 10 ft/sec.

It is said that at top speeds a document can be located in seconds. Insertion of the magazine lights the screen and starts the film drive motor. The magazine cannot be removed until all film is rewound.

### *Heat-Resistant Zinc Borosilicate Glasses*

Glass that can resist both high temperature and thermal shock and yet maintain good optical quality is needed for glazing windows in supersonic aircraft so that visual and photographic observations can be made with a minimum of distortion.

To obtain a thermal-shock-resistant glass of optical quality, the zinc borosilicate glass-forming system was investigated at the National Bureau of Standards, Washington, D.C. To conduct the investigation, glass specimens were prepared in the laboratory by varying the content of the three major components, $ZnO$, $B_2O_3$ and $SiO_2$. Properties which were determined for these glasses included sag point, liquidus temperature, refractive index, modulus of elasticity, thermal expansion, chemical durability, and surface devitrification.

For further technical details, see "Properties of Zinc Borosilicate Glasses," by E. H. Hamilton, R. M. Waxler and J. M. Nivert, Jr., *J. Research, NBS, 62:* 59 (Feb. 1959) RP 2930.

### *Proceedings of Cathode-Ray Tube Recording Symposium, Dayton, Ohio, Jan. 13–14, 1959*

On Jan. 13 and 14, 1959, a Cathode-Ray Tube Recording Symposium was held in Dayton, Ohio, to bring together representatives of the electronics and photographic industries and the military to present papers and discuss problems of common interest.

An objective of the symposium was to lay the groundwork for establishing common nomenclature and formulating standards for the measurement of cathode-ray tube parameters in terms which are compatible with photographic values. Approximately 275 representatives from 130 photographic, electronic and weapons systems organizations, and representatives from the Air Force, Army and Navy attended.

The papers presented at the symposium were: "Military Display and Recording Requirements," by C. B. Krumm; "Optimizing Video Display and Recording," by Frank L. Palazzo; "CRT Parameters," by W. E. Zunke; "Mechanics of Recording," by Lt. Col. Fred M. Crawford; "Sensitometry of Films Used for Cathode Ray Tube Recording," by Jack C. Lewis; "High Resolution Cathode-Ray Tube Face Using Fiber Optics," by N. S. Kapany and D. F. Capellaro; "The Role of Fiber Optics in Data Recording," by W. L. Hyde; "Cathode-Ray Tube Recording Cameras," by Henry A. Cubberly; "Methods of Determining Spot Size," by B. N. Manning; "Airborne Rapid Process-

ing," by J. B. Taylor, Z. Takats and H. Fledl; "Characteristics of Photographic Film as a Recording Medium," by Albert J. Derr; and "An Accurate Method of Measuring the Spot Size of High Resolution Cathode-Ray Tubes," by Lawrence E. White.

The two-day meeting was concluded with a panel discussion on the subject "Critical Problems in Video Recording." Panel members were drawn from both military and commercial organizations.

The symposium was sponsored by Systems Development Corp., 7100 Old Xenia Pike, Dayton, Ohio, in cooperation with the Strike and Recording Camera Section of the Aerial Reconnaissance Laboratory, WADC.

Papers presented at the symposium have been published in a well-illustrated loose-leaf volume entitled "Proceedings of the CRT Symposium," by the Systems Development Corp.

### *Notes on Tropical Photography*

For those interested in tropical photography there is available from the Sales Service Div., Eastman Kodak Co., Rochester, N. Y. an extensively revised Kodak publication of 35 pages, Pamphlet C-24, titled as above.

The pamphlet is prepared for photographers in southern sections, such as along the Gulf Coast, where humidities and temperatures sometimes approach tropical conditions, and for photographers in the tropics or planning to go there.

The pamphlet contains a summary of recommended precautions for tourists and residents, sources of trouble, materials and equipment, exposure information, processing recommendations, proper storage of processed films, and preservation of black-and-white prints in the tropics.

---

# *1959 Annual Conference* 26 to 30 October 1959

## Edgewater Beach Hotel · Chicago, Illinois

The next National Conference of the Society has been scheduled for October 26 through 30, 1959, at the Edgewater Beach Hotel, Chicago, Ill. Planning for the Conference is well under way.

An extensive papers program is being prepared under the guidance of Charles E. Ives, Papers Chairman, Research Laboratories, Eastman Kodak Company, Rochester 4, N.Y. There will be exhibits of special photographic instruments and equipment. Exhibits Chairman is Arthur E. Neumer, Jr., Hawk-Eye Works, Eastman Kodak Company, 20 Avenue E, Rochester 21, N.Y. Conference Coordinator is Ira R. Kohlman, Colorfax Laboratories Inc., 1160 Bonifant St., Silver Spring, Md.

---

# *The Society of* Photographic Scientists and Engineers

*Box 1609 • Main Post Office • Washington, D.C.*

## OFFICERS

| | |
|---|---|
| *President* | GEORGE T. EATON, Building 59, Kodak Park, Rochester 4, New York |
| *Executive Vice President* | STEVEN LEVINOS, Ansco, Binghamton, New York |
| *Engineering Vice President* | JOHN A. MAURER, 116–118 West 29th Street, New York 1, New York |
| *Editorial Vice President* | PETER KRAUSE, 295 Riverside Drive, Johnson City, New York |
| *Financial Vice President* | HERBERT MEYER, 325 Sequoia Drive, Pasadena 2, California |
| *Secretary-Treasurer* | NORTON GOODWIN, 826 Connecticut Avenue NW, Washington 6, D.C. |
| *Managing Secretary* | EDWARD S. COBB, Box 1609, Main Post Office, Washington, D.C. |

## CHAPTERS *and* CHAPTER OFFICERS

| | | |
|---|---|---|
| *Binghamton, New York* | *President* | IRA B. CURRENT, 26 Woodland Avenue, Binghamton, New York |
| | *Secretary* | E. SCUDDER MACKEY, Stone Road, RD No. 2, Binghamton, New York |
| *Boston, Massachusetts* | *President* | NICHOLAS CEDRONE, 73 Pond Street, Waltham, Massachusetts |
| | *Secretary* | ARTHUR J. ROSENBAUM, 44 Gleason Street, Framingham, Massachusetts |
| *Cleveland, Ohio* | *President* | R. E. BIRR, c/o General Electric Lamp Division, Nela Park No. 281, Cleveland 12, Ohio |
| | *Secretary* | CLINTON K. HAMLINK, 2230 South Overlook Road, Cleveland 6, Ohio |
| *Ithaca, New York* | *President* | COLONEL WILLIAM ALLEN, 216 Forest Home Drive, Ithaca, New York |
| | *Secretary* | DAVID O. FLETCHER, 1314 East State Street, Ithaca, New York |
| *Monmouth, New Jersey* | *President* | JOSEPH MANGIARACINA, 30 Brook Avenue, Little Silver, New Jersey |
| | *Secretary* | MISS MARILYN LEVY, 100 McLaren Street, Red Bank, New Jersey |
| *New York, New York* | *President* | FRANK G. BACK, 55 Sea Cliff Avenue, Glen Cove, New York |
| | *Secretary* | LT. HAYDEN B. PEAKE, Army Pictorial Center, 35-11 35th Avenue, Long Island City 1, New York |
| *Rochester, New York* | *President* | JAMES C. GRIFFIN, Haloid Xerox Inc., 282 Hollenbeck St., Rochester, New York |
| | *Secretary* | W. F. WALKER, Research Laboratories, Eastman Kodak Company, Rochester 4, New York |
| *Southern California* | *President* | CLAYTON S. CHAPEN, 652 Calle Miramar, Redondo Beach, California |
| | *Secretary* | ROBERT J. KEIDATZ, 7519 Baird Avenue, Reseda, California |
| *Chicago* | *President* | HENRY COOPMANS, 9118 Greenwood Avenue, Ballard Acres, Des Plaines, Illinois |
| | *Secretary* | ROBERT J. MAZOR, 1438 West 123rd Street, Chicago 43, Illinois |
| *Washington, D.C.* | *President* | KENNETH B. LUDWIG, 1054 31st Street, N.W., Washington 7, D.C. |
| | *Secretary* | LOUIS WERNER, 3610 North Powhatan Street, Arlington 13, Virginia |

# *Sustaining Members* / Society of Photographic Scientists and Engineers

Abrams Instrument Corporation

Aero Service Corporation

Ansco Division, General Aniline & Film Corporation

Atkinson Laboratory, Incorporated

Bar-Ray Products, Incorporated

Bausch & Lomb Optical Company

Bell & Howell Company

Charles Beseler Company

Burke & James, Incorporated

Chemco Photoproducts Company, Incorporated

Chicago Aerial Industries, Incorporated

Consolidated Film Industries

E. I. du Pont de Nemours & Company

Eastman Kodak Company

Edgerton, Germeshausen & Grier, Incorporated

The EdnaLite Optical Company, Incorporated

Elgeet Optical Company, Incorporated

Fairchild Camera & Instrument Corporation

Farrand Optical Company, Incorporated

Oscar Fisher Company, Incorporated

The F-R Corporation

General Electric Company

General Film Laboratories Corporation

Graflex, Incorporated

Grant Photo Products, Incorporated

W. & L. E. Gurley Company

Haloid Xerox Incorporated

Hardale Associates

Hi-Speed Equipment, Incorporated

Houston Fearless Corporation

Charles A. Hulcher Company, Incorporated

Philip A. Hunt Company

Hycon Manufacturing Company

The Kalart Company, Incorporated

Kollmorgen Optical Corporation

LogEtronics Incorporated

L-W Photo Products Company

J. A. Maurer, Incorporated

The Morse Instrument Company

National Research and Chemical Company

North American Aviation, Incorporated

Pako Corporation

Photogrammetry, Incorporated

Polaroid Corporation

Rolor Industrial Corporation

Simmon Brothers, Incorporated

Technicolor New York Corporation

Tiffen Marketing Company

Viewlex, Incorporated

Wollensak Optical Company

Zoomar, Incorporated